Tumor Targeted Multifunctional Poly(amidoamine) (PAMAM) Dendrimers to Promote Delivery of Poorly Soluble Chemotherapeutic Agent Paclitaxel in Cancer

THESIS

Submitted in partial fulfilment

of the requirements for the degree of

DOCTOR OF PHILOSOPHY

by

ROMPICHARLA S V KIRAN

ID No. 2014PHXF0010H

Under the supervision of

Dr. SWATI BISWAS

BITS Pilani
Pilani | Dubai | Goa | Hyderabad

2018

BIRLA INSTITUTE OF TECHNOLOGY AND SCIENCE, PILANI

CERTIFICATE

This is to certify that the thesis entitled "**Tumor Targeted Multifunctional Poly(amidoamine) (PAMAM) Dendrimers to Promote Delivery of Poorly Soluble Chemotherapeutic Agent Paclitaxel in Cancer**" and submitted by **ROMPICHARLA S. V. KIRAN** ID No. **2014PHXF0010H** for award of Ph.D. of the Institute embodies original work done by him under my supervision.

Signature of the Supervisor:

Name in capital letters: **SWATI BISWAS**

Designation : **Assistant Professor**

Date:

Acknowledgements

This thesis work would not have been possible without the guidance, support and help of several individuals. I thank everyone directly or indirectly involved in the successful completion of this work.

Looking back, connecting all the dots since I took up this journey, I realize the value of encouragement and support from my research guide. I owe utmost gratitude to my research supervisor, Dr. Swati Biswas, Assistant Professor, Department of Pharmacy, BITS Pilani, Hyderabad Campus for her undying support and mentorship. Her scientific acumen, understanding nature, encouragement and personal guidance have provided the framework for this thesis work.

I am extremely thankful to Dr Balaram Ghosh, Department of Pharmacy, BITS Pilani Hyderabad for providing constructive criticism to my work as Doctoral Advisory Committee (DAC) member and taking out time for relevant discussions regarding the study throughout this work.

I am grateful to Dr. V. V. Vamsi Krishna, Department of Pharmacy, BITS Pilani Hyderabad who acted as Doctoral Advisory Committee (DAC) member for his detailed constructive comments and support throughout this work.

I thank Prof. Souvik Bhattacharyya, Vice Chancellor, Prof. G. Sundar, Director, BITS Pilani, Hyderabad Campus, Prof. S. C. Sivasubramanian, Acting Registrar, Prof. Sanjay Kumar Verma, Dean, Academic Research, Prof. Niranjan Swain, Dean, General Administration, Prof. P. Yogeeswari, Associate Dean, Sponsored Research and Consultancy Division, and Prof. Vidya Rajesh, Associate Dean, Academic Research Division, BITS-Pilani, Hyderabad, for providing excellent working facilities and an absorbing research environment.

Thanks are due to Prof. D. Sriram, Head, Department of Pharmacy, BITS Pilani Hyderabad for his constant support to provide the best laboratory facilities possible.

I owe my most sincere gratitude to all faculty members of Department of Pharmacy, especially, Prof. P. Yogeeswari, Prof. A. Sajeli Begum, Dr. Onkar Prakash Kulkarni, Prof. Punna Rao Ravi, and Dr. Arti Dhar who were always available to hear me out and suggest solutions to any problems. I also thank former Head, Department of Pharmacy, BITS Pilani Hyderabad, Prof. Shrikant Y. Charde for his support.

I gratefully acknowledge the financial assistance from Department of Biotechnology (DBT), Government of India, New Delhi.

Working in the lab would not have been easy without the help of my labmates. I thank Dr. Omkara Swami Muddineti, Ms. Preeti Kumari, Ms. Prakruti Trivedi, Mr. Himanshu Bhatt, Ms. Anusha, Ms. Yamini and Mr. Ganesh for their support.

I thank my seniors and my colleagues who helped me in my work. Thanks are due to Dr Praveen, Dr Suman, Dr Anup, Dr. Shailender, Dr. Hasitha, Dr Sudeep, Prasanthi, Shubhmita, Shubham, Rimpy, Teja, Avantika, Ekta, Nikhila, Siva Krishna, Priyanka Reddy, Jaspreet, Suresh, Asha, Lokesh, Girdhari Roy, and Deepanjan for their support. I am indebted to my friends, Swathi, and Sravan, for being understanding and motivating me throughout this journey.

I sincerely thank the staff of BITS Pilani Hyderabad Ms. Saritha, Mr. Praveen, Ms. Bhagyalaxmi, Mr. Narendra Verma, Mr. Rajesh, Mr. Srinivas, Ms. Rekha, and Ms. Sunitha, for their humble gesture and kind support to me during my stay at BITS Pilani Hyderabad.

I would like to thank the Department of Science and technology (DST) and Centre for International Cooperation in Science (CICS) for providing travel support in presenting my research at international conferences.

I owe my loving thanks to my parents and family, without whose encouragement and understanding it would have been impossible for me to finish this work.

Rompicharla S V Kiran

Abstract

Dendrimers have gained much attention in the recent years for their unique architecture and feasibility of surface modification to cater various functions in drug delivery. They have been successfully explored for delivery of poorly soluble anti-cancer molecules to different types of cancers. The purpose of the present research is to study the delivery potential of dendrimers in targeting anti-cancer agents specifically to tumors by utilizing various benefits they offer in improving the biopharmaceutical properties of the drugs. The current thesis focuses on the delivery of paclitaxel (PTX), a poorly soluble chemotherapeutic agent to cancer cells utilizing poly(amidoamine) (PAMAM) dendrimers as delivery system. Initially, PTX was covalently attached to the generation 4.0 PAMAM dendrimer via a succinate linker using acid/amine coupling reaction to yield G4-PTX. Polyethylene glycol has been conjugated to the amine terminals of the G4 PAMAM dendrimer-PTX conjugate to improve the distribution and decrease the toxicity of cationic dendrimers. In the first part of the study, G4-PTX-PEG was anchored with octa-arginine (R8), a cell penetrating peptide to improve the penetration of conjugate into the cells. The synthesized dendrimers were characterized by proton NMR, gel permeation chromatography (GPC), and zeta potential measurements to confirm the formation of conjugates. From the GPC analysis, it was observed that approximately 2.5 molecules of PTX, 10.5 molecules of PEG and 1.8 molecules of R8 were attached to each G4 PAMAM dendrimer molecule. Hemolytic toxicity of the dendrimer conjugates revealed that PEGylated dendrimers were non-toxic to the cells and R8 modification did not cause any toxicity. The synthesized constructs were evaluated in human cervical cancer cells (HeLa) as monolayers as well as 3D multicellular spheroids. The R8 tagged

conjugate was found to internalize efficiently into the cancer cells as assessed by microscopy and flow cytometry. The cytotoxic potential of PTX was significantly improved upon conjugation with PAMAM dendrimers. Presence of R8 further augmented the delivery of PTX to cancer cells. The studies in 3D spheroids clearly demonstrated the advantage of tagging R8 to the surface of dendrimers which enhanced the penetration into spheroids thereby delivering higher drug load to cancer cells.

In the next study, active targeting strategy was used to have a better control on delivery of the drug to cancer cells. Biotin, a micronutrient essential for normal cellular functions and receptors of which are overexpressed in cancer cells has been covalently attached to G4-PTX-PEG. The biotin targeted and non-targeted conjugates were evaluated *in vitro* in human lung cancer cells (A549) which overexpress biotin receptors. HABA/Avidin assay showed an attachment of 20.98 molecules of biotin per dendrimer. Biotin saturation studies in A549 cell lines were performed to determine the mechanism of uptake into cells. It was noticed that the biotin tagged dendrimer conjugates were internalized actively via the vitamin biotin receptors. The G4-PTX-PEG-Biotin conjugate showed the highest cytotoxicity in cell monolayers as well as 3D spheroids in comparison to G4-PTX-PEG and free drug.

Altogether, these studies demonstrated the ability of multifunctional PAMAM dendrimer system in efficiently delivering PTX to cancer cells thereby improving the cytotoxic potential. Therefore, the newly developed PAMAM dendrimer system holds great potential in delivering chemotherapeutics to cancer clinically.

TABLE OF CONTENTS

List of figures

List of tables

Abbreviations and symbols

^{1}H NMR	Proton Nuclear Magnetic Resonance
A549	Human alveolar adenocarcinoma cell
DAPI	4',6-diamidino-2-phenylindole
DCC	N,N'-Dicyclohexylcarbodiimide
DCM	Dichloromethane
DIPEA	N,N-Diisopropylethylamine
DLS	Dynamic Light Scattering
DMEM	Dulbecco's modified Eagle's media
DMF	Dimethyl formamide
DMSO	Dimethyl sulphoxide
DSC	Differential scanning calorimetry
EDC	1-Ethyl-3-(3-dimethylaminopropyl)carbodiimide
EDTA	Ethylene diamine tetra acetic acid
EPR	Enhanced Permeability and Retention
F	Fluorescein
FBS	Fetal bovine serum
FITC	Fluorescein isothiocyanate
FTIR	Fourier transform infrared spectroscopy
G4	Generation 4.0
GPC	Gel Permeation Chromatography;
IC_{50}	Half maximal inhibitory concentration
MTT	3-[4,5-Dimethylthiazol-2-yl]- 2,5-diphenyltetrazolium bromide
MW	Molecular weight
MWCO	Molecular weight cut-off
NHS	N-hydroxy succinimide
NMR	Nuclear Magnetic Resonance;
PAMAM	Poly(amidoamine)
PBS	Phosphate buffered saline
PDI	Polydispersity index
PEG	Poly (ethylene glycol)
PI	Propidium iodide

PTX	Paclitaxel
R8	Octa-arginine
rpm	Rotation per minute
RT	Room temperature
SD	Standard deviation
UV	Ultraviolet
λ_{max}	Wavelength maxima for UV-absorbance
µg	Microgram
µL	Microlitre
µM	Micromolar
^{o}C	Degree centigrade
mg	Milligram
min	Minute
mL	Millilitre
mm	Millimetre
nm	Nanometre
mmol	Millimole

Chapter 1

Introduction

1.1 Cancer

Cancer is a term used for a group of diseases in which cells divide abnormally in an uncontrolled fashion and are able to invade adjacent or distant organs or tissues. The process of cancer spreading to various parts of body is called metastasis and is a major factor for deaths caused by cancer. It can occur and affect nearly all parts of the human body at all ages irrespective of the gender. Cancer is a leading cause of death globally and accounted for 7.6 million deaths (around 13% of all deaths) in 2008 (Ferlay et al. 2010). Deaths from cancer worldwide are projected to continue to rise to over 13.1 million in 2030 (Noor Kamil 2015; Senapati et al. 2018).

In India, cancer is now the second major cause of mortality after cardiovascular disease. As per GLOBOCAN 2012 report by World Health Organization, cancer accounts for approximately 949,000 new cases every year with 634,000 deaths in 2008. Prevalence rates of Breast, Cervical and Oral Cancer in India are alarmingly high when compared to global incidence rates. Over 50% of cancer deaths in India are caused because of lung and oral cavity cancer in males and breast and cervical cancer in females. Statistics show that every 8 minutes one woman dies of cervical cancer in India. Further, one in every two women newly diagnosed with breast cancer dies of it in India (Ferlay et al. 2015; Bray et al. 2013).

Cancer of oral cavity (105,000 new cases and 42,000 deaths annually), lungs (47,000 new cases and 42,000 deaths), stomach (21,000 new cases and 21,000 deaths), colorectal (20,000 new cases and 14,000 deaths), and pharynx constitute the most frequently affecting cancers in men whereas breast (115,000 new cases and 54,000 deaths), cervix (134,000 new cases and 73,000 deaths), colorectal, ovary (28,000 new cases and 20,000 deaths), and oral cavity (36,000 new cases and 26,000 deaths) cancers comprise the top 5

cancers in women (Saranath and Khanna 2014; Ferlay et al. 2015). It was also reported that death of 1 in 5 males and 1 in 20 females was caused due to smoking and tobacco related diseases which accounted to estimated 930,000 deaths in 2010 ('Cancer Statistics'). However, the mortality rate has declined in the last 5years due to a better understanding of cancer biology and improved diagnostic devices and treatments.

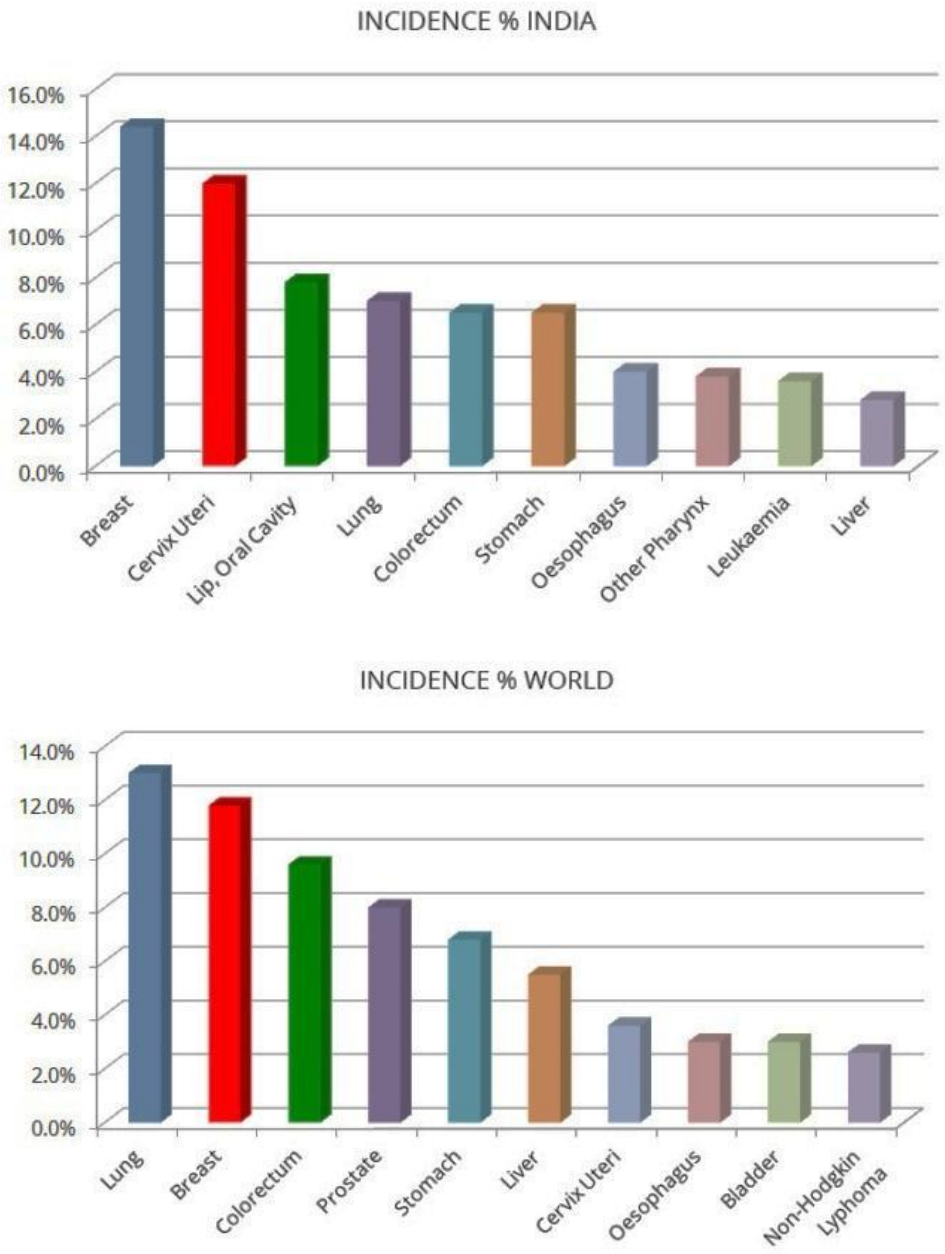

Figure 1.1 Incidence of cancers in India and World as per GLOBACAN 2012 report.

The transformation of normal cell into a cancer cell is the consequence of interaction of genetic factors of a person with external carcinogenic agents such as: Tobacco, food contaminants, water pollutants, ultraviolet radiation, and certain viral or bacterial infections. Lifestyle related factors like excessive alcohol use, unhealthy diet, and physical inactivity also pose considerable risk of developing cancer (Nair, Varghese, and Swaminathan 2005; Ingole, Kakde, and Bonde 2016).

Human body is composed of more than trillions of cells which are fundamental units of life (Sherwood 2015). As a general mechanism, normal cells develop and divide to form fresh cells as per the need of the human body. They eventually die as they grow old or become damaged and new cells replace the old cells. In a healthy human being, there is a right number of each type of cell. This is controlled by the cells themselves by producing signals which direct them when to divide and when not to. In the process, if any fault occurs in signal transmission, cells may start growing uncontrollably leading to irregularities. This abnormal behavior of cells leads to events where they ignore control signals making the old or damaged cells continue to live when they should perish, and new cells form when they are not required resulting in tumor formation. They lose their ability to distinguish its own boundary and spread across the body to places where they do not belong. The process by which cells divide is called cell division. Cells have a control center called nucleus and contains the genetic material deoxyribonucleic acid (DNA). This DNA is part of the genes which controls the cellular division and functions depending on the body's need. DNA is the blueprint for everything the cell does (O'Connor, Adams, and Fairman 2010).

In a human cell, the DNA is arranged in 46 distinct sections called chromosomes. Altogether more than 10,000 genes are present in the chromosomes. Each of these genes

direct cells to make a different protein following a series of biochemical reactions ('Cancer Registration and Surveillance Modules').

Certain genes direct the cell to synthesize structural proteins, which form the building blocks whereas some other genes make the cell to produce hormones, growth factors or cytokines, which travel out of the cell and establish communication with other cells. A type of proteins called regulatory proteins is manufactured by some genes which control the function of proteins or convey other genes when to turn "on" or "off." (Griffiths AJF 2000; Lodish H 2000)

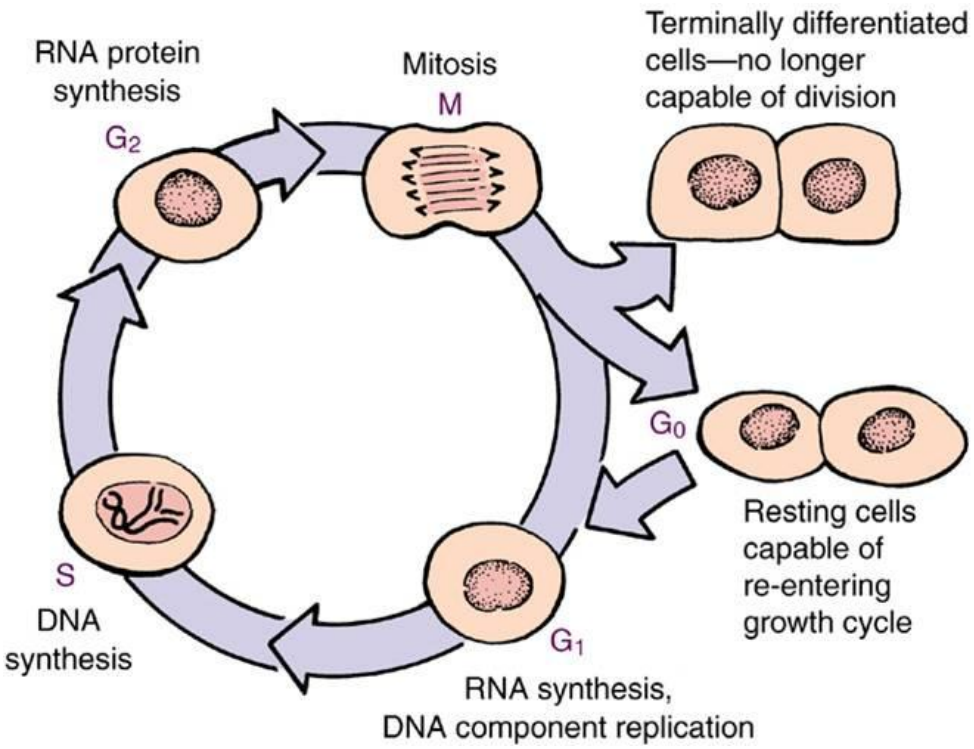

Figure 1.2 Diagram representing phases of cell cycle and events occurring at each phase. Reproduced from www.nursingbuddy.com/2011/02/16/introduction-to-cell-physiology/

Cells divide from parent to daughter cells by mitosis process and this series of events is called cell cycle. Cell cycle consists of mitosis phase (M phase) and a synthetic phase called S Phase. DNA is synthesized during S phase. Between M phase and S phase is G1

phase where RNA, proteins, and enzymes needed for DNA synthesis in S phase are produced. After S phase is the G2 phase which prepares the cell for M phase. G0 phase is the resting phase where we see non-dividing cells. Various checkpoints alongside each step of the cell cycle make sure that everything goes the way it should. These normal cells are highly specialized and very specific in the functions they perform (Hartwell and Weinert 1989).

1.2 Cancer cell biology

In cancer cells, during the process of cell division, genes undergo mutation leading to formation of defective cell. These defective cells further undergo cell division without control making more and more copies of that cell. Mutations are changes that happen to genes making it incapable of performing its own functions. Mutation can happen by chance or due to multiple reasons such as environmental causes, chemical exposure, and life style habits (White et al. 2014).

In general, two types of gene mutations can occur. One is dominant mutation and the other is recessive mutation. These mutations can affect three main types of genes namely; proto-oncogenes, tumor suppressor genes, and DNA repair genes (Vogelstein and Kinzler 2004). Dominant mutation is caused by an anomaly in one gene in a pair. For example, a mutated proto-oncogene leads to production of a faulty protein which instructs the growth factor receptor to be constantly open on the cell surface, when no growth factor is present to liaison. Further, it sends a message to the cell to constantly divide. This dominant "gain of function gene" is cancer-causing and is termed an oncogene (onco = cancer) ('Cancer Registration and Surveillance Modules').

In recessive mutation, both genes in a pair get damaged. An example of this type of mutation is alteration in function of tumor suppressor genes or anti-oncogenes. A tumor

suppressor gene called p53 synthesizes a protein that shuts "off" the cell cycle and thus helps to regulate the cell growth. It controls the formation of potential cancerous cells by repairing or destroying the faulty cells (Vogelstein and Kinzler 2004).

If one of two p53 gene in the pair undergoes mutation, the other gene will still be capable of controlling the cell cycle. On the other hand, if both genes are transformed, the "off" switch is lost, and the cell division is no more under control (Floor et al. 2012).

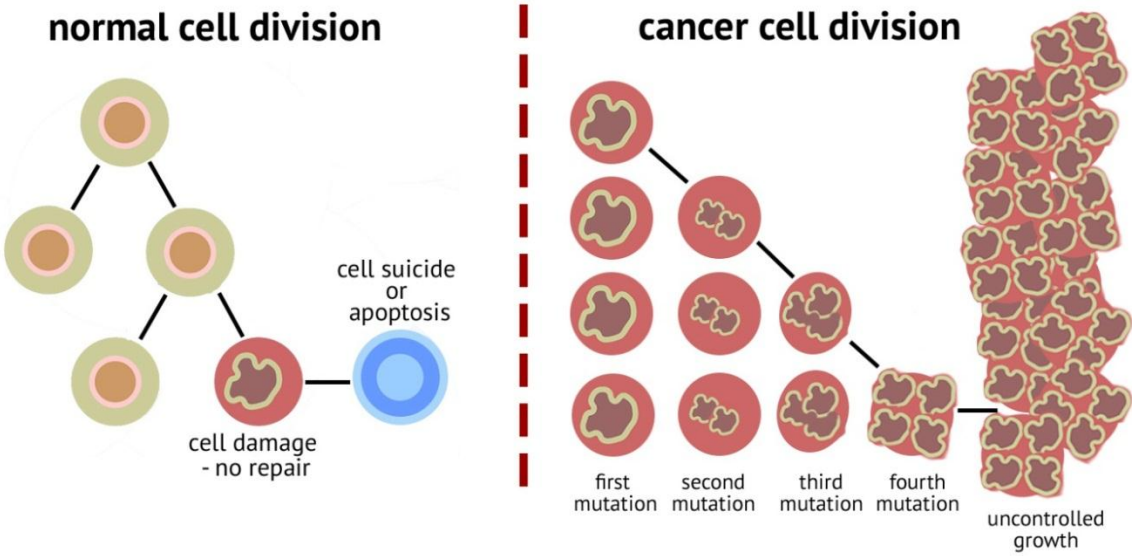

Figure 1.3 Diagrammatic representation of cell division in normal cells and cancer cells. Reproduced from www.philpoteducation.com/mod/book/view.php?id=779&chapterid=1123#

Mutated cells undergo uncontrolled growth leading to tumor formation. Unusual cell division can take place either when oncogenes are activated or when tumor suppressor genes fail to express. In fact, for a normal cell to become malignant, several mutations are required. In certain cases, both types of mutations — dominant and recessive — may occur. Similarly, DNA repair genes are which have a function of fixing damaged DNA, if mutated, tend to develop further alterations in other genes. Altogether, these mutations may cause the cells to become cancerous. These alterations are sometimes called

"drivers" of cancer. Irregular cell division can also be triggered by viruses. In such cases, even if the genes appear normal, the protein may not operate ordinarily because the cell contains a cancer-producing virus (Lodish H 2000).

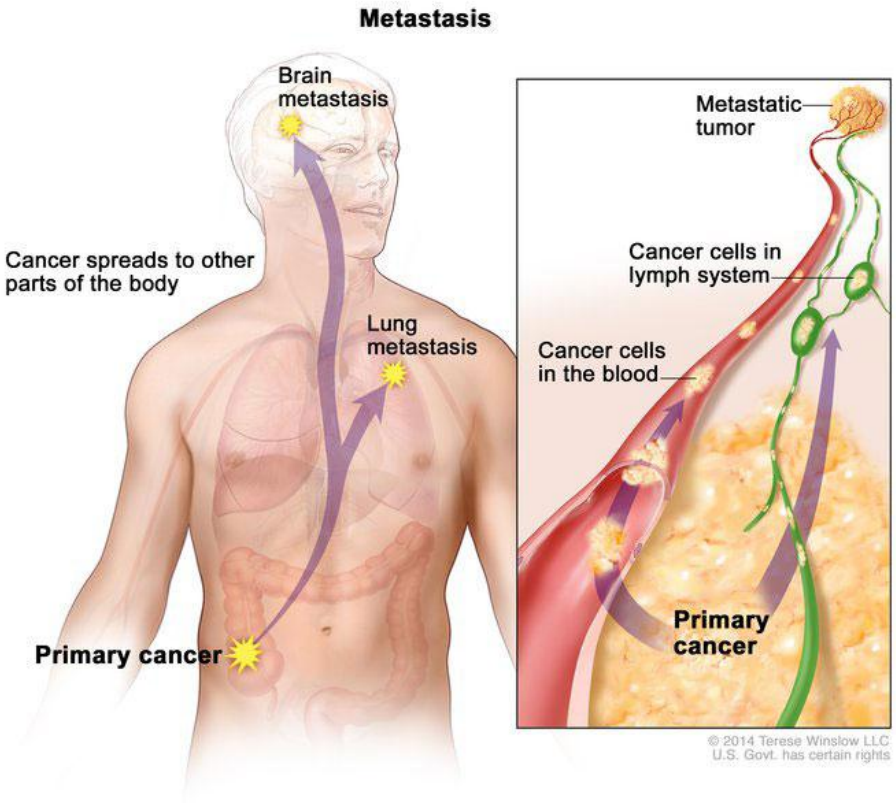

Figure 1.4 Pictorial representation of how metastasis occurs from primary tumors leading to one or more metastatic tumors in different parts of the body. Reproduced from www.cancer.gov published by National Cancer Institute, USA.

All the above mentioned factors may lead to formation of tumors usually solid in nature. Some cancers do not form solid mass for which cancer of blood (leukemia) is an example. The site where the cancer starts is called the primary tumor. It can localize at the place where it began or can invade adjacent tissue, enter lymph nodes or blood circulation spreading cancer wherever it reaches. This is called metastatic tumor and is most common cause of death in people who die of cancer. Based on the histological site where cancer arises, cancers are grouped into 6 major categories namely carcinoma,

sarcoma, myeloma, leukemia, lymphoma, and mixed types ('Cancer Registration and Surveillance Modules').

1.2.1 Hallmarks of Cancer

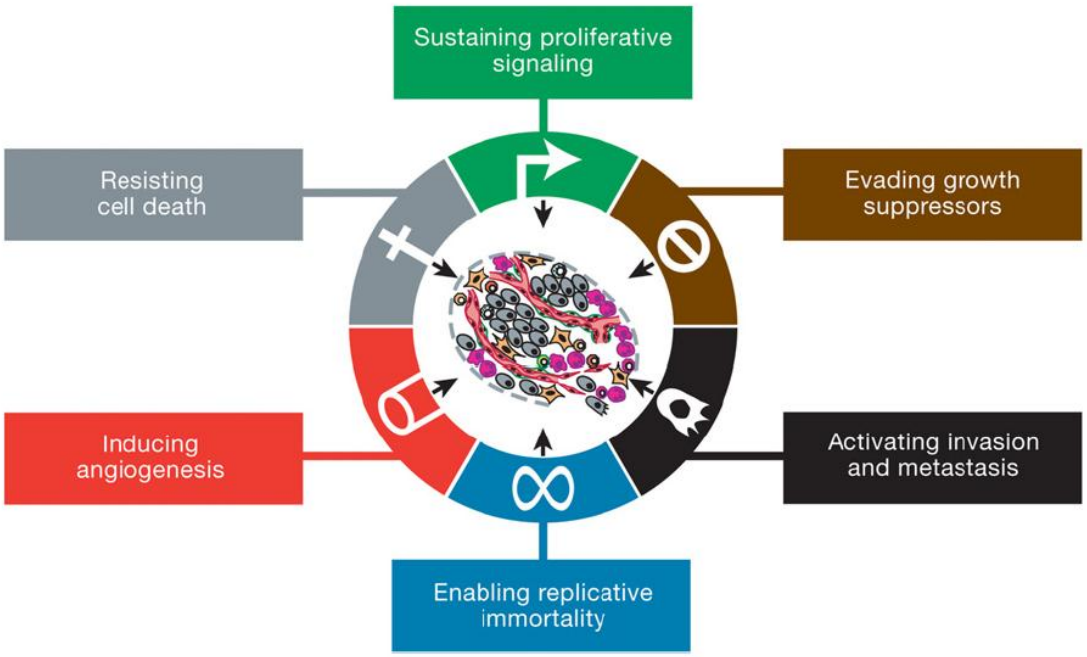

Figure 1.5 Hallmarks of cancer (Hanahan and Weinberg 2011)

Prof. Hanahan and Prof. Weinberg in their article 'Hallmarks of cancer: The next generation' (Hanahan and Weinberg 2011) have proposed six hallmarks of cancer which constitute an organizing principle that provides a logical framework for understanding the complexities of cancer biology. With remarkable scientific progress in the last decade it has been clearly understood and solidified that elaborating the behavior of cancer cells alone cannot sufficiently explain the biology of cancers. Instead, the contributions of the tumor microenvironment to tumorigenesis must also be comprehended. The six hallmarks of cancer are sustaining proliferative signaling, evading growth suppressors, resisting cell death, enabling replicative immortality, inducing angiogenesis, and activating invasion and metastasis.

Apart from the above six, two additional hallmarks were perceived to be emerging and were proposed along with their enabling characteristics. Deregulating cellular energetics and, avoiding immune response are the two emerging hallmarks which are explained as alteration of cellular metabolism to promote cancer cell proliferation and evasion of immunological destruction by T and B lymphocytes, natural killer cells and, macrophages (Hanahan and Weinberg 2011).

1.3 Cancer treatment and chemotherapy

Current cancer management majorly consists of surgical intervention, chemotherapy, and radiation therapy or a combination of these options (Jia and Jia 2012). Traditional ways to target cancer cells include obstruction of DNA synthesis and mitosis which kills rapidly proliferating cancer cells. As these are non-targeted mechanisms, normal healthy cells most often are also damaged, causing severe inadvertent side effects including but not limited to nausea, loss of appetite, bone marrow suppression, alopecia and, hypersensitivity reactions. Moreover, the serious and severe side effects caused by chemotherapeutic agents are the leading reasons for high mortality rate in cancer patients. Additionally, most chemotherapeutic drugs do not have ideal physicochemical properties for formulation and have low access to tumors in vivo. This leads to higher doses being administered further causing increased toxicity and multidrug resistance (Tripodo et al. 2014).

Some of the chemotherapeutic classes include alkylating agents, antimetabolites, antimicrotubule agents, antitumor antibiotics, topoisomerase inhibitors etc. Alkylating agents act by binding to DNA thereby interfering with DNA replication and further cell division.

Nitrogen mustards (cyclophosphamide, ifosfamide, chlorambucil, melphalan), tetrazines (dacarbazine, mitozolamide), nitrosoureas (carmustine, lomustine), mitomycin C are some of the examples of alkylating agents. Organoplatinum complexes such as cisplatin, carboplatin, and oxaliplatin act by crosslinking with DNA strands inhibiting DNA, RNA, and protein synthesis (Pratt, Ensminger, and Ruddon 1994).

Antimetabolites are another class of anti-cancer agents which possess structural similarity to endogenously available vitamins, nucleosides, or amino acids and act by inhibiting the enzymes or incorporating into DNA to further block the synthesis of DNA, RNA, or proteins in cancer cell. Folate antagonists (methotrexate, pemetrexed), purine analogues (cladribine, fludarabine, pentostatin, mercaptopurine), pyrimidine analogues (fluorouracil, capecitabine, gemcitabine), and hydroxyurea fall in the class of anti-metabolites (Scholar 2007).

Taxanes (paclitaxel, docetaxel, and cabazitaxel), and vinca alkaloids (vincristine, vinblastine, vinorelbine) act on the spindle apparatus during cell division. Topoisomerases are enzymes that function on the 3D structure of DNA by cleaving//unwinding/rejoining DNA strands for replication. Camptothecin analogues (irinotecan, topotecan), anthracyclines (doxorubicin, daunorubicin, epirubicin, idarubicin), epipodophyllotoxins (etoposide, tenoposide) are some of the examples of topoisomerase inhibitors (Freres, Jerusalem, and Moonen 2017).

Cytotoxic agents primarily affect cells which undergo rapid cell division and so do not precisely target cancer cells in the G0 phase of cell cycle. Further, they have limited effect on aspects of cancer progression like metastasis, and tissue invasion. They show similar toxicity to cancer as well as normal cells. Apart from the cytotoxic drugs, monoclonal antibodies (mAbs; trastuzumab, bevacizumab), hormonal agents (tamoxifen,

letrozole, bicalutamide etc.) that act specifically on receptors and modulate their function were developed for use in treatment of cancer (Gerber 2008).

1.3.1 Limitations of conventional cancer chemotherapy

Although the conventional chemotherapy regimens are being followed in treatment of various cancers either alone or in combination with other treatment strategies, they pose several limitations as enumerated below.

Poor aqueous solubility: Most of the chemotherapeutic agents are poorly soluble in water and require solvents in formulation of their dosage forms. These agents suffer meager bioavailability and requires frequent and high dosing to reach the therapeutic concentrations. To formulate intravenous dosage forms, the active agents must be capable of going into solution in aqueous media for them to stay in the system. For example, Paclitaxel (PTX), a highly successful chemotherapeutic agent suffers very low solubility of less than 0.5 mg/L (Kakde et al. 2011). Cremophor EL (castor oil derivative) and dehydrated alcohol had to be used in its formulation which causes toxicities of heart, kidney, brain, systemic toxicity, and peripheral neuropathy along with hypersensitvity reactions. On the other hand, surfactants when employed in the formulation to solubilize the drug, may lead to precipitation of drug *in vivo*, due to their high critical micelle concentration in physiological fluids.

Non-specific toxicities: Conventional anticancer agents when administered by intravenous route, pass through the blood circulation and reaches cancer cells as well as normal cells. Such drugs which are currently in use often show unwanted toxicities due to their broad distribution in the body resulting in serious adverse effects such as bone marrow depression, systemic toxicity, hair loss, anemia, weight loss, nausea, diarrhea, infertility, cardiovascular toxicity, vomiting etc. to name a few. Also, cells have slowly

attained drug resistance to these single agent therapies (Stortecky and Suter 2010). The absence of selectivity in mechanism of action is a conspicuous drawback of conventional chemotherapy. Most number of anti-cancer drugs does not act on intracellular mechanisms exclusive to cancer cells but on pathways common in both normal and cancerous cells.

Uptake by reticuloendothelial system (RES): Macrophages and monocytes present in the reticular connective tissue (ex: liver, spleen) compose the reticuloendothelial system and are responsible for rapid clearance of hydrophobic agents from the blood circulation (Kakde et al. 2011). They remove the cell debris, foreign substances, and pathogens from the circulation by phagocytosis. As most of the cancer chemotherapeutics are hydrophobic in nature, they get engulfed by the RES which results in rapid clearance of drug from the blood stream. Therefore, high concentrations of drug needs to be administered to reach the therapeutic concentrations at the target site. Hydrophobicity of the delivery system along with its particle size properties and surface charge influences the uptake by RES.

To overcome this problem, the delivery system can be coated by polyethyleneglycol (PEG) which is a synthetic, water-soluble polymer. PEG improves the hydrophilicity of the system and masks it from being identified by macrophages. It inhibits opsonization and protein adsorption of the delivery system which improves its circulation time. This technique has been effectively used to minimize the rapid clearance of drug delivery systems and improving the overall half life of the drug (Mishra, Nayak, and Dey 2016).

Multidrug resistance (MDR): One of the major problems associated with conventional chemotherapy is the cells acquiring resistance to drugs. Resistance could occur by cellular or non-cellular mechanisms (Kakde et al. 2011). The cellular mechansim involves a

plasma membrane receptor protein P-glycoprotein (P-gp) which repels the drugs out of the cell obstructing intracellular accumulation of therapeutic agents. P-gp is the major efflux protein in the body belonging to the family of ATP binding cassette (ABC) transporters (Chidambaram, Manavalan, and Kathiresan 2011).

P-gp transporter protein is overexpressed in cancer cells and diminishes the entry and retention of drug in the cells. This phenomenon is majorly observed when drug diffuses passively into the cell through the lipid cell membrane. After entering into cell, anti-cancer agents, using the energy of ATP hydrolysis forms transmembrane channels by binding to P-gp and expel these molecules out of the cell. Such actives which are susceptible to P-gp efflux are called P-gp substrates. Doxorubicin, docetaxel, paclitaxel, actinomycin D, etoposide are few of the anti-cancer agents which are P-gp substrates (Bar-Zeev, Livney, and Assaraf 2017). Oral bioavailbility of such molecules is seriously comprimised. The co-administration of inhibitors of P-gp was investigated to improve the delivery to cancer cells. For example, a delivery system encapsulating elacridar, a P-gp inhibitor along with paclitaxel in a micellar system was reported to overcome the multidrug resistance problem of paclitaxel (Wang et al. 2015).

Multidrug-resistance-associated protein 1 (MRP1) and Breast cancer resistance protein (BCRP) are two other major drug transporters after P-glycoprotein. MRP1 was reported to be overexpressed in cancers of lung, colon and different forms of leukaemia (Chai, To, and Lin 2010). Further, high first-pass metabolism of taxoids by P-450 enzymes also contribute to their poor oral bioavailability.

Also, poor vascularization of tumor regions reduces the drug access to the entire cancer tissue leading to poor therapeutic efficacy in cancer cells. Some of the basic drugs get ionized in the acidic environment of the tumor which prevents their movement across the cell membrane. High interstitial pressure and low microvascular pressure may also hold

back the extravasation of drug molecules. Apart from the drug efflux pumps, cancer cells also show drug resistance by decreasing the uptake of drug, increasing the drug metabolism, altering the drug targets, impair apoptotic pathways and cell cycle checkpoints (Bar-Zeev, Livney, and Assaraf 2017).

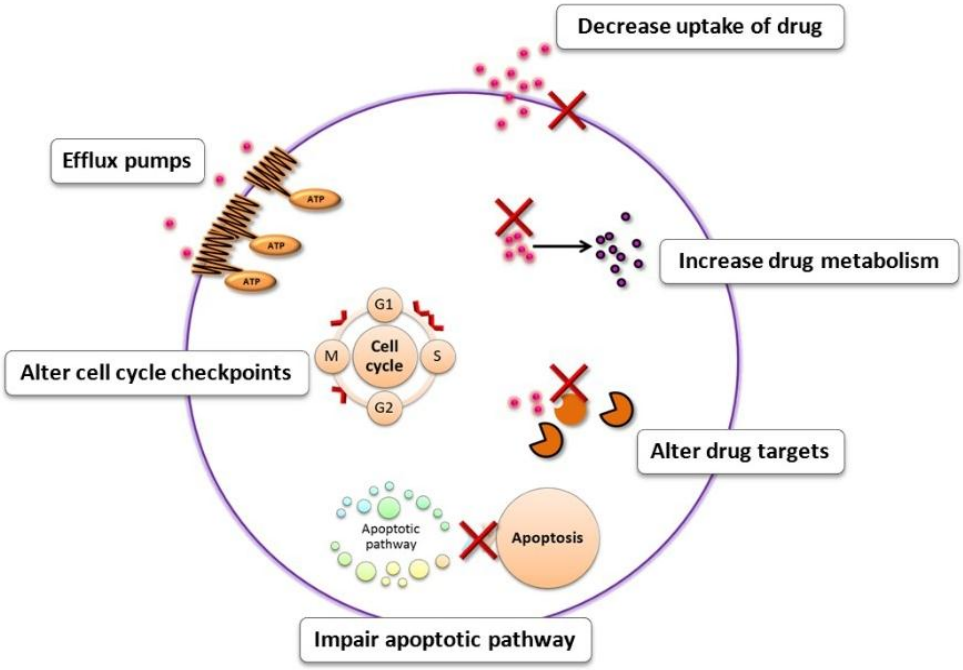

Figure 1.6 Mechanisms of cancer cell resistance towards anti-cancer drugs (Chai, To, and Lin 2010).

As a solution to overcome the pitfalls of conventional chemotherapy, pursuit for effective therapeutic approaches warrants more attention, and understanding.

The aim of the ideal cancer chemotherapy is to deliver the right amount of drug at a controlled rate and for adequate period of time to the site of action (tumor) to achieve the desired therapeutic outcome, causing no harm to the normal cells at the same time. To accomplish this objective, the delivery systems should be designed so as to hold required amount of therapeutic agent and eliminate the setbacks associated with bioavailability, biodistribution, clearance, non-specific toxicities, and drug resistance. The delivery system should be able to remain in the blood circulation for prolonged time, with tumor

specificity, retention in tumor, and tunable drug release, providing the maximum pharmacological efficacy of the drug.

1.4 Nano drug delivery

Nanotechnology is a rapidly growing field that has gained great attention in drug delivery and cancer theranostics (Conniot et al. 2014). Nanomedicines in cancer aim to improve the pharmacokinetics and distribution of anti-cancer drugs which increases their specificity to cancer cells. Various nanotechnology based products have already established their benefits clinically and made their way into the market. Further, there are more than 60 active clinical trials going on involving nano drugs most of which are for anti-cancer drug delivery. The years from 2013 to 2015 had witnessed the highest number of nanoformulation based applications of clinical trials to USFDA suggesting the high potential of nanotechnology based products in treatment of various diseases (Ventola 2017).

The nanometer size (1-1000 nm) and, high surface to volume ratio of these materials gives them unique biological advantage which allows them to carry, bind, and absorb a variety of drugs, genetic material, peptides and, diagnostic agents with great efficacy (Senapati et al. 2018). Nanoformulations are capable of enhancing the solubility of poorly soluble drugs, and improving the bioavailability of poorly absorbed drugs.

Nanocarriers investigated in the cancer chemotherapy can be classified majorly into targeted and non-targeted delivery systems. Liposomes, polymeric nanoparticles, nanocrystals, dendrimers, polymeric micelles, albumin bound nanoparticles, metal nanoparticles, and polymer-drug conjugates are some of the widely explored nano systems for delivery of chemotherapeutic agents (Peer et al. 2007).

The drug is either entrapped in the delivery system or covalently conjugated to the system. Entrapment of drugs in the nano systems prevents the degradation of drugs in the biological system and also by-passes first pass metabolism leading to enhanced bioavailability (Bobo et al. 2016). As the solubility of drug improves when encapsulated, it prevents the precipitation of drug *in vivo*.

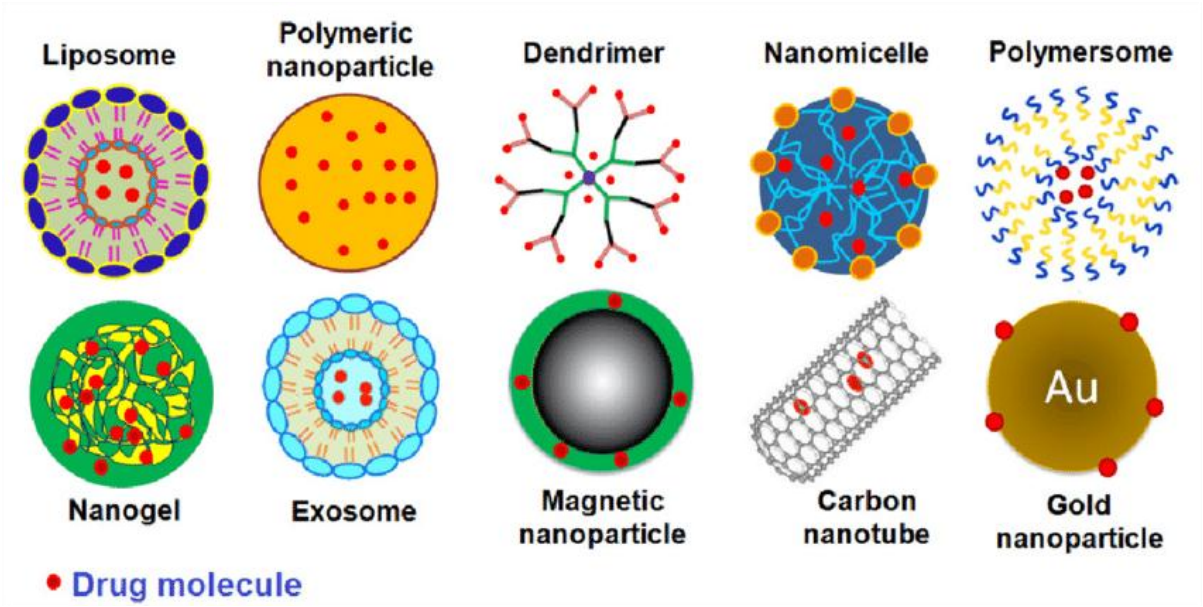

Figure 1.7 Types of nano systems investigated for cancer drug delivery (Agrahari 2017)

The first clinical trial of nanoformulations for chemotherapeutic drug delivery dates back to mid-1980s, and in 1995 the first nanosystem liposomes incorporating doxorubicin had hit the clinic (Li et al. 2017). Consequently, various nanoparticulate systems for the delivery of anti-cancer agents have been investigated owing to the benefits they offer such as enhancing solubility and stability of hydrophobic drugs, decreasing non-specific uptake, prolonging circulation time, evading undesirable off-target effects, improving cellular association, and effective targeting of tumors.

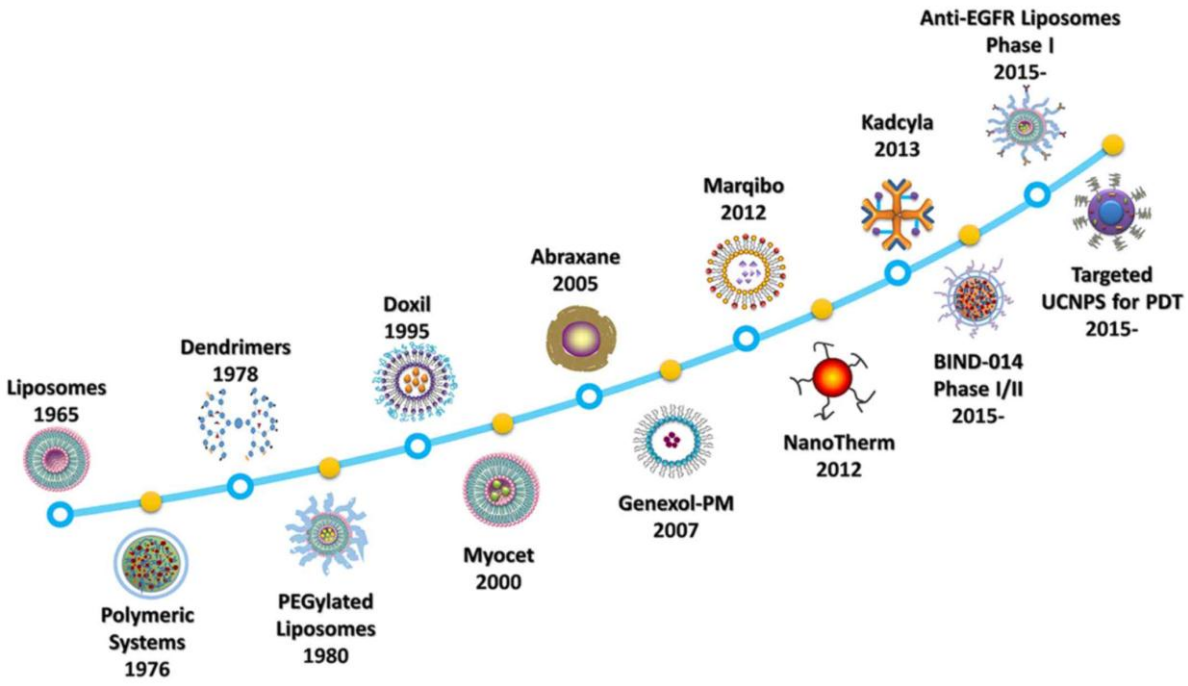

Figure 1.8 Timeline of development of nano drug delivery systems for biomedical applications (Li et al. 2017).

Advantages of nanocarrier systems:

- Nanocarriers improve the therapeutic index of drugs encapsulated in comparison to their conventional delivery systems.
- They increase the drug efficacy by maintaining the steady state therapeutic concentrations by controlling the drug release over a period of time.
- Nanocarriers are capable of evading phagocytosis by macrophages by surface modification with hydrophilic polymers such as polyethyleneglycol.
- The surface of nanocarriers can be tuned to attach a variety of ligands which can actively target the receptors specific to the cell.
- Due to the nano size of the system, they can accumulate in the tumor tissue passively by enhanced permeation and retention (EPR) effect.

- Polymers used for formulation of nanocarriers such as poloxamers act as P-gp inhibitors and thereby reverse the multidrug resistance which improves the intracellular drug concentration.

Doxil (Doxorubicin hydrochloride) was the first USFDA approved liposomal formulation for the treatment of ovarian cancer and multiple myeloma. The liposomal doxorubicin was found to be effective in humans with increase in the area under the curve (AUC) by 300-fold and reduced clearance 250-fold compared to free doxorubicin (Ventola 2017). Myocet is another liposomal formulation which is made up of phosphatidylcholine and choline and entraps doxorubicin citrate. Liposomal formulations encapsulating cisplatin, oxaliplatin are currently under clinical trials (Babu et al. 2014).

Another nanoformulation Abraxane, which is albumin bound particles of paclitaxel has been approved for treatment of various cancers. It was found to be well tolerated compared to the conventional paclitaxel formulation which contains cremophor EL as the solubilizer (Ventola 2017). This has facilitated Abraxane to be administered at desired quantities to achieve maximum benefits. Opaxio, a polyglutamic acid conjugated paclitaxel nanodrug is under investigation.

Also, a polymeric micelle based formulation of paclitaxel (Genexol-PM) has been approved for the treatment of metastatic breast cancer and has shown better therapeutic profile compared to conventional formulations. Nanocarriers possess the prowess to be delivered actively or passively to the target site by various approaches. Most of the approved nanoformulations are passively targeted and accumulate in the cancer tissue by a phenomenon called enhanced penetration and retention (EPR) effect (Prabhakar et al. 2013).

1.5 Targeted drug delivery

Targeted drug delivery of nanocarriers enables the selective and efficient localization of therapeutic molecules in the target site while restricting the access to adjacent normal tissues. This helps in reducing the non-specific toxicities, maximizing the therapeutic index, and improving the biodistribution of drug which is a major aspect in triumph of anti-cancer drug delivery. Cancer targeting by nanoscale systems can be accomplished based on the considerations of leaky vasculature of tumors, angiogenesis, and ligand based approach for over expressed receptors in cancer, EPR effect, and intracellular targeting. Particle size, potential, hydrophilic-lipophilic properties, and chemical attachment of ligands are few of the factors which should be looked into for effective targeting of nanodrug delivery systems (Kakde et al. 2011).

1.5.1 Passive tumor targeting

The conventional anticancer drugs are non-selective to tumor and unevenly distributed in the body, causing relatively low therapeutic index. Due to this reason, the treatment of common solid tumors with chemotherapy alone becomes difficult. Nanocarriers having chemically conjugated or physically encapsulated drugs have been an attractive approach to improve the tumor targeting efficiency. Recent studies indicated that nanoparticles display prolonged circulation in the blood and accumulation in the tumor without the use of targeting ligands revealing the existence of passive targeting (Duncan 2003). The tumor blood vessels are commonly described by abnormalities including comparatively high percentage of proliferating endothelial cells, enhanced tortuosity, and formation of abnormal basement membrane.

The rapid vascularization to provide nutrients and oxygen to the growing cancer cells results in the defective vascular structure, thus decreasing the lymphatic drainage and

rendering the permeability of macromolecules through vessels. This passive targeting mechanism was first reported by Maeda *et al*. termed as "Enhanced Permeation and Retention (EPR) effect" (Maeda 2001; Matsumura and Maeda 1986). After the identification of EPR effect, many studies have investigated the passive targeting of macromolecules and nanocarriers such as polymeric micelles, liposomes, and dendrimers due to EPR effect in solid tumors, thus enhancing the therapeutic efficacy.

The nanocarriers having following characteristics are important for the EPR effect. (i) The ideal particle size of the nanocarrier should be in the range of 10 to 100 nm. However, for effective extravasation through the fenestrations in leaky vasculature, size should be less than 400 nm. Whereas, to prevent the specific internalization by liver, nanocarrier size need to be less than 100 nm, and to escape the filtration by the kidneys, the size need to be greater than 10 nm. (ii) The surface charge of the nanocarriers should be anionic or neutral to avoid renal elimination. (iii) The nanocarriers should avoid the uptake by reticuloendothelial system, which destroys any foreign particle through opsonization followed by phagocytosis (Malam, Loizidou, and Seifalian 2009; Gullotti and Yeo 2009).

Nonetheless, the passive targeting also possesses few limitations.

(i) The degree of tumor vascularization and angiogenesis plays major role in passive targeting of nanocarriers, and it will differ with tumor nature and anatomical location (Bae 2009)

(ii) High interstitial fluid pressure of solid tumors circumvents effective internalization and consistent distribution of drugs in the tumor (Heldin et al. 2004). The increased interstitial fluid pressure of tumor related with poor lymphatic drainage describes the link between nanocarrier size and the EPR effect: long-circulating nanocarriers in the size

range of 100 nm are more retained in the cancer cells, while smaller particles diffuse easily (Pirollo and Chang 2008).

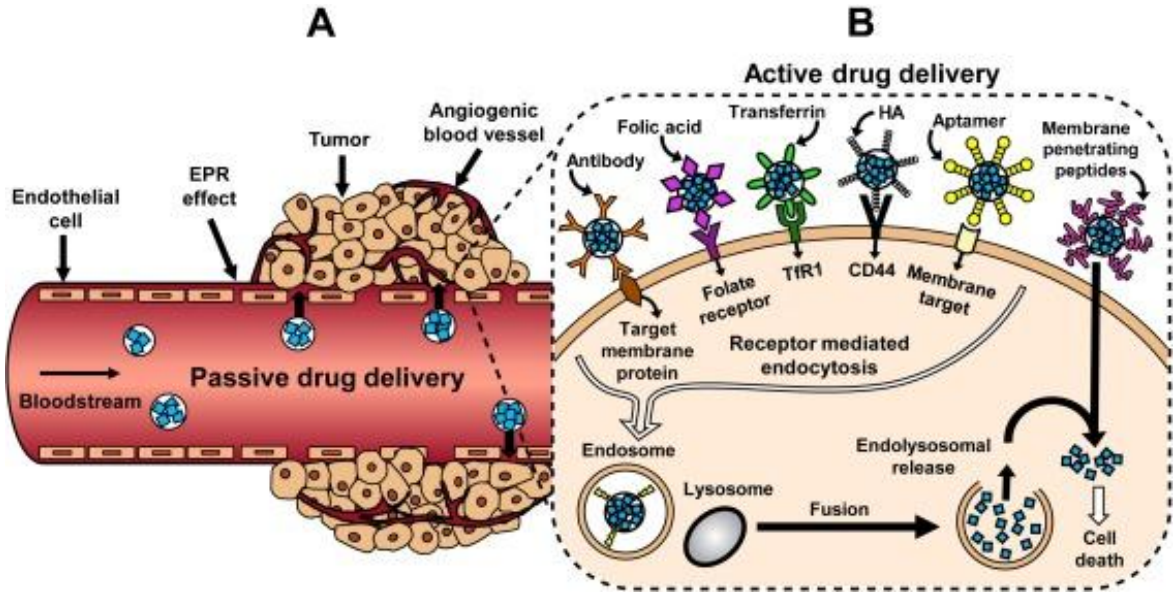

Figure 1.9 Representation of passive and active tumor targeting approaches (Bar-Zeev, Livney, and Assaraf 2017).

1.5.2 Active tumor targeting

In active tumor targeting, the surface of the nanocarriers is fabricated with targeting ligands which usually binds to appropriate receptors expressed on the cancer cell. The ligand is selected which binds to the overexpressed receptors on the tumor cells or tumor vasculature and expressed at low level on normal cells. The targeting ligands helps in decreasing the adverse side effects by delivering the drug to the specific site of action, but also assists cellular internalization of the drug by receptor-mediated endocytosis, which is an energy dependent process needing a considerably lower concentration gradient across the plasma membrane than simple endocytosis. Active targeting ligands are either non-antibody ligands (peptidic or not) or monoclonal antibodies (mAbs) and antibody fragments (Köhler and Milstein 1975; Bannon-Peppas and Blanchette 2004; Sudimack and Lee 2000; Bellocq et al. 2003).

Some of the widely used ligands for active targeting of nanocarriers include transferrin, folic acid, biotin, hyaluronic acid, lactoferrin, angiopep, cyclic RGD peptide etc. The delivery of anti-cancer molecules was efficient with improved therapeutic activity and reduced side-effects when they are targeted actively to the cells. Transferrin receptor (TfR) is one of the over-expressed receptors in fast growing cells. It is about 10 times over-expressed in cancer cells in comparison to normal cells. In one study, greater accumulation of paclitaxel at the tumor site was reported when polymeric nanoparticles were modified with transferrin on the surface. Another important target for active-targeting is the Folate receptor which is overexpressed in various cancers, such as malignancies of the ovary, brain, kidney, breast, myeloid cells and lung. Folic acid is a crucial vitamin required for the biosynthesis of nucleotide bases and is ingested in higher amounts by rapidly proliferating cells (Leamon and Reddy 2004).

In another study, Trastuzumab, a monoclonal antibody which binds to human epidermal growth factor 2 (HER2) was tagged to PAMAM dendrimers for active delivery of paclitaxel. The trastuzumab conjugated dendrimers were proved to deliver paclitaxel in an efficient way (Ma et al. 2015).

Biotin is example of small molecule targeting agent which offers many advantages over large peptides in terms of uptake and immunogenicity. It is essential in role of cell growth and metabolic reactions. Biotin receptors are over-expressed in various cancers in comparison to normal cells. SN-38, a camptothecin derivative showed pronounced uptake in cancer cells on biotinylation of nanocarrier system (Mehdizadeh et al. 2017; Nateghian et al. 2016).

Vega et al. reported the monoclonal antibody-based targeting of micelles in treatment of cancer (Vega et al. 2003). The epidermal growth factor receptor (EGFR), a transmembrane glycoprotein with an intracellular tyrosine kinase domain, which is

overexpressed on the cells of more than one-third of all solid tumors, was targeted with the mAb C225 (Wen et al. 2001). As this mAb attaches to the outer domain of EGFR, it is more suited for actively delivering the micellar carriers to a variety of cancers (Mendelsohn 1997). When cancer cells clump and reach a size of about 2-3 mm, flow of oxygen and nutrients to the cancer is suppressed. This causes induction of tumor angiogenesis allowing tumors to develop past their diffusion boundary (Greish 2007). The regulators of this process can be exploited to target drugs and inhibit angiogenesis to inhibit further tumor progression. Active targeting to αvβ3 integrin with the micelle-conjugated cyclic pentapeptide c(Arg-Gly-Asp-d-Phe-Lys) (cRGDfK) was explored by Nasongkla *et al*. (Nasongkla et al. 2004).

1.5.3 Intracellular Targeting

In order to elicit the desired pharmacological effects, drug molecules are required to be efficiently localized in specific location or organelle of the cell. This is also a pre-requisite to boost the efficacy and efficiency of drug treatment, and decrease the unwanted effects. For example, targeting nucleus for gene and antisense therapy, mitochondria for pro-apoptotic drugs, lysosomal compartment for lysosomal enzymes, cytoplasm for siRNA and mRNA to elicit their biological activity (Cerrato, Künnapuu, and Langel 2017). One such approach of intracellular targeting to specific organelles can be achieved by special class of peptides called cell penetrating peptides.

1.5.3.1 Cell penetrating peptides

A major issue with chemotherapy is the ineffective penetration of drug molecule in the tumor (Ruoslahti 2017). Penetration into cancer tissue is a noteworthy concern with nanoparticle drugs as well. To understand why this happens, we need to look the anatomy of a tumor. The tumor environment is made of dense connective tissue stroma which does

not allow free movement of drug molecule into the tumor cells (Ruoslahti 2017; Uchida et al. 2011). Moreover, the leaky vasculature in the tumor forms a high osmotic pressure zone within the tumor not allowing fluid to penetrate in, and hence, the chemotherapeutics cannot enter freely. Due to all of this, the tumor cells towards the core of the tumor receive little to no drug at all.

As a result of this, the cells receiving little drug concentrations are prone to becoming drug resistant over multiple drug administrations (Ruoslahti 2017). This situation can be addressed efficiently by using a class of peptides called cell penetrating peptides (CPPs).

CPPs are short chain peptides which contain 7-30 amino acid residues and are usually positive in net charge at physiological pH. These peptides are also called membrane translocation sequences (MTSs), Protein transduction domains (PTDs), or Trojan peptides. The first and foremost advantage of CPPs is their capability to deliver cargos through the cell membrane, which are many times higher than their own molecular weight. CPPs can be either cationic or amphipathic. Tat and Penetratin are the first discovered CPPs for their cell penetrability. More than 100 peptides were reported till date to possess the similar properties. Most of the CPPs are cationic, assume amphipathic structures and are rich in lysine and arginine residues (Hackett 2012).

CPPs can be broadly classified into three categories- primary amphipathic, secondary amphipathic, and non-amphipathic peptides. The primary amphipathic CPPs usually contain greater than 20 amino acids and are made of sequential hydrophilic and hydrophobic amino acids. They internalize into the cell by endocytosis as well as direct translocation through the cell membrane. The secondary amphipathic CPPs are generally shorter than the aforesaid peptides. The non-amphipathic CPPs are shortest of all and are capable of penetration into cells merely based on their cationic nature (Hackett 2012).

The mechanism of cellular internalization primarily is the endocytosis. It was debated that CPPs use clathrin/caveolin mediated endocytosis, macropinocytosis as a mode of entry. The cationic CPPs rich in arginine (poly-arginines) were reported to establish electrostatic interactions and hydrogen bonding between the guanidine group of arginine and the negatively charged cell membrane (like heparin sulphate proteoglycans, phosphates or carboxylates) before undergoing endocytosis or macropinocytosis (Papadopoulou and Tsiftsoglou 2013; Shin et al. 2014). The mechanism of internalization largely depends on the nature of CPP employed such as its length, charge, amphiphilicity along with the properties of cargo being transported. It further depends on the type of cell target and the CPP to cell ratio employed (Papadopoulou and Tsiftsoglou 2013).

In general, CPPs have only the arginine residues common and peptides comprising of only arginine resides were highly effective in terms of membrane translocation (Futaki et al., 2001a). The properties of CPPs such as inertness, low toxicity, and low immunogenicity (Torchilin et al., 2003; Jarver and Langel, 2004) make them preferred approach to improve cell penetration of cargoes.

Also, these peptides can effectively deliver a variety of cargoes to intracellular and even intranuclear compartment in almost all the exposed cells within minutes. They enhance the circulation of the active agent within the tumor due to their penetrability. CPPs can be used to enhance drug efficacy to the tumor or impart a dose-sparing effect largely reducing the drug side effects.

Among polyarginines, the optimum number of arginine residues needed for maximum activity was shown to be around 8 (Deshpande et al. 2018). A reduction in the activity was reported for polyarginines longer or shorter arginine residues than 8. Therefore, the CPP, octa-arginine (R8) can be regarded as a basic or a proto-type of the protein

transduction domains. It was hypothesized that the uptake mechanism of CPP conjugated systems depends on the peptide density attached to the surface of the cargo (Khalil et al. 2008, 2006). Khalil *et al.* Studied that the mechanism of cellular internalization of liposomes modified with a low R8 density shifted from clathrin-mediated endocytosis to macropinocytosis when the density of R8 was increased (Koshkaryev, Piroyan, and Torchilin 2013; Khalil and Harashima 2018). Further, PEGylation of CPP-cargo system shields the delivery system from the proteolytic enzymes in blood circulation. This improves the half time of the system by reducing the filtration by kidneys due to increase in size (Koren and Torchilin 2012). R8 was studied for its ability to improve the anti-cancer drug delivery by various research groups.

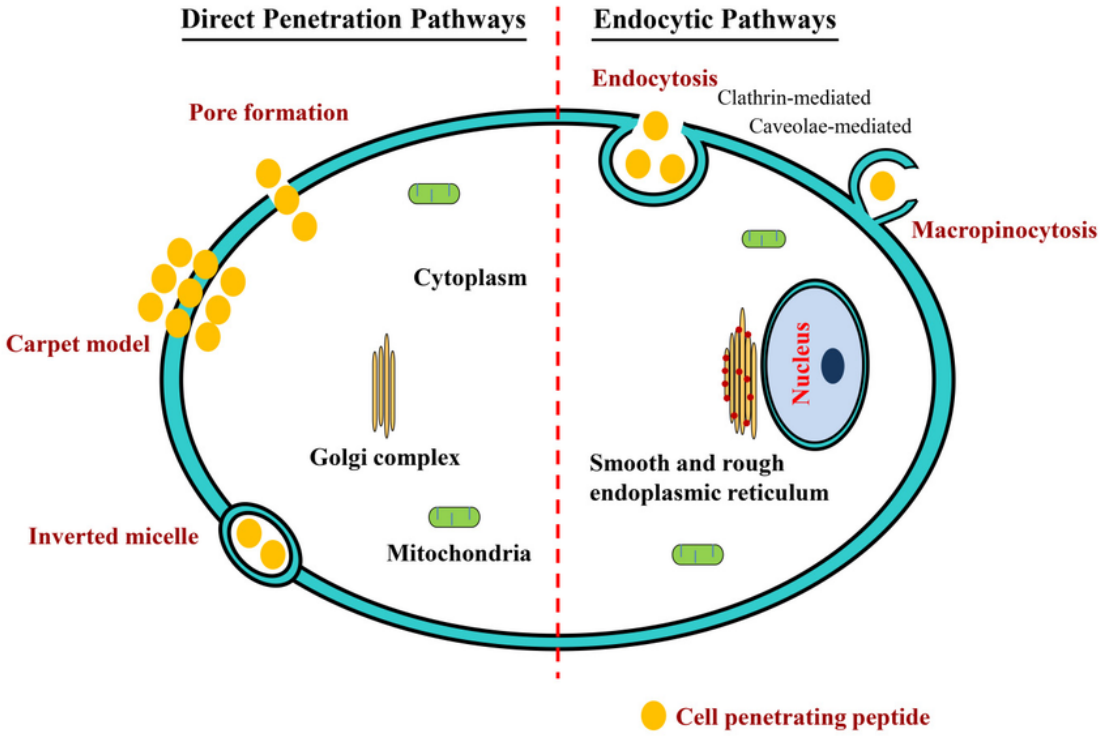

Figure 1.10 Mechanism of cellular internalization of cell penetrating peptides (Layek, Lipp, and Singh 2015).

Biswas S. *et al.* have worked on surface functionalization of doxorubicin loaded liposomes using octa-arginine for enhanced anti-cancer activity. Arg8 was conjugated to PEG-DOPE co-polymer. The modified liposomes significantly improved the intracellular and intratumoral delivery of doxorubicin as studied by flow cytometry and confocal laser scanning microscopy (Biswas, Dodwadkar, et al. 2013).

Dubikovskaya *et al*. conjugated octa-arginine (Arg8/R8) to taxol, an anticancer drug, via a disulfide bond, which exhibited the effect of preferentially unloading taxol inside the cells. Both R8-taxol and taxol alone were tested against ovarian cancer models with OVCA-429 (taxol-sensitive) or OVCA-429T (taxol-resistant) cells implanted in the peritoneal cavity of mice. The results indicated that R8-taxol and taxol had comparable effects against taxol-sensitive tumors. On the other hand, when studied against a taxol-resistant cancer model, R8-taxol administered mice had significantly higher survival rates in comparison to only taxol treated mice (Shin et al. 2014; Dubikovskaya et al. 2008).

P.Deshpande *et al.* have formulated a dual functional liposomal system with transferrin and octa-arginine as the surface ligands for delivery of doxorubicin. The dual targeted carrier was found to be more effective in delivering to tumor cells than the free drug (Deshpande et al. 2018).

In another study, Y Cui et al. have developed a reduction degradable polymeric micelles system which was decorated with polyarginine to deliver doxorubicin to the cancer cells. The polyarginine tagged micelles were observed to be localized more in the tumor due to the cell penetrating activity of polyarginine (Cui et al. 2016).

Table 1.1 List of Cell Penetrating Peptides (CPPs) explored in research (Papadopoulou and Tsiftsoglou 2013)

CPP	**Origin**	**Aminoacid (aa) Sequence / Physicochemical nature**	**Length (aa)**
TAT	HIV-1 TAT (transactivator factor of transcription)	YGRKKRRQRRR Cationic peptide	11
Penetratin (Antp)	*Drosophila* homeotic transcription factor encoded by *antennapedia* gene	RQIKIWFQNRRMKWKK Amphipathic peptide	16
VP22	herpes simplex virus VP22 transcription factor	DAATATRGRSAASRPTERPR APARSASRPRRPVD Amphipathic peptide	35
poly-Arginines	chemically synthesized	R7, R8, R9 Cationic peptides	9 / 8
Transportan	galanin -mastoparan	GWTLNSAGYLLGKINLKALA ALAKKIL Chimeric - Amphipathic peptide	27
TP10	truncated form of Transportan	AGYLLGKINLKALAALAKKI L Chimeric - Amphipathic peptide	21
pVEC	Vascular Endothelial (Ve) - Cadherin	LLIILRRRIRKQAHAHSK Amphipathic peptide	18
Pep-1	Trp-rich motif-SV40 NLS	KETWWETWWTEWSQPKKK RKV Chimeric - Amphipathic peptide	21
C105Y	peptide based on the residues 359-374 of alpha1-antitrypsin	CSIPPEVKFNKPFVYLI Amphipathic peptide	17
PFVYLI	derived from the synthetic peptide C105Y	PFVYLI Hydrophobic peptide	6
CADY	chemically synthesized, combining aromatic (W) and cationic (R) residues	GLWRALWRLLRSLWRLLWR A Amphipathic peptide	20
CAPHs	chemically synthesized with cationic amphiphilic polyproline helices	P11LRR to P14LRR Cationic - Amphipathic peptides	14 to 17

1.6 Dendrimers

Dendrimers are expected to be one of the more useful nanodrug delivery systems to date. Dendrimers are a unique class of nanostructured, hyperbranched polymers that possess a narrow mass and poly-dispersity (Layek, Lipp, and Singh 2015). They have tree-like architecture with exponential number of branches radiating from the core.

The term ‘‘dendrimer’’ is coined from two greek words, ‘dendron’, meaning tree, and ‘meros’, meaning part. Prof. Tomalia and his group developed the first class of dendrimers. Size of the dendrimers is mainly dependent on the number of layers of branching called generations. They confer a spherical shape with internal solvent-filled void cavities which can be used for drug encapsulation. The surface groups of dendrimers offer an advantage to perform for wide range of chemical modifications as per the requirement (Sharma, Gautam, and Gupta 2011).

Dendrimers consist of three basic parts: A central core, branches and, the terminal functional groups (Kesharwani, Jain, and Jain 2014). They are highly symmetric functional polymers and can be tailored to deliver a wide variety of molecules to the target site by either physical encapsulation or chemical conjugation onto the surface which make them suitable drug carriers (Menjoge, Kannan, and Tomalia 2010). Modification of branches or end groups can be performed to alter their permeability properties or toxicity.

Dendrimers are effectively being utilized in delivery of vaccines, drugs (small molecules and peptides), and genes. They have applications in solubilization of poorly soluble drugs, gene therapy, drug delivery, immunoassays, imaging and diagnosis. Dendrimers have been explored for administration of nanodrug formulations cutaneously, intravenously, orally, rectally, and vaginally and were found to be well tolerated.

Dendrimers can be synthesized from monomers following different strategies majorly: Divergent synthesis, Convergent synthesis, Self-assembling synthesis, Lego chemistry, and Click chemistry (Menjoge, Kannan, and Tomalia 2010).

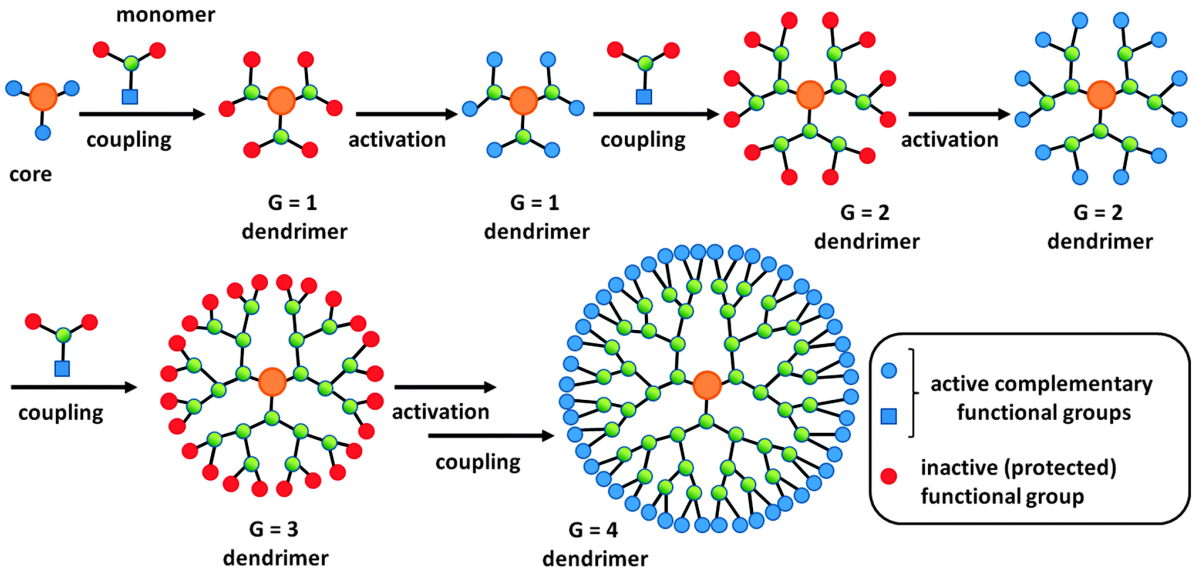

Figure 1.11 Divergent method of dendrimer synthesis (Sowinska and Urbanczyk-Lipkowska 2014)

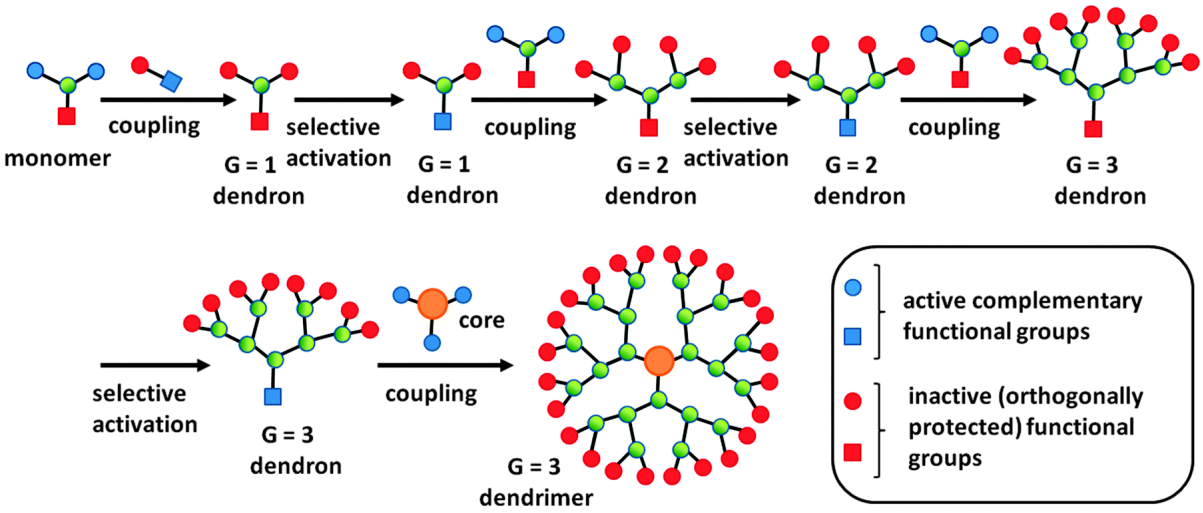

Figure 1.12 Convergent method of dendrimer synthesis (Sowinska and Urbanczyk-Lipkowska 2014).

1.6.1 Types of dendrimers

There are different families of dendrimers which serve multiple applications in environmental, industrial, and medical fields.

They are: Poly(amidoamine-organosilicon) dendrimers (PAMAMOS), Poly(amidoamine) dendrimers (PAMAM), Poly(propylene imine) dendrimers (PPI), Poly(ethylene imine) dendrimers (PEI), Poly(etherhydroxylamine) dendrimers (PEHAM), Poly(L-glutamic acid) dendrimers, Melamine dendrimers, Chiral dendrimers, Liquid crystalline dendrimers, Tecto dendrimers and, Hybrid dendrimers (Pourianazar, Mutlu, and Gunduz 2014; Menjoge, Kannan, and Tomalia 2010).

1.6.2 PAMAM dendrimers

The first dendrimer class to be available commercially was PAMAM dendrimers (STARBURST PAMAM) invented by Tomalia group. They are the widely referenced and well characterized family of dendrimers in the literature for biomedical applications. PAMAM dendrimers consist of initiator core, symmetric branches leading to terminal functional groups on the surface. Each branching unit is termed a generation (G). For the PAMAM series, the molecular diameter increases by about 1 nm with each generation and ranges from1.1 to 12.4 nm as they multiply from generations 1 to 10 (Menjoge, Kannan, and Tomalia 2010). The shape of the dendrimers is affected by the number of generations. They take the elliptical shape at lower generations which becomes spherical with increase in each generation. The number of generation also affects the molecular weight, size, and the number of surface groups.

PAMAM dendrimers commercially available have multiple options for core materials which includes ethylenediamine, diaminobutane, diamonododecane, diaminohexane, and cystamine. The terminal groups on surface can be of hydroxyl, carboxylic acid, or amine

functionality. One of the major advantages of PAMAM dendrimers is their spherical, globular structure resembling endogenous proteins (Pourianazar, Mutlu, and Gunduz 2014). This architecture allows its uptake and circulation in the body.

Table 1.2 Table showing different generations of PAMAM dendrimers and their characteristics (Tomalia 2005).

Generation	No. of terminal groups	molecular weight	diameter (nm)
0	4	609	1.5
1	8	1,522	2.2
2	16	3,348	2.9
3	32	7,001	3.6
4	64	14,307	4.5
5	128	28,918	5.4
6	256	58,140	6.7
7	512	116,585	8.1

1.6.3 PEGylated PAMAM dendrimers

Although PAMAM dendrimers have significant advantages in drug delivery, it also has some limitations because of its cationic nature. This high positive charge on the surface of dendrimers results in their interaction with cell membranes and causes toxicity (Jain et al. 2010). However, the toxicity is dependent on the generation of dendrimer and concentration. Modifying the surface of dendrimer masking the positive charge can significantly reduce the toxicity of dendrimers. Fortunately, there are various strategies investigated to overcome the cytotoxicity and hemolytic toxicity of dendrimers without losing their properties (Kesharwani, Jain, and Jain 2014).

Conjugation of surface groups with polyethylene glycol chains is called PEGylation and is an effective and simple way to minimize the toxicity of cationic dendrimers. PEG is a non-toxic, non-immunogenic polymer which enhances the circulation time and biocompatibility of PAMAM dendrimers in the body. Reduction in the overall positive charge by PEGylation prevents the interaction of dendrimers with RBCs and hence can significantly decrease hemolytic toxicity (Luong et al. 2016). Acetylation, glycolsylation, amino acid or peptide conjugation, DNA/gene/antibody conjugation are additional methods to reduce the toxicity.

PEGylated PAMAM dendrimers are one of the most efficient carrier systems for delivery of chemotherapeutic drugs to tumor site. It also helps improve the biodistribution and pharmacokinetics due to its stealth nature of avoiding opsonization and macrophage uptake (Layek, Lipp, and Singh 2015). Higher drug loading, and controlled drug release property was observed with PEGylated PAMAM dendrimers. PEG can also be used as a linker to attach drugs/targeting ligands to the terminal groups avoiding steric hindrance (Luong et al. 2016). It also improves solubility of drugs, and increases drug loading capacity. Further, partial conjugation of PEG on the nanoconjugates imparts optimal cationic charge for cellular association and help in endocytosis of PEG-PAMAM conjugates (Kesharwani, Jain, and Jain 2014).

PEGylation acts as a shield and reduces the interaction of enzymes which degrades the loaded drug/genes/peptides. Based on the above advantages, PEGylation is considered a mandatory step to deliver the anti-cancer molecules to tumor site in a safe and effective way.

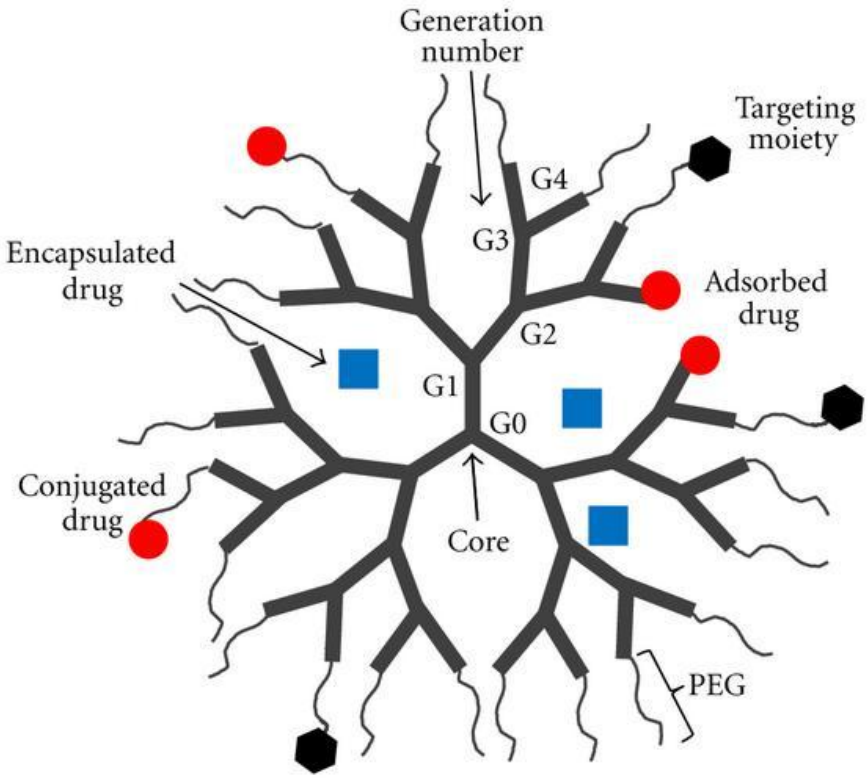

Figure 1.13 Fabrication of dendrimers for targeting and delivery of drugs by surface modification or physical entrapment (Lee and Nan 2012).

1.6.4 PAMAM dendrimers in drug delivery

PAMAM dendrimers of generation 3.0 to 5.0 are most widely explored for the delivery of drugs and macromolecules. PAMAM dendrimers offer wide choice of load to be delivered to the target site owing to its versatility in physical holding of drugs or chemical conjugation. In covalent linkage of drugs, the amount of drug conjugated can be tuned by the number of generations (which increases the length of the branching arms) and the release can be ensured by constructing easily cleavable drug – dendrimer linkage (Zhang and Chatterjee 2007). The benefits of dendrimers over polymer-drug conjugates in terms of solubility, release and penetration of drugs were reported by Mignani S *et al.* (Mignani et al. 2013).

In one study, G5 PAMAM-Biotin-FITC conjugated dendrimer was synthesized and characterized by ^{1}H-NMR and UV-Vis Spectroscopy. The confocal microscopy and flow cytometry studies revealed that the uptake of conjugate in HeLa cells was much higher than the conjugate without Biotin, which suggests the use of Biotin as a targeting ligand to deliver chemotherapeutic agents (Yang et al. 2009).

Sharma A *et al.* have synthesized a G4 PAMAM-Gallic acid conjugate and characterized using UV, IR, Mass and NMR techniques. Cytotoxicity study was done in MCF-7 cell line using MTT assay. The conjugate was found to have more efficacy and selectivity towards cancer cell when compared to normal cell (Sharma, Gautam, and Gupta 2011). In another study, for mitochondrial targeting triphenylphosphonium conjugated, acetylated, G5 PAMAM dendrimer has been synthesized. Acetylation was done to reduce non-specific interactions. FITC-conjugate was observed visually under fluorescence microscopy to assess its trafficking towards mitochondria. Results suggested that the conjugate efficiently targeted mitochondria and non-specific toxicity was also reduced (Biswas et al. 2012).

Biswas S. *et al.* investigated the use of dendrimer in SiRNA delivery. They have synthesized a triblock co-polymeric system, poly(amidoamine) dendrimer (generation 4)-poly(ethylene glycol)-1,2-dioleoyl-sn-glycero-3-phosphoethanolamine. Stable polyplexes were formed with excellent serum stability, cellular internalization and a significantly higher cellular uptake and transfection efficiency (Biswas, Deshpande, et al. 2013).

In another study Debnath *et al.* synthesized a dendrimer-curcumin conjugate which is water soluble. Cytotoxicity of the conjugate is assessed in SKBr3 and BT549 breast cancer cell lines using MTT assay. Results witnessed the enhanced efficacy of curcumin conjugated with dendrimer (Debnath et al. 2013).

Huihui Liao and Hui Liu along with their co-workers encapsulated Doxorubicin in PEGylated G5 PAMAM dendrimer. Methoxy PEG with COOH end group was conjugated to amine terminated G5 PAMAM dendrimer. The conjugate loaded with Doxorubicin was water soluble and stable. Cytotoxicity using MTT assay was performed in HeLa cells which was effective than unconjugated doxorubicin (Liao et al. 2014).

1.6.5 Paclitaxel

Paclitaxel (PTX) is a widely used anti-cancer agent which acts by hyperstabilization of spindle apparatus by polymerizing the tubulin. This disrupts the normal spindle dynamics leading to inhibition of cell division. It is a microtubule inhibitor. Paclitaxel blocks G2/M phase of cell cycle (Horwitz 1994). Paclitaxel was isolated from the bark extract of pacific yew tree Taxus brevifolia. It induces apoptosis by binding to and blocking the function of the apoptosis inhibitor protein Bcl-2 (B-cell Leukemia 2) (Wang et al. 2015).

Paclitaxel is approved for the treatment of Kaposi's sarcoma and cancers of lung, ovary, and breast. Inspite of its huge therapeutic potential, paclitaxel suffers serious limitations of poor aqueous solubility, lack of cancer specificity, and substrate to P-gp efflux proteins (Sarisozen, Abouzeid, and Torchilin 2014). In order to overcome low aqueous solubility of PTX, formulations based on Cremophor EL (e.g. Taxol®) were developed and administered via slow intravenous infusion following dilution with normal saline (0.9% NaCl) or dextrose (5%) solutions. However, Taxol® exerts serious adverse effects such as neurotoxicity and nephrotoxicity because of the excipient Cremophor EL which was used to solubilize PTX (Yuan et al. 2016). Consequently, Cremophor EL-free formulations of PTX have been investigated and attempts to improve its therapeutic efficacy were made by incorporating PTX in different nanocarrier systems.

Numerous trials were reported to improve the solubility and efficacy of PTX. The C2′ position of PTX has been extensively explored for the development of prodrugs which enhance the water solubility and anticancer activity. "Taxoprexin" (PTX-docosahexaenoic acid) and "Opaxio" (poly-L-glutamic acid-PTX) are two C2 conjugates of paclitaxel which are currently under clinical trials (Ojima et al. 2016).

1.6.5.1 Physicochemical properties of paclitaxel

Paclitaxel ($C_{47}H_{51}NO_{14}$; molecular weight: 853.9 g/mol), is a cyclodecane derivative isolated from the bark of the Pacific yew tree, *Taxus brevifolia* aand other *Taxus spp*. Sold under the brand name Taxol®, it is a fine, white to off-white crystalline powder which is poorly soluble in water. Paclitaxel is soluble in alcohols (methanol: 50mg/ml; ethanol: 1.5mg/ml) and DMSO (50mg/ml). Paclitaxel is rapidly degraded in weakly alkaline, aqueous solutions with minimum degradation observed between pH 3–5.

Paclitaxel melts at 213°C and has a logP~3, with the UV absorption maxima at 227 nm. The chemical structure of paclitaxel is shown in Figure 1.14. It has 4 hydrogen bond donors and 14 hydrogen bond acceptors ("National Center for Biotechnology Information, PubChem Compound Database; CID=36314").

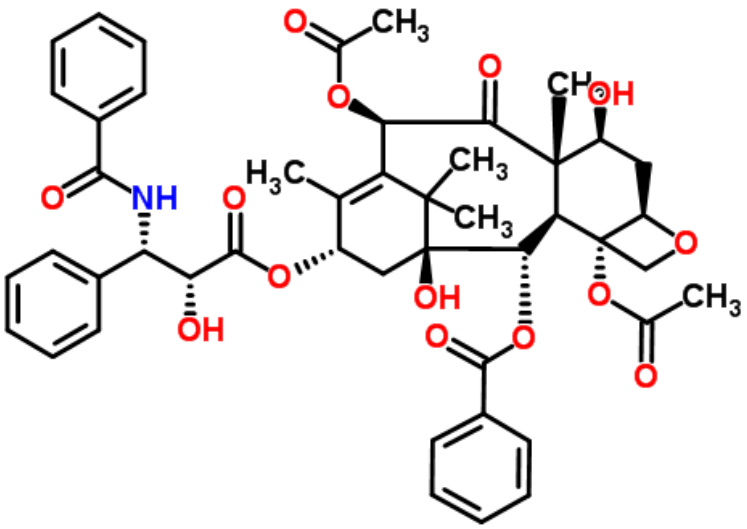

Figure 1.14 Chemical structure of Paclitaxel

IUPAC name : (2α,5β,7β,10β,13α)-4,10-Diacetoxy-13-{[(2R,3S)-3-(benzoylamino)-2-hydroxy-3-phenylpropanoyl]oxy}-1,7-dihydroxy-9-oxo-5,20-epoxytax-11-en-2-yl benzoate

1.7. Objectives

The main objective of the proposed research was to synthesize and evaluate multifunctional PAMAM dendrimer conjugates for delivery of an anti-cancer agent, paclitaxel (PTX). The clinical application of PTX has several limitations because of its poor solubility, non-specific distribution, and drug efflux by P-gp transporters. This attempt was made to overcome the aforementioned problems by delivering PTX intracellularly. To that end, PAMAM dendrimer – PTX conjugate was prepared, PEGylated, and anchored with octa-arginine (a CPP), or Biotin (a targeting moiety) for effective delivery to cancer cells. The major objectives and specific aims of this thesis are:

Objective 1: To synthesize octa-arginine (R8) conjugated multifunctional G4 PAMAM dendrimer system to deliver PTX.

Specific aims:

(i) To synthesize G4 PAMAM-PTX conjugate with help of succinate linker.

(ii) To PEGylate G4 PAMAM-PTX which yields G4 PAMAM-PTX-PEG.

(iii) To anchor cell penetrating peptide octa-arginine (R8) to G4 PAMAM-PTX-PEG.

(iv) To characterize the conjugates using ^{1}H NMR, zeta potential, and GPC analysis.

(v) To evaluate synthesized conjugates *in vitro* in cancer cell monolayers.

(vi) To evaluate the efficacy of the multifunctional dendrimer conjugate in 3D tumor cell spheroids.

Objective 2: To develop biotin tagged multifunctional G4 PAMAM dendrimer system to deliver PTX.

Specific aims:

(i) To synthesize G4 PAMAM-PTX conjugate with help of succinate linker.

(ii) To PEGylate G4 PAMAM-PTX which forms G4 PAMAM-PTX-PEG.

(iii) To anchor targeting ligand, Biotin to G4 PAMAM-PTX-PEG.

(iv) To characterize the conjugates using ^{1}H NMR, zeta potential, and HABA assay.

(v) To evaluate synthesized conjugates *in vitro* in cancer cell monolayers.

(vi) To evaluate the efficacy of the multifunctional dendrimer conjugate in 3D tumor cell spheroids.

Chapter 2

Octa-Arginine Modified Poly(Amidoamine) Dendrimers for Improved Delivery and Cytotoxic Effect of Paclitaxel in Cancer

2.1 Abstract

Cell penetrating peptides (CPP) have the ability to penetrate the cell membrane and have been associated with various cargos for their facile intracellular translocation. The current study involves the synthesis of a CPP, octa-arginine (R8)-modified poly(amidoamine) dendrimer of generation 4 (G4), which has additionally been PEGylated and conjugated to the poorly soluble anticancer drug, paclitaxel (PTX). The synthesized dendrimer conjugates were characterized by ^{1}H NMR and zeta potential measurements and evaluated *in vitro* in cell monolayers and 3D spheroids. Cellular uptake study in human cervical cancer cell line (HeLa) revealed that R8 modification significantly improved the cell association of conjugates. G4-PTX-PEG-R8 conjugate demonstrated enhanced cytotoxic potential and higher induction of apoptosis compared to free PTX and G4-PTX-PEG. Further, the penetrability of fluorescently labeled F-G4-PTX-PEG-R8 was evaluated in 3D spheroids of HeLa at various depths by using confocal microscopy. G4-PTX-PEG-R8 induced cell death and inhibited the growth in 3D spheroids as competently as in monolayers. The enhanced intracellular translocation of R8-modified dendrimers resulted in improved anticancer efficacy of PTX. Therefore, the newly developed dendrimer system is efficient for the intracellular delivery of PTX in cancer cells and has a strong potential to be utilized as an effective chemotherapeutic agent for cancer.

2.2 Introduction

Cancer is considered as one of the world's most life-threatening diseases with millions of new cases reported every year (Cui et al. 2016; Estanqueiro et al. 2015). Even though the extensive research has resulted in advanced understanding of cancer, development of more sensitive detection methods, and invention of chemotherapy drugs with superior efficacy compared to previous discoveries, the ability to deliver the drug molecules to the tumor tissue, and specifically to the intracellular compartment of the cancer cells remains a challenge (Shin et al. 2014). The conventional cancer chemotherapy suffers disadvantages such as low solubility, poor permeability, fast clearance, non-specific toxicities, poor biodistribution, and emergence of multiple drug resistance due to chronic drug exposure, which leads to meager therapeutic response and patient incompliance (Kesharwani and Iyer 2015). To address the above concerns, nano drug delivery systems have attracted great interest due to the wide range of benefits they offer and significant progress has been achieved in taking these systems into clinic (Ma et al. 2015). Various nano-sized systems such as liposomes, polymeric micelles, lipid nanoparticles, nano-structured lipid carriers, drug conjugates, dendrimers, and nano-suspensions have been proven to efficiently target and deliver the active moieties to cancer either passively or actively (Shin et al. 2014; Kulhari et al. 2016; Estanqueiro et al. 2015; Akhter et al. 2017; Zhou et al. 2017).

Dendrimers are a class of three-dimensional tree like branched polymers in nanometer size range, monodisperse in nature and highly ordered structure with a central core branching out to a choice of functional groups at the periphery (Kwak et al. 2015; Svenson and Tomalia 2012). Poly(amidoamine) dendrimers (PAMAM) gained reputation from the last decade due to their unique advantages over other delivery systems and have

been extensively used in delivery of small molecules, peptides, and genetic material in various disease conditions (Kesharwani, Jain, and Jain 2014). The empty internal cavities of the PAMAM dendrimer could physically hold the entrapped drugs whereas the surface groups (NH_2, OH, and COOH groups) can bind the molecules covalently (He et al. 2011; He et al. 2015; Ma et al. 2015; Singh et al. 2016). PAMAM dendrimers have been investigated for their efficiency in delivery of anti-cancer agents such as doxorubicin (Fu et al. 2014; Wang, Cao, et al. 2011), docetaxel (Kulhari et al. 2016), paclitaxel (Khandare et al. 2006), methotrexate (Jiang et al. 2010), 2-methoxy estradiol (Wang, Guo, et al. 2011) etc. effectively to tumor site either in physically entrapped or chemically conjugated form. Further, the availability of react-able functional groups on dendrimer surface allows them to be anchored by a variety of peptides/ligands/antibodies to target cancer cells (Zhu et al. 2014; He et al. 2015). In general, the nanocarrier systems passively enter the tumor tissue via leaky vasculature by a phenomenon known as enhanced permeation and retention (EPR) effect (Gillies and Frechet 2005; Cui et al. 2016; Rompicharla et al. 2017). However, following accumulation in the tumor microenvironment by EPR effect, the drug-loaded nanocarriers need to translocate through the cell membrane to reach the intracellular compartment to exert the therapeutic potential. The set back is usually the poor permeability of the nanocarriers through the cell membrane, which usually occurs via energy-dependent endocytosis (Biswas, Dodwadkar, et al. 2013).

Invention of cell penetrating peptides (CPPs) has offered great benefits in this regard and improves the cellular internalization of a variety of molecules (Kuwada et al. 2011; Kloß et al. 2009; Madani et al. 2011). CPPs are peptides consisting usually of less than 35 amino acid residues (Bolhassani, Jafarzade, and Mardani 2017). They have been explored in a wide variety of theranostic applications in cancer, including the intracellular delivery

of small anticancer drugs, macromolecules, and nanoparticle systems (Dissanayake et al. 2017; Liu et al. 2015; Li et al. 2016). Cationic peptides which are rich in arginine residues were employed as CPPs such as TAT peptide (TATp), penetratin, low molecular weight protamine (LMWP) and oligoarginines (Shin et al. 2014; Milletti 2012; Kang et al. 2014). Octa-arginine (R8), a short chain peptide having 8 arginine residues was investigated by many researchers and proved to be efficient in transporting a variety of cargoes into the cells (Yamada, Hashida, and Harashima 2015; Biswas, Deshpande, et al. 2013; Kitagishi et al. 2015). In the present study, we have synthesized a multifunctional PAMAM dendrimer conjugate of generation 4, which couples an anti-cancer agent Paclitaxel (PTX), polyethylene glycol (PEG) and a CPP, R8. The R8 modification was expected to promote intracellular translocation of the nano-construct allowing delivery of PTX in high concentration in the intracellular compartment for enhanced cytotoxic effect. The final conjugate and the intermediates were characterized, and were evaluated in the Human cervical cancer (HeLa) cell line in monolayers and 3D spheroidal system.

2.3 Materials and methods

2.3.1 Materials and cell lines

Dendrimer of generation 4 with ethylenediamine core and surface amino groups (G4 PAMAM) was purchased from Dendritech (USA). Paclitaxel (PTX) was obtained as a gift sample from Fresenius Kabi India Pvt., Ltd. (Gurgaon, India). Methoxy-polyethyleneglycol-succinimidyl carboxymethyl ester (mPEG-SCM ester, MW 2000 Da) was obtained from Jenkem Technology (USA). N-ethyldiisopropylamine (DIPEA) was obtained from Avra Chemicals, India. NHS-Fluorescein was obtained from Thermo Scientific (USA). Octaarginine (R8) peptide was custom synthesized from USV Limited (Mumbai, India). N-(3-Dimethylaminopropyl)-N′-ethylcarbodiimide hydrochloride

(EDC. HCl, 98%) and N-Hydroxysuccinimide (NHS, 98%) were obtained from Sigma Aldrich Chemicals (USA). Regenerated cellulose dialysis membrane (MWCO 2 kDa, 3.5 kDa and 14 kDa) was obtained from Spectrum Laboratories, Inc. (USA). N,N'-Dicyclohexylcarbodiimide (DCC) was purchased from Spectrochem Chemicals Ltd. (India). All the other chemicals and solvents obtained commercially were of analytical grade.

Human cervical carcinoma cells, HeLa were obtained from National Center for Cell Sciences (NCCS, Pune, India). DMEM (Dulbecco's minimum essential medium) supplemented with 10% FBS and 1% penicillin-streptomycin solution (Himedia Labs, Mumbai) was used as the growth medium. Cells were maintained in a humidified incubator at 37°C and 5% CO_2.

2.3.2 Synthesis of multifunctional PAMAM dendrimer

2.3.2.1 Synthesis of fluorescent labeled G4 PAMAM dendrimer

G4 PAMAM dendrimer was fluorescent tagged as per the previously described method with a slight modification (Biswas et al. 2012). Briefly, 100 mg of G4 PAMAM dendrimer was dissolved in DMF. NHS Fluorescein dissolved in DMF was added to the dendrimer solution (molar ratio 1:1) dropwise under inert atmosphere. The mixture was stirred for 8 h at room temperature in dark. DMF was removed under vacuum and the product was dialyzed for 48 h to remove the unattached NHS Fluorescein. The product was lyophilized and stored until further use. The scheme of synthesis of the modified dendrimer has been represented in Figure 2.1.

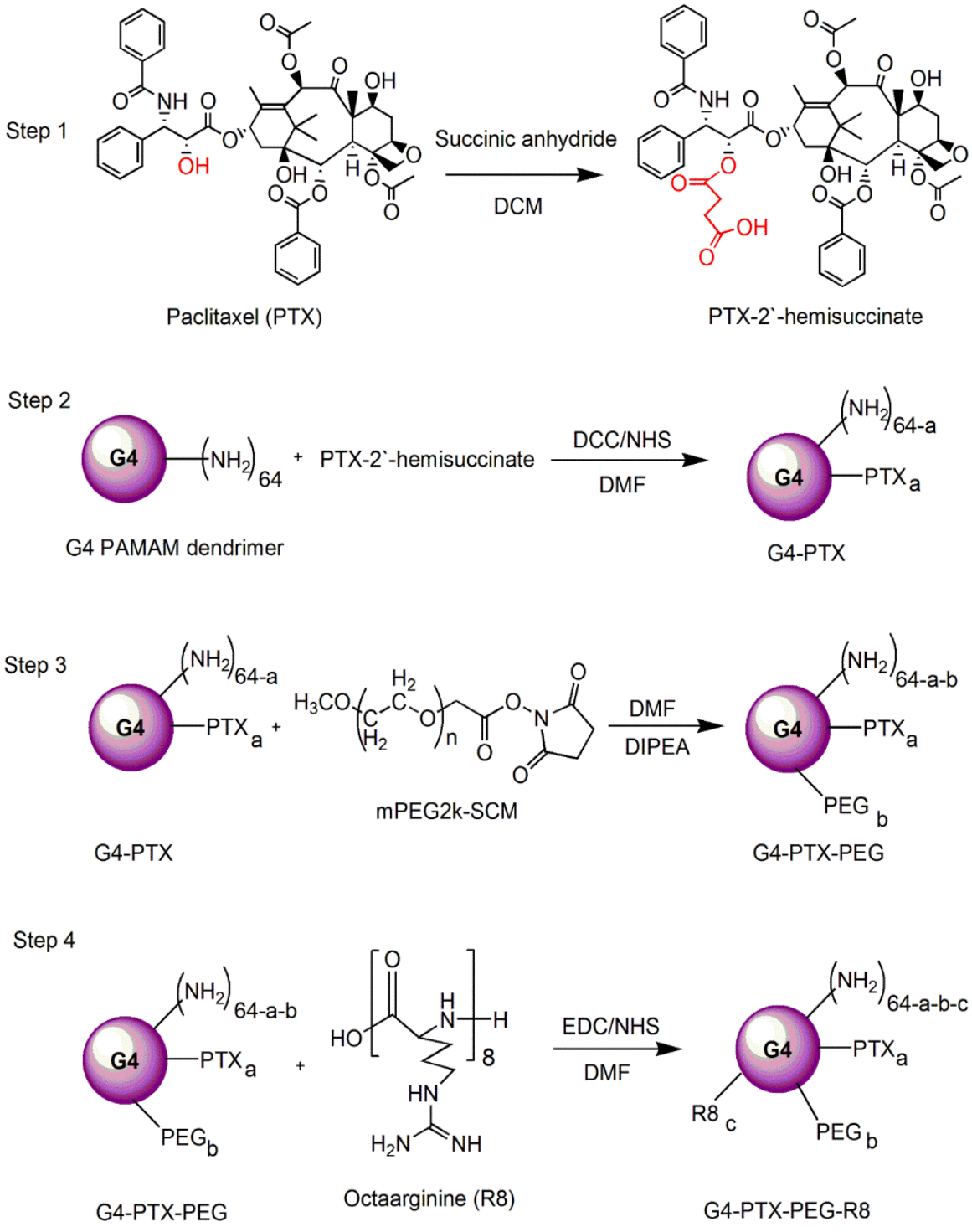

Figure 2.1 Schematic representation of step-by-step synthesis of multifunctional G4 PAMAM dendrimer conjugates.

2.3.2.2 Synthesis of G4-PTX

Paclitaxel has a 2`-OH group which was activated to hemisuccinate using succinic anhydride. Briefly, To 25 mg of Paclitaxel (PTX) in DCM, 4.4 mg of succinic anhydride (molar ratio of 1:1.5) was added under stirring in presence of dry pyridine and continued for 3 days [36]. After the reaction, product was extracted using ethyl acetate and vacuum dried to get the PTX-2`-hemisuccinate as white powder. PTX-2'-hemisuccinate was activated with DCC/NHS in DMF for 6-8 hours at room temperature to make it react readily with the amine terminals of G4 PAMAM dendrimer [37]. To the G4 PAMAM Dendrimer (50 mg) in DMF, activated PTX NHS ester (molar ratio of 1:4) was added drop wise under nitrogen. The reaction was continued overnight and the DMF was evaporated under vacuum. The formed product was dialyzed extensively for 48 h using 3500 Da MWCO dialysis membrane. A white fluffy solid of G4-PTX conjugate was obtained after lyophilization.

2.3.2.3 Synthesis of G4-PTX-PEG

To the synthesized G4-PTX conjugate, mPEG SCM ester of molecular weight 2 kDa was attached as described below. The mPEG SCM (molar ratio 12:1) in DMF was added under stirring to the solution of G4-PAMAM-PTX in a RBF. DIPEA (20 µl) was added as a base to the reaction mixture. The reaction was continued overnight and DMF was evaporated under vacuum. Reaction mixture was dialyzed for 48 h using 12-14 kDa MW cutoff dialysis membrane. Solid G4 PAMAM-PTX-PEG was obtained after lyophilization. The attachment of PEG to dendrimer was characterized and confirmed by change in zeta potential, proton NMR and GPC analysis.

2.3.2.4 Conjugation of octaarginine(R8) onto G4-PTX-PEG

Carboxy terminal of R8 was activated using EDC/NHS and was reacted with previously synthesized G4-PTX-PEG at a molar ratio of 3:1 in DMF. The final conjugate G4-PTX-PEG-R8 was collected as a solid after freeze drying following dialysis of the product after the reaction.

2.3.3 Characterization of multifunctional conjugate

All the synthesized conjugates were characterized by proton NMR (300 MHz, Bruker, USA) and zeta potential analysis. To determine the relative molecular weights of synthesized conjugates, gel permeation chromatography (GPC) analysis was performed. Zorbax GF-250 (9.4 mm ID X 25 cm X 4-4.5 µ) size exclusion analytical column was used to run the samples in a HPLC system (Agilent 1100 series). Tris buffer (50 mM) and KCl (100 mM) was used as eluting phase in isocratic mode at a flow rate of 1 ml/min. A calibration curve was plotted with the standard molecular weight compounds prior to analyzing the samples. Zeta potential of the conjugates was determined using a Malvern Zetasizer (Nano ZS, Malvern Instruments, UK).

2.3.4 Hemolytic toxicity study

Hemolytic toxicity study was performed to assess the safety of synthesized multifunctional conjugate, which was executed following a previously reported procedure (Kumari et al. 2017). Briefly, 5 ml of rat whole blood was collected in heparinzed vials from which erythrocytes (RBCs) were separated by centrifugation at 3000 rpm for 30 min. A 5% RBC suspension was prepared by diluting the cells with PBS after thorough washing.

Further, 100 µL of 5% RBC solution was incubated for 1 h at 37 °C with 900 µL of multifunctional dendrimer conjugate (without PTX) dissolved in PBS at 5 mg/ml and 10 mg/ml concentrations. Triton-X 100 (1% solution) and PBS were used as positive and negative control respectively. Following incubation, samples were centrifuged and the absorbance of Hemoglobin (Hb) in the supernatant was measured by microplate reader (Spectramax™, Molecular Devices, USA). The degree of hemolysis was calculated on the basis of Hb absorbance (Abs) at 576 nm and derived from the following formula:

$$\%\ Hemolysis = \frac{Abs_{sample} - Abs_{negative\ control}}{Abs_{positive\ control} - Abs_{negative\ control}}\ X\ 100$$

2.3.5 Confocal microscopy

To assess the internalization of multifunctional dendrimer conjugate visually, confocal microscopy was used. HeLa cells were seeded onto circular coverslips placed in 12-well culture plates at a cell population of 50,000 cells/well. Following day, F-G4-PEG and F-G4-PEG-R8 (20 µg/ml) were added to the wells and incubated at 37 °C for 1 h and 4 h. After the incubation period, cells were washed three times with sterile PBS, treated with DAPI (1 µg/ml) for 5 min, washed and fixed with 4% *para*-formaldehyde for 15 min. The coverslips were then mounted cell-side on the microscopic slides with the help of a mounting medium (Fluoromount-G). Slides were observed using confocal microscope (Leica DMi8, Leica Microsystems, Germany) and fluorescence images of cells were captured in FITC and DAPI filters. Picture files were processed using Image *J* software.

2.3.6 Cellular uptake by flow cytometry

The HeLa cells were seeded in 6-well microplates at a cell population of 0.6×10^6 cells/well and allowed for attachment of cells overnight. On the following day, F-G4-PEG and F-G4-PEG-R8 were added to the cells at a concentration of 20 µg/ml and

incubated for 1 h and 4 h at 37 °C. Post-incubation, cells were washed with PBS and then harvested. The cells were centrifuged and were re-suspended in PBS prior to analysis by flow cytometer (Amnis, EMD Millipore, USA). Cells without any treatment were used as control. For each sample, a minimum of 10,000 events were collected. The geo mean fluorescence of the cells was calculated from the IDEAS software V6.0.

2.3.7 Cytotoxicity Study

The cytotoxicity of free PTX, G4-PTX-PEG, and G4-PTX-PEG-R8 was determined by MTT assay. HeLa cells were seeded at a density of 10,000 cells/well in 96-well plates on the day before treatment. Formulations equivalent to a PTX concentration ranging from 0-50 µg/ml were added to the wells and incubated at 37 °C and 5% CO_2 for 24 h and 48 h. After the specified time interval, formulations were discarded and treated with 50 µl of MTT reagent (5 mg/ml solution). The 96-well plates were incubated for another 4 h, MTT reagent was removed, and DMSO (150 µl) was added to each well to dissolve the purple colored formazan crystals. The absorbance at 570 nm was measured using a microplate reader (Spectramax™, Molecular Devices, USA) keeping a wavelength of 630 nm as reference. Cells without treatment were used as control. Percentage cell viability was derived from the absorbance of sample against absorbance of control.

2.3.8 Apoptosis

AnnexinV FITC/PI double staining assay was carried out to determine the extent of induction of apoptosis in HeLa cells. Free PTX, G4 PTX PEG and G4 PTX PEG R8 were added to 6-well plates seeded with HeLa cells at a density of 0.6×10^6 cells/well and incubated for 24 h. The concentration of PTX in each formulation was equivalent to 25 µg/ml. The study was performed as per the manufacturer's protocol. After treatment, cells were harvested, washed with ice-cold PBS and suspended in 100 µl AnnexinV binding

buffer. Then, cells were stained with 5 µl AnnexinV and 10 µl PI solution and incubated at room temperature for 15 min. At last, 400 µl of AnnexinV binding buffer was added to the samples and analyzed using flow cytometer (Amnis, EMD Millipore, USA). Untreated cells were used as control for the study. Data was processed using IDEAS software version 6.0 and a scatter plot was plotted with green (FITC) channel on X-axis and red (PI) channels on Y-axis. The dot plot was divided into four quadrants representing live cells (Q1), early apoptotic (Q2), late apoptotic (Q3) and necrotic (Q4) cells.

2.3.9 Evaluation of multifunctional dendrimer conjugates in 3D spheroid model

2.3.9.1 Formation of HeLa spheroids

HeLa cancer cell spheroids were prepared by liquid overlay method (Sarisozen, Abouzeid, and Torchilin 2014; Perche and Torchilin 2012). Briefly, serum free MEM medium with 1.5% (w/v) agar was prepared and sterilized. 50 µL of the agar solution was added to the bottom of each well of the 96 well plates to prevent cell adhesion. In case of 8-well glass chamber slides, 200 µl of agar solution was added. Plates were allowed to cool down for 45 min before use. HeLa cells were harvested, counted and then seeded at a density of 8,000 cells per each well. Plates were centrifuged at 1500 rcf for 15 min at room temperature. The formation of spheroids was continuously monitored using an inverted microscope (Leica DMi8, Leica Microsystems, Germany). Spheroids of 3 – 5 days old were used in the further studies.

2.3.9.2 Penetration efficiency in 3D cancer cell spheroids

The penetration of F-G4-PTX-PEG and F-G4-PEX-PEG-R8 through the spheroids was evaluated by confocal microscopy after 1 and 4 h of incubation. Following that, the tumor spheroids grown in the 8-well glass chamber slides were washed with PBS and then

observed by laser scanning confocal microscope (Leica DMi8, Leica Microsystems, Germany). Z-stack images were obtained from the surface towards the tumor spheroid equatorial plane at 10 μm intervals of thickness. All images were taken using a 10X objective. Images were analyzed using Image *J* software.

2.3.9.3 Uptake of dendrimer conjugates in 3D spheroids by flow cytometry

Uptake of multifunctional dendrimer conjugates in 3D cultured spheroids was assessed quantitatively by flow cytometry. Five-day-old spheroids were incubated with F-G4-PEG and F-G4-PEG-R8 for 1 h and 4 h. At each time point, 10 spheroids were collected as one replicate to achieve sufficient cell count. The spheroids were washed with PBS and broken down using Accutase cell detachment solution. The cells were dispersed as a suspension and Accutase was neutralized with FBS. Then, cells were centrifuged again and re-suspended in PBS to further analyze them using flow cytometer. A minimum of 10,000 events were collected for each sample. Same instrument conditions were maintained to study the uptake in monolayers and spheroids. Geo mean fluorescence exhibited by F-G4-PTX-PEG and F-G4-PEX-PEG-R8 treated spheroids was plotted as a bar diagram.

2.3.9.4 Inhibitory effect on the 3D spheroids

The 3D spheroids were incubated with free PTX, G4-PTX-PEG, and G4-PTX-PEG-R8 at a PTX concentration of 25 μg/mL. Growth medium was replaced after 24 h. The media was further changed on alternate days. The extent of inhibition of growth in spheroids was observed under inverted microscope (Leica DMi8, Leica Microsystems, Germany) at 10X magnification and images were captured. The data is represented as mean diameter of three spheroids with standard deviation.

2.3.9.5 In vitro cytotoxicity in spheroids

Cytotoxicity imposed by various PTX formulations in 3D spheroids was studied using Presto blue assay following the manufacturer's instructors. Visually compact spheroids (typically 3-5 days after seeding) were treated with free PTX, G4-PTX-PEG, and G4-PTX-PEG-R8 (concentration: 25 μg/mL) for 24 h. A group of 10 spheroids were included for each treatment. After the treatment period, the spheroids were washed with PBS and added with 50 μL of cell detachment solution (Accutase^{TM}) and incubated for 10 min at 37 °C. After that, the spheroids were gently shaken and the resulting suspension was centrifuged at 1200 rpm for 5 min. Samples for analysis were prepared by re-suspending the cell pellet in 90 μL of growth medium and adding 10 μL of Presto Blue reagent. The samples were incubated at 37 °C for 2 h. The absorbance was measured at 570 nm using 600 nm as reference.

2.3.9.6 Live/Dead cell assay in 3D spheroids

To assess the distribution of live and dead cell population in the 3D spheroids after various PTX treatments, calcein blue assay was performed. Briefly, the spheroids were treated with free PTX, G4-PTX-PEG, and G4-PTX-PEG-R8 at a PTX concentration of 50 μg/mL. After the incubation period of 24 h, the spheroids were washed with PBS and stained with calcein blue AM reagent and propidium iodide (PI). Calcein blue AM ester passively diffuses into the cells and gets cleaved by the intracellular esterases in viable cells. The resultant calcein blue retains in the cell and emits blue fluorescence. Further, dead cells are stained by PI can be observed using red filter of fluorescence microscope (Leica DMi8, Leica Microsystems, Germany). Images were captured and processed using Image J software.

2.3.10 Statistical analysis

All experiments were performed in triplicate and data are expressed as mean ± SD. The statistical significance among the groups was established using Student's *t*-test using Graph Pad prism 5 (GraphPad Software, Inc.; San Diego, CA). Any value with *p* less than 0.05 were considered statistically significant. The representation of *, ** or ##, *** or ### in figures corresponds to *p* values < 0.05, 0.01 and 0.001, respectively.

2.4 Results and Discussion

2.4.1 Synthesis and characterization of multifunctional dendrimer conjugate

Activated PTX, which is PTX-2`-hemisuccinate was confirmed by Mass spectrometry. A Peak at 954.5 (MH+) and 976.5 (MNa+) was observed corresponding to the hemisuccinate form of PTX (Figure 2.2). The proton NMR of the final conjugates G4-PTX-PEG and G4-PTX-PEG-R8 was represented in Figure 2.5. In the NMR spectrum, peaks at δ (ppm) 7-8.5 correspond to the aromatic groups of the PTX molecule. The protons of PEG chains can be seen at δ (ppm) 3.2-4.1 and dendrimeric protons from δ (ppm) 1.5-3.5. The signal at δ (ppm) 1-1.5 relates to the methylene protons of R8. These signals confirm the structure of G4-PTX-PEG-R8. The reduction in the intensity of PTX signals could be due to formation of micellar structure of dendrimer in D_2O.

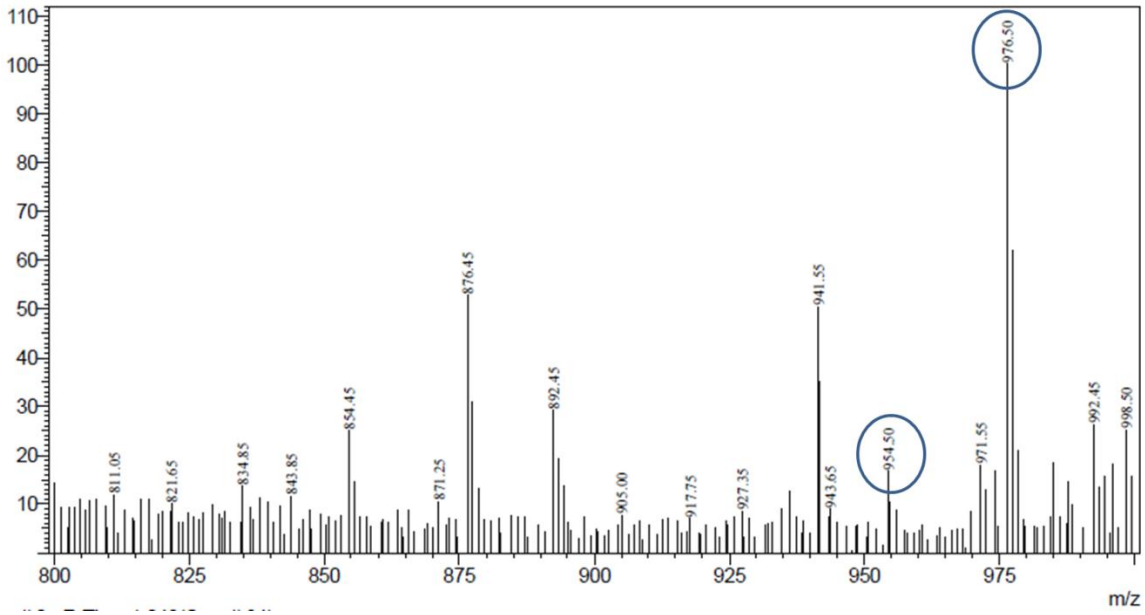

Figure 2.2 Mass spectrum depicting the m/z at 954.5 (MH+) and 976.5 (MNa+) corresponding to PTX-2'-hemisuccinate in positive ion mode.

Proton NMR spectra of intermediates is provided in Figure 2.3 and2.4.

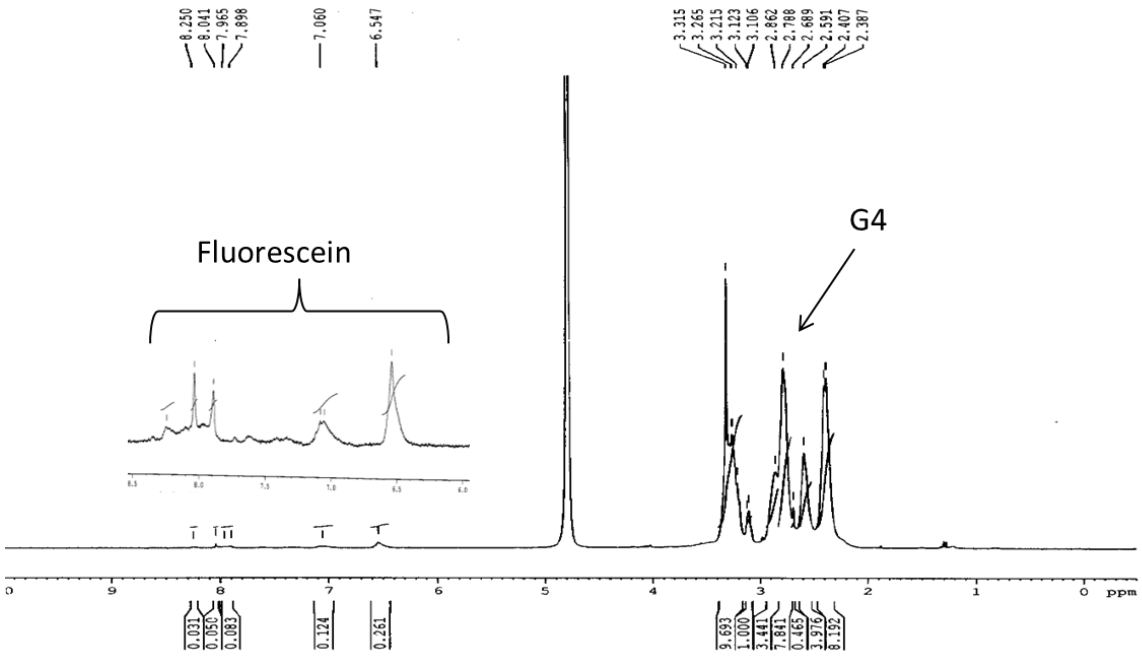

Figure 2.3 ^{1}H NMR spectrum of F-G4 in D2O at 300 MHz

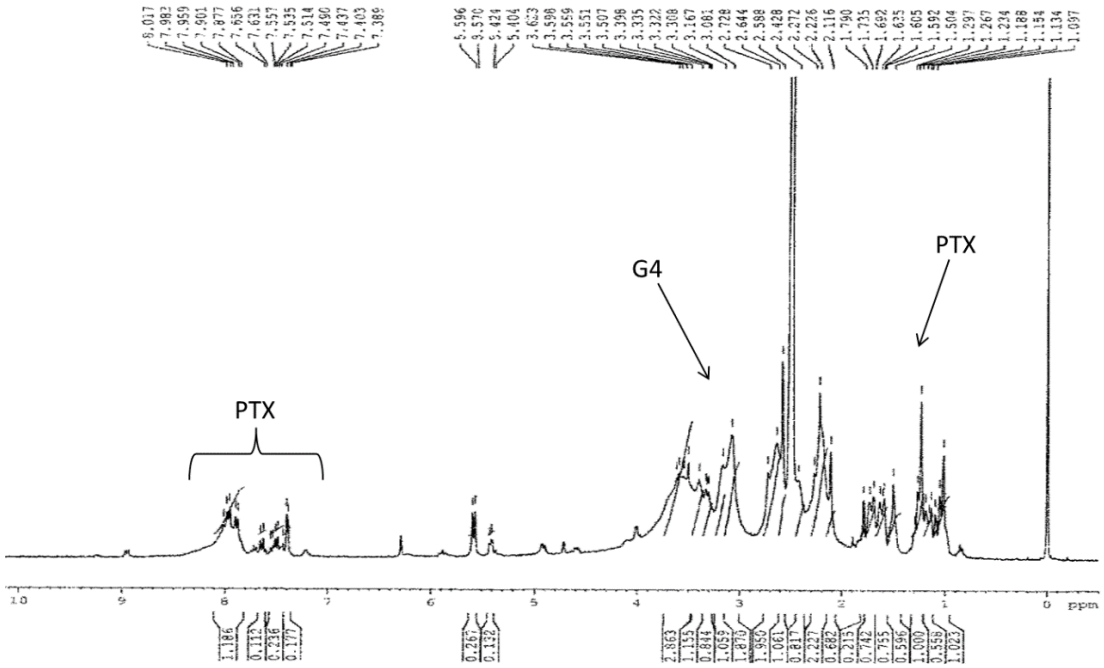

Figure 2.4 ^{1}H NMR spectrum of G4-PTX in d6-DMSO at 300 MHz.

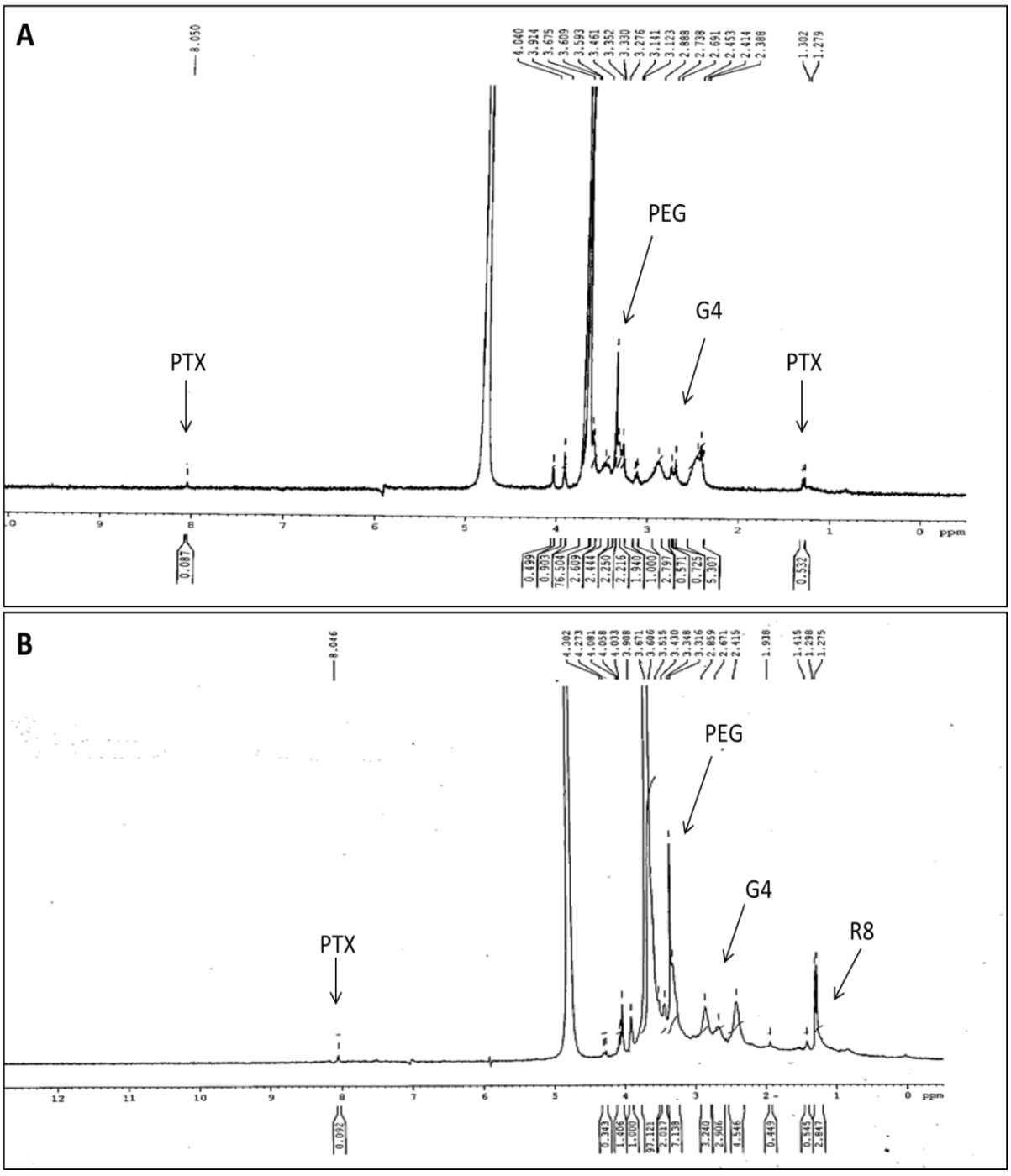

Figure 2.5 ^{1}H NMR spectrum of (A) G4-PTX-PEG and (B) G4-PTX-PEG-R8 in D2O at 300 MHz.

The relative molecular weight acquired from the GPC was used to calculate the approximate number of molecules attached to each dendrimer molecule. It was observed that approximately 2.5 molecules of PTX, 10.5 molecules of PEG and 1.8 molecules of R8 were attached to each G4 molecule (See Table 2.1). In addition, a change in the zeta potential value as shown in Table 2.2 at each synthesis step supports the formation of the conjugates.

Table 2.1 Relative mass and approximate number of molecules attached to each dendrimer as determined by GPC analysis.

Multifunctional Conjugate	**Relative Mass (Da)**	**No. of molecules attached approximately per each dendrimer**
G4	14843	-
G4-PTX	17263	2.53 of PTX
G4-PTX-PEG	38391	10.56 of PEG
G4-PTX-PEG-R8	40779	1.88 of R8

Table 2.2 Zeta potential values of multifunctional dendrimer conjugates (Mean±SD, n=3)

Dendrimer conjugate	**Zeta potential (mV)**
G4	16.4±0.93
G4-PTX	10.67±1.09
G4-PTX-PEG	4.73±0.26
G4-PTX-PEG-R8	9.42±1.01

2.4.2 Hemolytic toxicity study

Hemolysis study was performed for the dendrimer conjugates G4-PEG and G4-PEG-R8 at 5 mg/ml and 10 mg/ml concentration along with plain G4 dendrimer to measure carrier mediated toxicity, if any. Results indicated that the synthesized dendrimer conjugates pose negligible toxicity to RBCs. At a concentration of 10 mg/ml plain G4 caused a hemolysis of 5.7% whereas both the conjugates G4 PEG and G4 PEG R8 caused around 2% hemolysis only. This can be attributed to the presence of PEG chains which reduces the surface charge in comparison to plain G4 thereby giving a protective shield. Further, R8 modification on the surface of G4 dendrimer also did not pose any significant toxicity proving the safety of the conjugate for systemic administration.The hemolysis percentage of the conjgates was represented in a bar diagram in Figure 2.6.

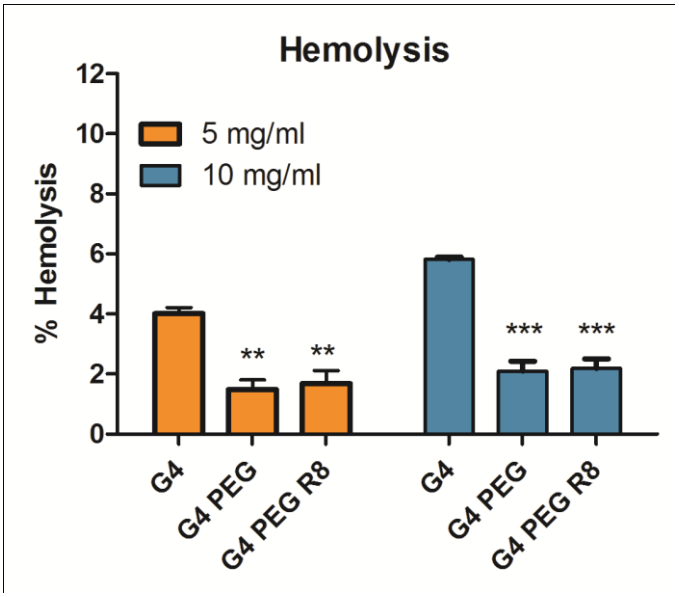

Figure 2.6 Percentage of hemolysis obtained from the interaction of the G4 conjugates with RBC suspension. Data is represented as Mean±SD, n=3. Statistical significance was determined for G4 PEG and G4 PEG R8 against plain G4 dendrimer.

2.4.3 Cellular Uptake by Confocal microscopy

HeLa cells treated with fluorescently labeled G4-PEG and G4-PEG-R8 for 1 h and 4 h were observed under confocal microscope to visualize the effect of R8 on the internalization of the conjugate. Brighter green fluorescence was detected in cytoplasm as well as nucleus with R8 attached dendrimer conjugate signifying higher cellular association relative to R8-unmodified conjugate. Confocal microscopy results are in agreement with flow cytometry data that the cells treated with F-G4-PEG-R8 demonstrated higher internalization compared to F-G4-PEG at both the time points. Photomicrographs of the cells after 1 h and 4 h incubation were represented in Figure 2.7A.

2.4.4 Cellular uptake by flow cytometry

To measure the cellular uptake of the multifunctional carrier system and to study the effect of R8 modification on internalization of the conjugate, flow cytometry experiment was carried out. From the results, a time dependent increase in the uptake was witnessed at 1 h and 4 h treatment. A 1.34 fold and 1.65 fold increase in the uptake was observed at 1 h and 4 h respectively for F-G4-PEG-R8 compared to F-G4-PEG. The flow cytometry data indicates that the R8 attachment promoted significantly higher cellular association of the R8-dendrimer-conjugate compared to unmodified dendrimer. Geo Mean Fluorescence of different treatments at 1 h and 4 h was represented as bar graph along with the histograms of events captured by flow cytometer in Figure 2.7B.

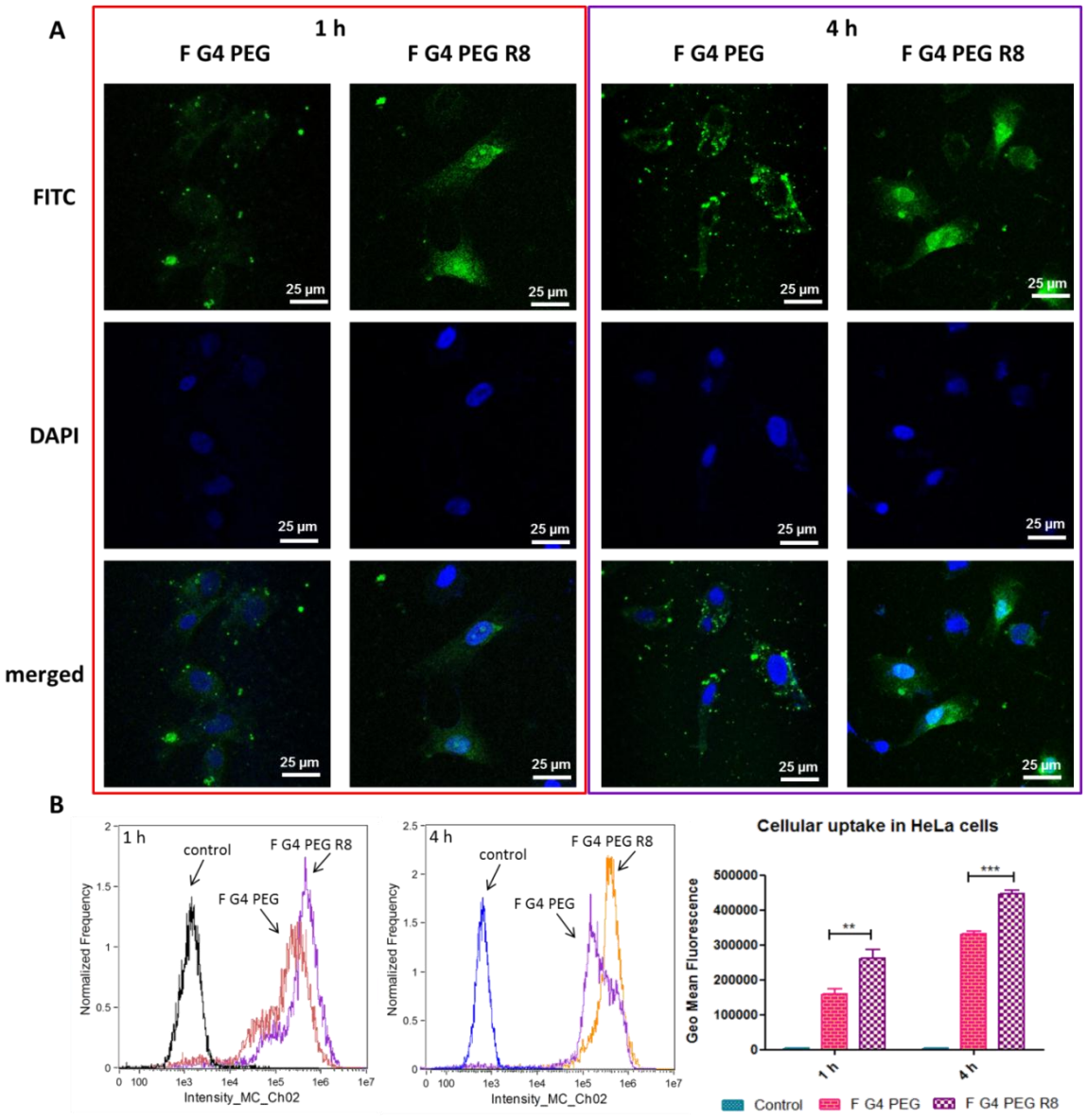

Figure 2.7 (A) Confocal microscopy images of HeLa cells after 1 h and 4 h of incubation with F-G4-PEG and F-G4-PEG-R8, (B) Cellular uptake of fluorescently tagged G4 conjugates with and without R8 modification in HeLa cells after 1 h and 4 h incubation as assessed by flow cytometer (Mean±SD, n=3).

2.4.5 Cytotoxicity Study

To determine the cytotoxic activity of PTX conjugates, MTT assay was executed. Cells were treated with free PTX, G4-PTX-PEG, and G4-PTX-PEG-R8 at 0-50 µg/ml concentration and incubated for 24 h and 48 h. The results of the study revealed that there was a time dependent and concentration dependent decrease in total cell viability (Figure 2.8). At the end of 24 h, G4-PTX-PEG-R8 exhibited 31.3±2.56% cell viability against 43.86±2.16% of G4-PTX-PEG and 52.04±1.19% of free PTX. Further, the cell viability reduced to 12.29±1.22%, 18.23±1.56%, and 28.95±2.49% for G4-PTX-PEG-R8, G4-PTX-PEG, and free PTX respectively after 48 h treatment. At all the concentrations, dendrimer conjugated PTX was more active than the free PTX. In addition, G4-PTX-PEG-R8 had highest cytotoxicity which can be attributed to its ability to penetrate efficiently into the cells resulting in accumulating PTX in higher amount in the tumor cells compared to unmodified G4-PTX-PEG or free PTX.

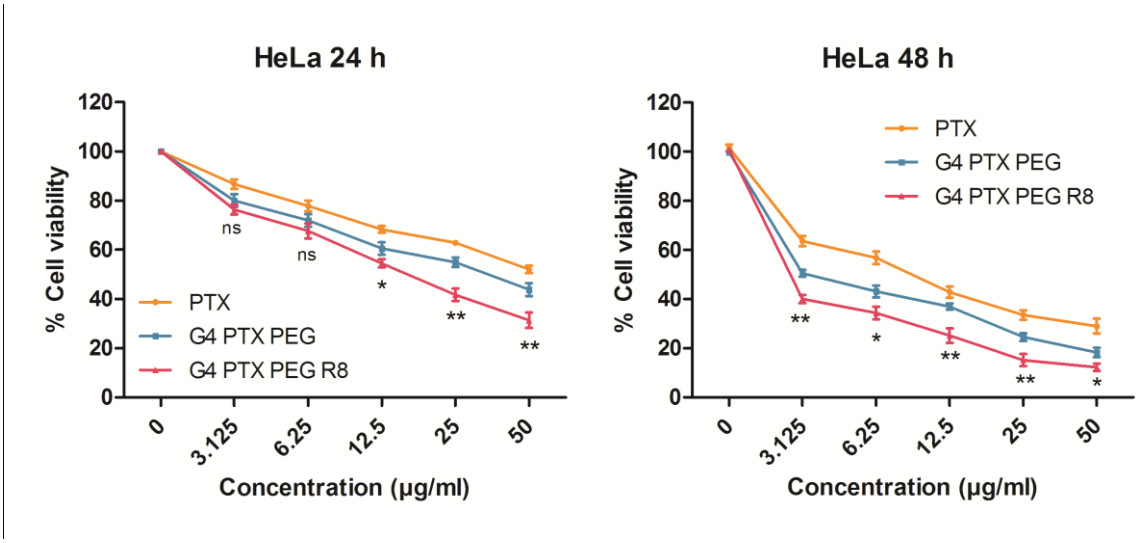

Figure 2.8 Percentage cell viability of HeLa cells treated with different concentrations of PTX, G4-PTX-PEG, and G4-PTX-PEG-R8 at 24 h and 48 h (Mean ± SD; n = 3).

2.4.6 Assessment of Apoptosis inducing potential

Annexin V FITC/PI double staining assay was carried out to measure the extent of apoptosis induced by free PTX and the dendrimer conjugates. The untreated cells did not show any signs of apoptosis or necrosis. As shown in Figure 2.9, after 48 h treatment, it was observed that G4-PTX-PEG-R8 induced a total apoptosis (Q2+Q3) of 89.5% whereas G4-PTX-PEG and free PTX induced 81.8% and 56.7% respectively. Both the dendrimer conjugates were superior compared to free PTX. The results were consistent with the MTT assay. Higher percentage of apoptosis is likely due to enhanced internalization of the R8-conjugate, more PTX was available for the cells which resulted in significant cell death.

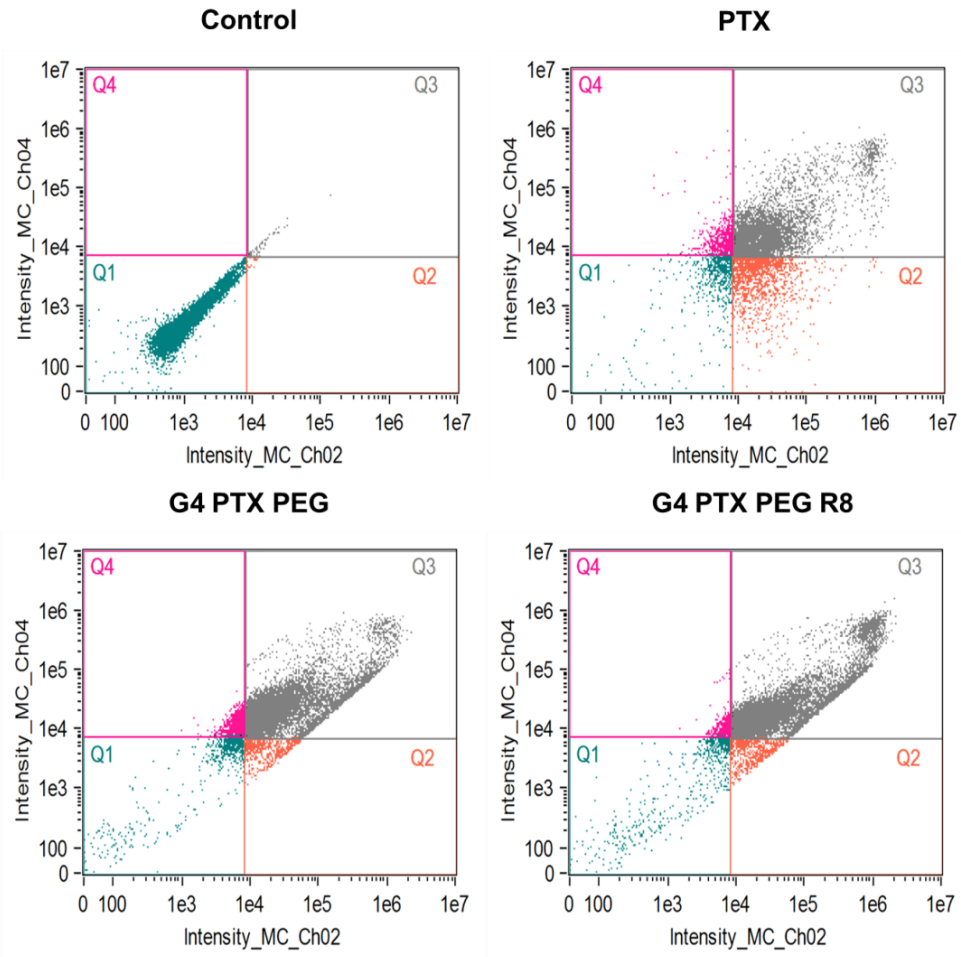

Figure 2.9 Quantitative estimation of apoptosis induced by various PTX treatments as studied by AnnexinV FITC/PI staining assay. (Q1 - Live cells, Q2 - Early apoptotic, Q3 - Late apoptotic, Q4 - Necrotic cells).

2.4.7 Penetration efficiency in 3D cancer cell spheroids

3D cell culture system, spheroids mimic the *in vivo* architecture and microenvironment of tumors owing to more natural morphology of cells in presence of extracellular matrix, and pH and oxygen gradients. Spheroids enhance the significance of *in vitro* results compared to 2D monolayers as they exhibit a drug resistance pattern similar to solid tumors (van den Brand et al. 2017; Yang et al. 2017). These properties make it an alternative to study the transport of molecules into the tumor tissue. From this study, it was observed from Z-stack confocal microscopy images that with increase in the incubation time, F-G4-PTX-PEG-R8 moved deeper into the spheroid towards the center compared to unmodified F-G4-PEG conjugate (Figure 2.10A). R8 being a cell penetrating peptide enhanced the internalization of the dendrimer conjugate into the spheroids. The observation indicated that R8-conjugation in dendrimers overcomes the poor permeability of the dendrimers into the deeper tumor tissues.

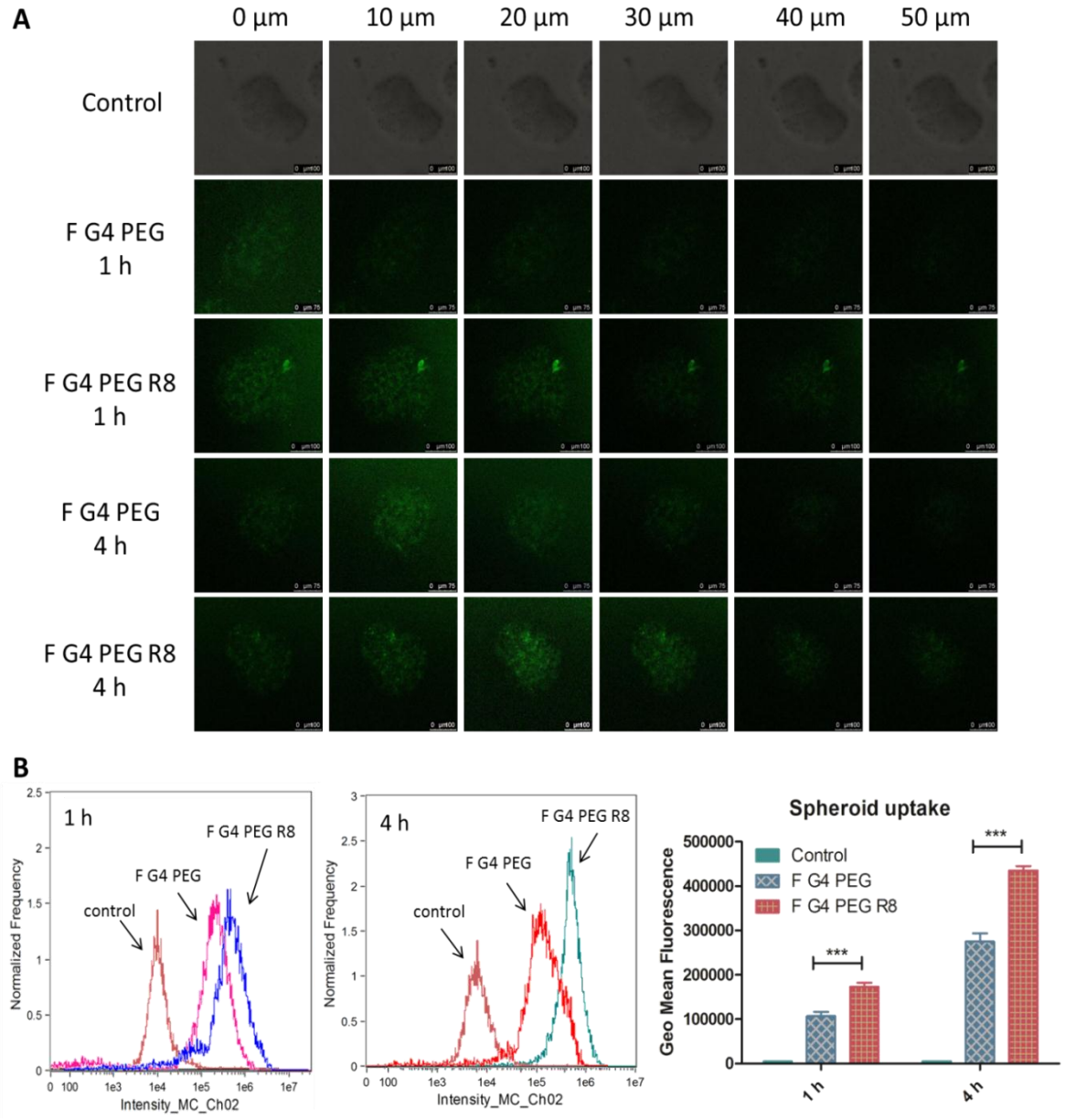

Figure 2.10 (A) Penetration of G4 conjugates in 3D cultured spheroids at various depths after 1 h and 4 h incubation captured as Z-stacks by confocal microscopy, (B) Quantitative assessment of cellular uptake in 3D spheroids treated with F-G4-PEG and F-G4-PEG-R8 by flow cytometry (Mean ± SD; n = 3).

2.4.8 Uptake of dendrimer conjugates in 3D spheroids by flow cytometry

The uptake of F-G4-PEG-R8 and F-G4-PEG in the 3D spheroids was quantified by breaking the spheroids and analyzing the samples using flow cytometer. Spheroids were treated with a cell detachment reagent, accutase to obtain single cell suspension. The F-G4-PEG-R8 conjugate entered the spheroids 1.58 folds and 1.62 folds higher in comparison to the F-G4-PEG after 1 h and 4 h of treatment, respectively as calculated by the geo mean fluorescence values. This result corroborates with the confocal microscopy data, where time-dependent increase in the fluorescence intensity was observed. Fluorescence intensity observed in spheroids was relatively less in comparison to monolayers which could be due to the difference in effective surface area available for penetration in both the systems. The study in 3D spheroids suggests that R8 attachment significantly improved the cellular association of the conjugate. Data obtained after analysis by flow cytometer was represented as Figure 2.10B.

2.4.9 Inhibitory effect on the 3D HeLa spheroids

Inhibition of progress of growth of 3D tumor spheroids was studied after treating the spheroids with free PTX, G4-PTX-PEG and G4-PTX-PEG-R8 for 24 h. The spheroids were monitored for 6 days and brightfield images were captured on Day 0, Day 3, and Day 6. The growth progression was analyzed by measuring the diameter of the spheroids. As represented in Figure 2.11A, it was witnessed that the growth was significantly inhibited in spheroids treated with dendrimer conjugates in comparison to free PTX. Also, a drastic increase in the diameter of control spheroids was observed over the period of time in comparison to drug treated spheroids with size reaching up to 1000 µm diameter.

The average diameter of spheroids at the end of 6 days was found to be 502 ± 8.7 µm, 658 ± 17.3 µm, 788 ± 43 µm, and 1016 ± 32 µm after treatment with G4-PTX-PEG-R8, G4-PTX-PEG, Free PTX, and control respectively. The data is represented as a line graph in Figure 2.11B. Octa-arginine (R8), being a cell penetrating peptide, helps the PTX to localize in the spheroids subsequently inhibiting their growth progression. Further, the uptake data also supports that the dendrimer conjugates internalize significantly into the spheroids over time which makes the drug more available at the target site to elicit therapeutic action. As the spheroid systems are simulation of in vivo tumors, it can be extrapolated that the R8 conjugated dendrimer can significantly reduce the tumor progression *in vivo*.

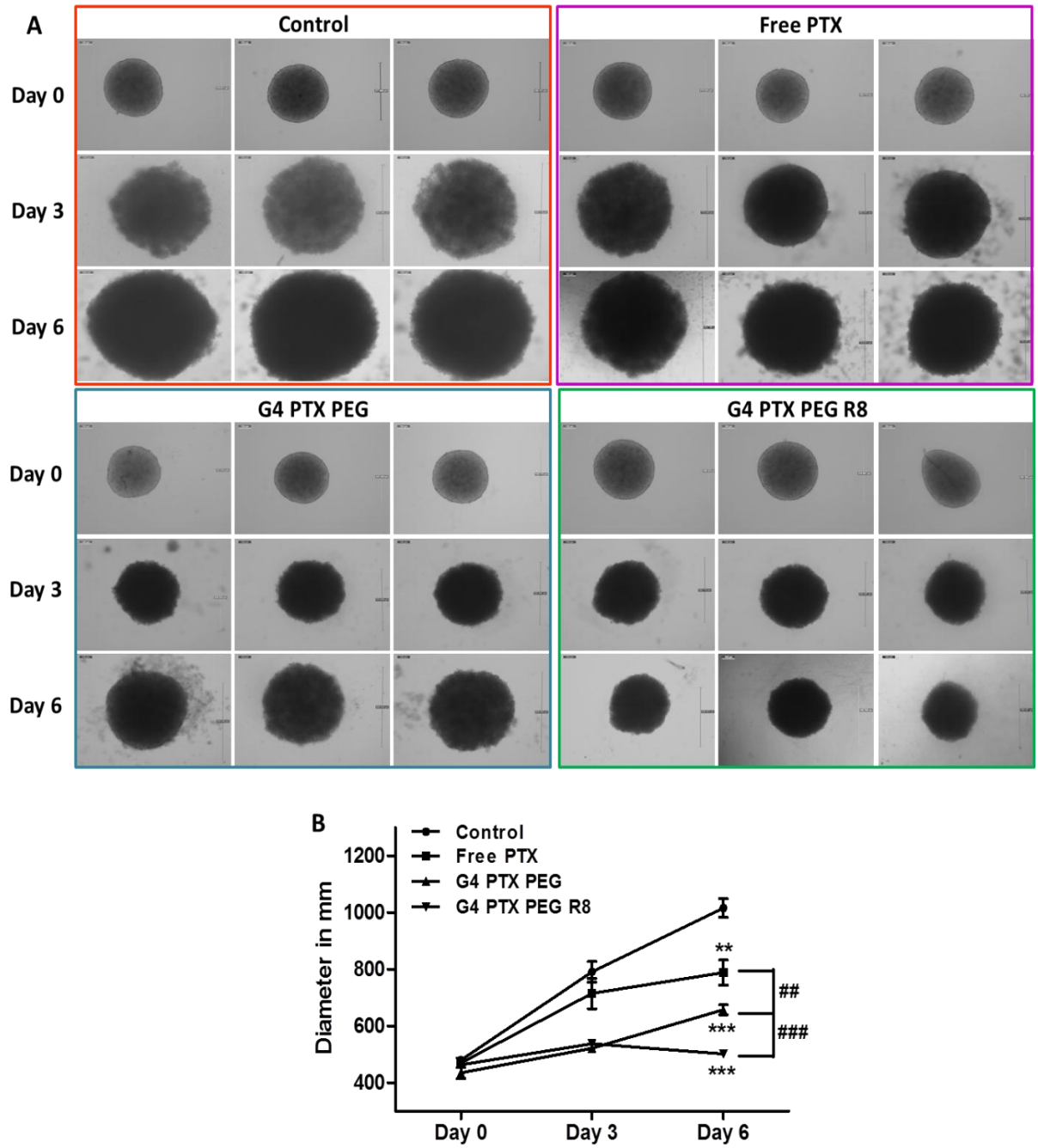

Figure 2.11(A) Photomicrograph of spheroids after different PTX treatments captured at Day 0, Day 3, and Day 6 using bright field microscope at 10X magnification. (B) Graphical representation of spheroid growth inhibition (Mean of diameter in µm ± SD; n = 3).

2.4.10 In vitro cytotoxicity in spheroids

Presto Blue assay was performed to determine the cytotoxic activity of PTX formulations in tumor spheroids. G4-PTX-PEG-R8 and G4-PTX-PEG showed higher cytotoxicity in comparison to free PTX after treatment for 24 h. The cytotoxicity was highest in case of G4-PTX-PEG-R8 with a cell viability of 39.8 ± 2.14% followed by G4-PTX-PEG and free PTX with a viability of 45.87 ± 2.5% and 62.27 ± 3.8% respectively. The data is represented as a bar graph in Figure 2.12.The dendrimer conjugates were found to be effective in tumor spheroids as was observed in the monolayers although a slight reduction in cytotoxicity was noted. This can be explained based on the fact that the diffusion of carrier system becomes limited in tumor spheroids compared to free access to cells in monolayers.

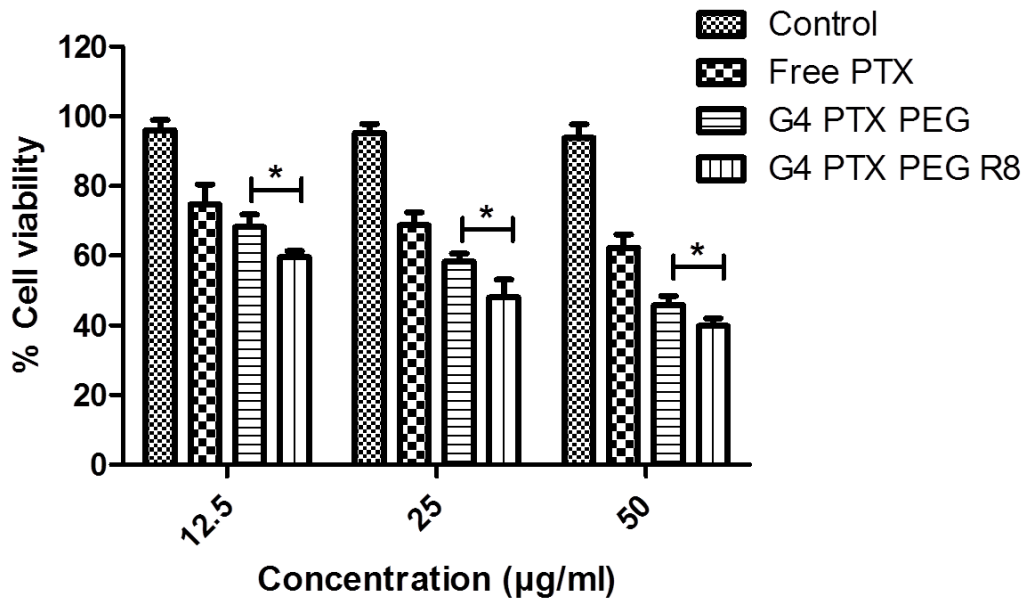

Figure 2.12 In vitro cytotoxicity induced by PTX, G4-PTX-PEG, and G4-PTX-PEG-R8 at 24 h in tumor spheroids as assessed by Presto Blue assay (Mean of percentage cell viability ± SD; n = 3).

2.4.11 Live/Dead cell assay in 3D spheroids

To visualize the live and dead population of cells as a response to treatment with PTX conjugates, the spheroids were incubated with Calcein Blue AM reagent. The calcein blue AM produces bright blue fluorescence due to intracellular esterase activity when internalized by live cells whereas the dead cells cannot transform the calcein blue AM reagent. On the other hand, dead cells can be identified by PI staining.

From the fluorescence micrographs of spheroids represented in Figure 2.13, it can be noticed that G4-PTX-PEG-R8 had maximum red fluorescence in comparison to G4-PTX-PEG and free PTX. Control spheroids did not show any dead population. In spheroids treated with free PTX, dead population was present mostly on the periphery indicating its inability to reach deeper parts of spheroid.

In case of G4-PTX-PEG and G4-PTX-PEG-R8, the dead population was seen evidently in the periphery as well as central parts of spheroid which can be attributed to its penetrability towards the core. R8 anchoring to the dendrimer conjugate resulted in superior penetration into the core of the spheroids and thereby higher drug accumulation and cell death.

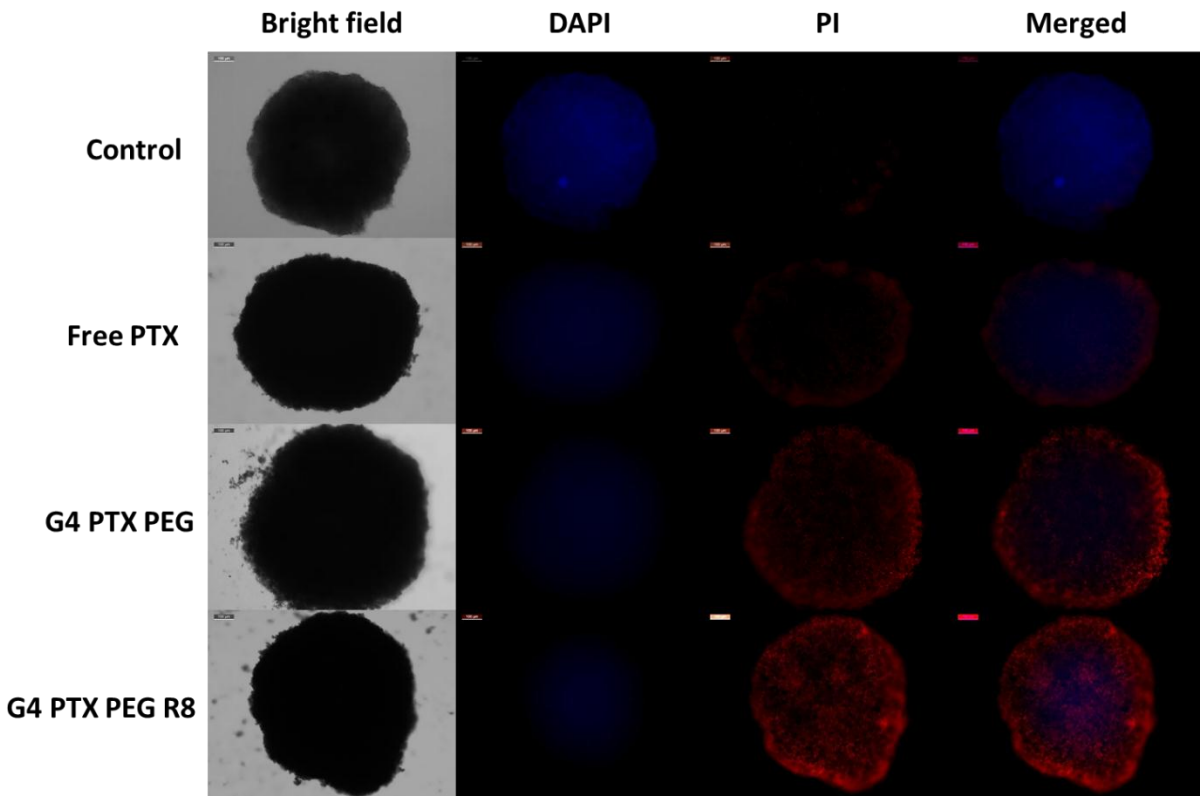

Figure 2.13 Live/dead cell micrographs of tumor spheroids captured using fluorescence microscope at 10X magnification. Red fluorescence (PI) depicts dead population and blue fluorescence (calcein blue) depicts live population.

2.5 Conclusion

Even though PAMAM dendrimers of various generations with ethylene diamine core has been utilized in delivering therapeutic cargo in cancer cells, cell membrane permeability is a challenge for this polar molecule. Therefore, a strategy needs to be undertaken to deliver the nanocarriers effectively in the intracellular compartment by facile translocation through the cell membrane. Here, we have developed an intracellularly targeted PAMAM nano-construct, G4-PTX-PEG-R8 by conjugating a potent cell penetrating peptide, R8 on the surface of the dendrimer. While PTX was conjugated on the dendrimer surface to prevent pre-mature drug release, anchorage of PEG on the surface was executed to impart the ability of long systemic circulation of the construct. GPC analysis indicated that approximately 2.5 molecules of PTX, 10.5 molecules of PEG, and 1.8 molecules of R8 were attached per molecule of G4 PAMAM dendrimer. Results obtained from hemolysis study indicated that the synthesized dendrimer conjugates, G4-PTX-PEG-R8 exhibited negligible toxicity to RBCs. MTT assay performed on HeLa cells demonstrated that G4-PTX-PEG-R8 exhibited highest cytotoxicity compared to the free PTX, and G4-PTX-PEG. G4-PTX-PEG-R8 demonstrated significantly higher cell membrane permeability in monolayers and spheroids of HeLa cells compared to G4-PTX-PEG, which led to the enhancement of the apoptosis inducing ability of G4-PTX-PEG-R8 as revealed by AnnexinV assay.

Further, in tumor spheroids which simulate in vivo tumors, the R8 conjugated dendrimer exhibited superior cytotoxicity and inhibition of growth.

In conclusion, G4-PTX-PEG-R8 could demonstrate tumor accumulation owing to long circulation property imparted by PEG chain followed by intracellular targetability by R8-conjugation. Therefore, the newly developed dendrimer-conjugate could be a promising chemotherapeutic agent for cancer treatment.

Chapter 3

Biotin Anchored Poly(Amidoamine) Dendrimers for Active Targeting of Paclitaxel in cancer

3.1 Abstract

Active targeting of chemotherapeutics is an effective way of delivering them specifically to the tumor site without damaging the normal healthy cells. A variety of ligands have been reported which actively target the corresponding receptors overexpressed on the surface of cancer cells. Biotin is a micronutrient essential for the cellular growth and is high in demand in most of the cancer cells. Consequently, biotin receptors are overexpressed in many cancer cell types which can be suitably targeted by nanocarriers anchored with biotin. In the current study, we have employed poly(amidoamine) (PAMAM) dendrimers of generation 4 (G4) to deliver paclitaxel (PTX), a poorly soluble anti-cancer agent precisely to cancer cells. Further, G4 PAMAM has been PEGylated and tagged with Biotin. The synthesized multifunctional PAMAM dendrimer conjugates were characterized by ^{1}H NMR and zeta potential analysis techniques. Further, the nano-conjugates were evaluated *in vitro* in cell monolayers and 3D spheroids. Cellular uptake and cytotoxicity studies in human non-small cell lung cancer cell line (A549) which has overexpressed biotin receptors showed that the biotin conjugation significantly improved the efficiency of the system. G4 PTX PEG Biotin has demonstrated higher cytotoxic potential compared to free PTX and G4 PTX PEG. Further, the penetration efficiency of dendrimer conjugates in 3D cancer spheroids was studied by confocal microscopy at various depths. G4 PTX PEG Biotin was found to induce superior cell killing in cell monolayers as well as 3D spheroids. The biotin modified conjugate demonstrated significant inhibition of growth of tumor spheroids. Therefore, the newly synthesized biotin anchored dendrimer system holds great potential in efficiently delivering PTX to biotin receptor overexpressed cancers.

3.2 Introduction

Cancer is the leading cause of death in the U.S. among people of ages less than 85 years. The number of patients suffering from different forms of cancer is on the raise due to factors like genetic effects, pollution, unhealthy lifestyle habits etc. Patients very commonly experience debilitating side effects while undergoing chemotherapy which can be acute, chronic, or even life-threatening (in some cases) at therapeutic doses of most of the anticancer drugs. Although the anticancer drugs are intended to be taken up by rapidly growing cancer cells, they are often taken up by other cells as well which is the reason for such side/off-target effects. Cytotoxic effect on the normal cells in a patient's body is the primary obstacle to the clinical application of otherwise potent anticancer drugs (Tripodo et al. 2014). The efficacy and tolerability of anticancer drugs can be increased by employing target specific DDS that can limit the associated side effects and thus improve the patient quality of life (Ren et al. 2015). Several potent chemotherapeutic agents like taxols, epirubicin, platinum compounds, methotrexate, doxorubicin (DOX) etc., cannot discriminate between healthy and cancer cells, especially when delivered as conventional dosage forms. This has limited their clinical potential due to severe undesirable side effects (Šimůnek et al. 2009; Yao et al. 2007; Celik et al. 2013; Abraham et al. 2005). To overcome such shortcomings, DDS with targeting moieties that specifically target cancer cells have been developed (Quan et al. 2014; Luo et al. 2014; Hao et al. 2015; Guo et al. 2014).

A successful cancer treatment wherein sufficient amount of drug has to reach the site of action cannot solely rely on EPR or passive targeting. Cancer cells need more micronutrients than normal cells for their proliferation and survival. As a consequence, cancer cells have overexpression of certain receptors which can be actively targeted using specific ligands (Russell-Jones et al. 2004). Different ligands like proteins, hormones,

vitamins, growth factors which can be identified by cancer cells, are attached to the backbone of the drug carrier system (Nateghian et al. 2016). If the circulation times are long enough, effective transport to the site of action and substantial uptake of drug via endocytosis can be possible through both - the EPR effect and active targeting of molecules (Brigger, Dubernet, and Couvreur 2002; Byrne, Betancourt, and Brannon-Peppas 2008; Chen et al. 2010).

Micronutrients are vital for normal cellular functions and biotin (vitamin H) is one of such essential micronutrients (Livaniou et al. 2000). Biotin, owing to its low molecular weight, relatively simple biochemical structure, and high tumor specificity, has drawn much attention from both pharmaceutical research and industrial communities. In order to thrive and multiply rapidly, cancer cells need extra biotin as compared to normal cells. Rapidly proliferating malignant cells often overexpress biotin-specific uptake systems on the cell surface which enables favorable integration of biotin or biotin conjugates at the tumor sites. Biotin overexpression is observed in wide types of cancers including renal (RENCA, RD0995), lung (A549, M109), ovarian (OV 2008, ID8), mastocytoma (P815) and breast (4T1, JC, MMT06056) cancer cell lines (Shi et al. 2014). This specific interaction of biotin and its receptors can be explored to increase the uptake of anticancer drugs by tumor cells (Yang et al. 2009; Bu et al. 2013; Yang et al. 2014). In the recent years, many researchers have demonstrated an increased uptake efficiency of anticancer drugs when delivered in biotin conjugated macromolecular carriers (Vadlapudi et al. 2013; Taheri et al. 2011; Yellepeddi, Kumar, and Palakurthi 2009; Tseng et al. 2009; Minko et al. 2002).

Dendrimers are hyperbranched macromolecules having monodispersed three-dimensional structure with specific molecular weight and host-guest encapsulation properties (Cheng et al. 2008; Esfand and Tomalia 2001). Poly(amidoamine) (PAMAM) dendrimers are the

first commercially used class of dendrimers for drug delivery investigations (Tomalia 2005). In general, the dendrimers possess vacant internal pockets which can encapsulate the hydrophobic cargoes (Jansen and Meijer 1994). In addition, the outer shell of dendrimers possess a wide number and variety of surface functional groups which can be conjugated or anchored with various moieties to serve multiple purposes (Majoros et al. 2006; Thomas et al. 2005). PAMAM dendrimers have been widely explored for delivery of poorly soluble anti-cancer agents to specific target sites (Milhem et al. 2000; Bhadra, Bhadra, and Jain 2005; Bhadra et al. 2003; Asthana et al. 2005; Najlah et al. 2006, 2007; D'emanuele et al. 2004). Ease of fabrication, nanometer size, biocompatibility, scalability are some of the properties which make dendrimers a potential drug delivery system (Svenson and Tomalia 2012; Duncan and Izzo 2005). Previous studies reported the active targeting of dendrimers by conjugation of ligands such as folic acid (Thomas et al. 2005), biotin (Yellepeddi, Kumar, and Palakurthi 2009; Xu et al. 2007), antibodies (Patri et al. 2004), peptides (Shukla et al. 2005), and epidermal growth factor (Barth et al. 2004) to dendrimers thereby enhancing the therapeutic potential of cancer chemotherapeutics.

In the present study, we have investigated the potential of biotin conjugated multifunctional PAMAM dendrimer system to effectively deliver paclitaxel (PTX), a chemotherapeutic agent which suffers poor physicochemical properties. Further, we have characterized the conjugates and evaluated the delivery system in biotin overexpressed human lung cancer cell line (A549). A 3D tumor spheroid model which mimics *in vivo* tumor has been employed to evaluate the uptake and therapeutic potential of the developed dendrimer system.

3.3 Materials and methods

3.3.1 Materials and cell lines

Dendrimer of generation 4 with ethylenediamine core and surface amino groups (G4 PAMAM) was purchased from Dendritech (USA). Paclitaxel (PTX) was obtained as a gift sample from Fresenius Kabi India Pvt., Ltd. (Gurgaon, India). Methoxy-polyethyleneglycol-succinimidyl carboxymethyl ester (mPEG-SCM ester, MW 2000 Da) was obtained from Jenkem Technology (USA). N-ethyldiisopropylamine (DIPEA) was obtained from Avra Chemicals, India. NHS-Fluorescein was obtained from Thermo Scientific (USA). N-(3-Dimethylaminopropyl)-N′-ethylcarbodiimide hydrochloride (EDC. HCl, 98%), Biotin and N-Hydroxysuccinimide (NHS, 98%) were obtained from Sigma Aldrich Chemicals (USA). Regenerated cellulose dialysis membrane (MWCO 2 kDa, 3.5 kDa and 14 kDa) was obtained from Spectrum Laboratories, Inc. (USA). N,N'-Dicyclohexylcarbodiimide (DCC) was purchased from Spectrochem Chemicals Ltd. (India). All the other chemicals and solvents obtained commercially were of analytical grade.

Human lung cancer cells, A549 were obtained from National Center for Cell Sciences (NCCS, Pune, India). DMEM (Dulbecco's minimum essential medium) supplemented with 10% FBS and 1% penicillin-streptomycin solution (Himedia Labs, Mumbai) was used as the growth medium. Cells were maintained in a humidified incubator at 37°C and 5% CO_2.

3.3.2 Synthesis of multifunctional PAMAM dendrimer

3.3.2.1 Synthesis of fluorescent labeled G4 PAMAM dendrimer

Fluorescently labelled G4 PAMAM dendrimer was prepared following the previously described method with a slight modification (Biswas et al. 2012). Briefly, 100 mg of G4 PAMAM dendrimer was dissolved in DMF. NHS Fluorescein dissolved in DMF was added to the dendrimer solution at a molar ratio of 1:1 dropwise under inert atmosphere. The solution was stirred at room temperature under dark conditions for 8 h. After the reaction, the solvent DMF was evaporated under vacuum and resulting product was subjected to dialysis to remove unconjugated fluorescein. Following dialysis for 48 h, the product was lyophilized and stored until further use.

3.3.2.2 Synthesis of G4-PTX

The 2`-OH group of paclitaxel was modified to its hemisuccinate form using succinic anhydride prior to reacting with amine groups of G4 PAMAM dendrimers. Briefly, to 25 mg of Paclitaxel (PTX) in DCM, 4.4 mg of succinic anhydride (molar ratio of 1:1.5) was added under stirring in presence of dry pyridine and the reaction was continued for 3 days. Following that, the product was extracted using ethyl acetate and vacuum dried to get the PTX-2`-hemisuccinate as white powder. The acid group of PTX-2'-hemisuccinate was activated with DCC/NHS in DMF for 6-8 hours at room temperature. The formed PTX-NHS ester is readily react-able with the amine terminals of G4 PAMAM dendrimer. A quantity of 50 mg of G4 PAMAM Dendrimer was dissolved in DMF, and activated PTX NHS ester was added drop wise under nitrogen at a molar ratio of 1:4. The reaction was continued overnight and the DMF was evaporated under vacuum. Dialysis of the product was carried against water for 48 h using 3500 Da MWCO dialysis membrane to

remove the impurities. A white fluffy solid of G4-PTX conjugate was obtained after lyophilization.

The scheme of synthesis of the multifunctional PAMAM dendrimer has been represented in Figure 3.1.

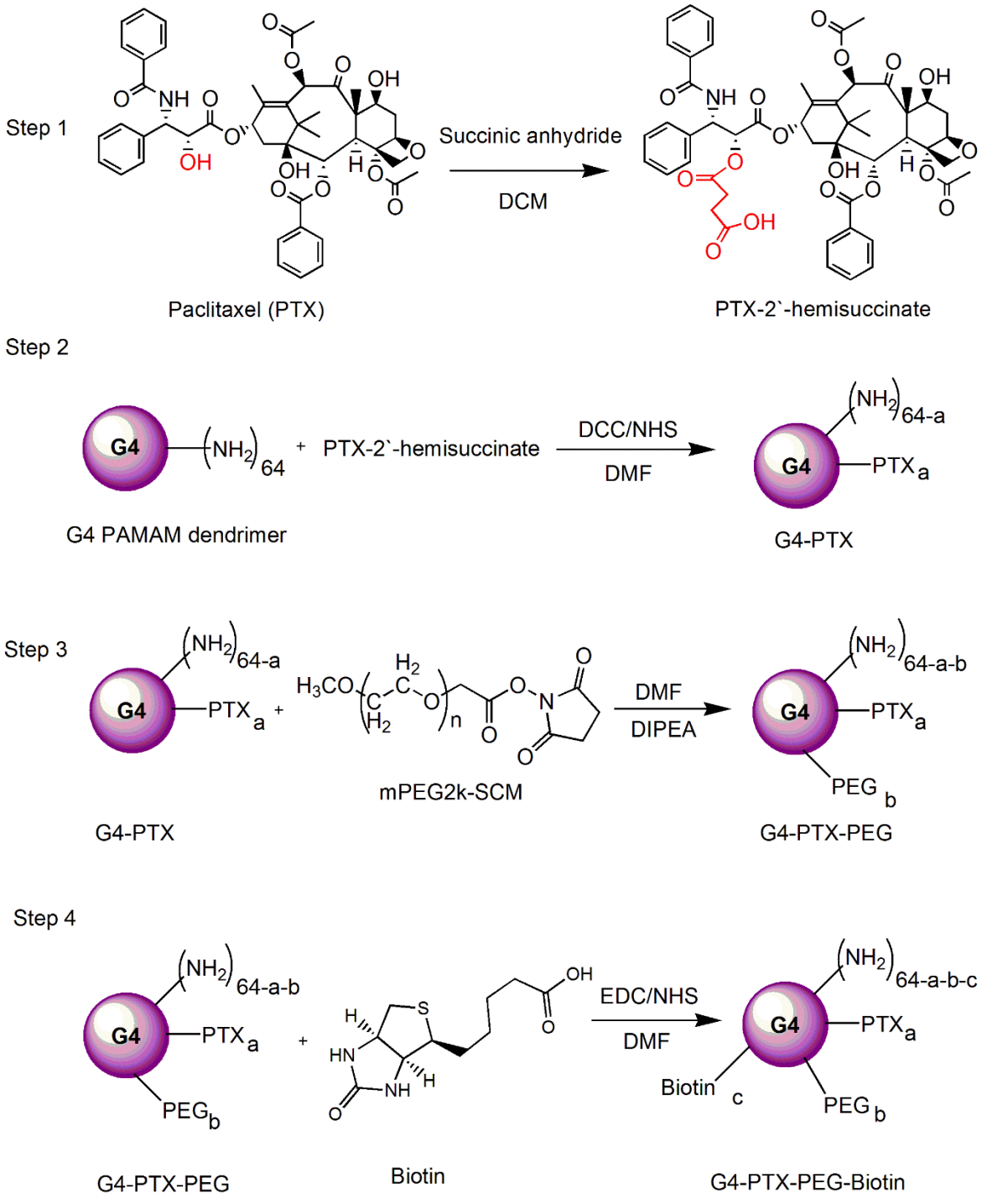

Figure 3.1 Schematic representation of synthesis of multifunctional G4 dendrimer conjugates

3.3.2.3 Synthesis of G4-PTX-PEG

The synthesized G4-PTX conjugate was PEGylated using mPEG SCM ester of molecular weight 2 kDa. To the solution of G4-PAMAM-PTX in DMF, mPEG SCM was added drop-wise at a mole ratio of 12:1. DIPEA (20 µl) was added as a base to the reaction mixture. The reaction was continued overnight and DMF was evaporated under vacuum. Following that, the reaction mixture was dialyzed for 48 h using 12-14 kDa MW cutoff (regenerated cellulose) dialysis membrane with frequent water changes. After dialysis, the product was lyophilized to obtain a solid white product of G4-PTX-PEG. The fluorescent tagged dendrimer conjugates were also prepared in the same manner. The attachment of PEG to PAMAM dendrimer was characterized and confirmed by measuring the zeta potential changes, proton NMR and GPC analysis.

3.3.2.4 Conjugation of Biotin onto G4-PTX-PEG

Biotin has a carboxyl group which was activated using EDC/NHS and was reacted with previously synthesized G4-PTX-PEG at a molar ratio of 30:1 in DMF. After the reaction, the DMF was evaporated under vacuum using rotary evaporator and product was dialyzed against water for 48 h. The final conjugate G4-PTX-PEG-Biotin was collected as a solid after freeze drying.

3.3.3 Characterization of multifunctional conjugate

Plain G4 PAMAM dendrimer, G4-PTX, G4-PTX-PEG, and G4-PTX-PEG-Biotin were characterized by proton NMR (300 MHz, Bruker, USA) and zeta potential analysis. To determine the relative molecular weights of synthesized conjugates, gel permeation chromatography (GPC) analysis was performed. Zorbax GF-250 (9.4 mm ID X 25 cm X 4-4.5 µ) size exclusion analytical column was used to run the samples in a HPLC system

(Agilent 1100 series). Tris buffer (50 mM) and KCl (100 mM) was used as eluting phase in isocratic mode at a flow rate of 1 ml/min. A calibration curve was plotted with the standard molecular weight compounds prior to analyzing the samples. Zeta potential of the conjugates was determined using a Malvern Zetasizer (Nano ZS, Malvern Instruments, UK).

3.3.4 HABA/Avidin assay

Biotin attachment to the dendrimer was quantitatively estimated using HABA/Avidin assay. This assay is based on the binding of the dye HABA (4'-hydroxyazobenzene-2-carboxylic acid) to avidin and the ability of biotin to displace the dye in stoichiometric proportions. HABA binds to avidin to produce a yellow-orange colored complex which absorbs at 500 nm. Biotin in the sample, if present, will displace the HABA dye and cause the absorbance to decrease. As per the manufacturer's protocol, to 900 µl of HABA/Avidin reagent, 100 µl of sample containing biotin dissolved in deionized water was added. The absorbance of the solution was recorded at 500 nm. Further, the biotinylation degree was calculated from the absorbance values obtained.

3.3.5 Confocal microscopy

Cellular internalization of multifunctional dendrimer conjugates was studied using confocal microscopy. Briefly, A549 cells were harvested from culture flasks at 80% confluence and counted. The cells were seeded at a cell density of 50,000 cells/well onto circular coverslips placed in 12-well culture plates. On the following day, conjugates F-G4-PEG and F-G4-PEG-Biotin (20 µg/ml) were added to the wells and incubated at 37°C for 1 h and 4 h. Also, to assess the mechanism of uptake of biotin tagged dendrimer conjugates, the cells were pre-incubated with excess free biotin (300 µm for 30 min) to saturate the biotin receptors. After the defined time, the well containing medium with free

biotin was removed and F-G4-PEG-Biotin was added to the cells. Prior incubation, cells were washed three times with sterile PBS, treated with DAPI (1 µg/ml) for 5 min, washed and fixed with 4% *para*-formaldehyde for 15 min. Using a mounting medium (Fluoromount-G), the coverslips were mounted cell-side on the microscopic slides. At 40 X magnification, cells were observed using confocal microscope (Leica DMi8, Leica Microsystems, Germany) and fluorescence images of cells were captured in FITC and DAPI filters. The obtained data were processed using Image *J* software.

3.3.6 Cellular uptake by flow cytometry

To quantitatively determine the cellular association of dendrimer conjugates, flow cytometry experiments were performed in A549 cells. The 6-well microplates were seeded with A549 cells at a cell density of 0.8×10^6 cells/well and allowed to attach overnight. Similar to the confocal microscopy study, biotin receptors were saturated by pre-incubating the cells with excess of free biotin (300 µm for 30 min) which receive F-G4-PEG-Biotin treatment to observe the mechanism of uptake by biotin receptors. Further, F-G4-PEG and F-G4-PEG-Biotin were added to the cells at a concentration of 20 µg/ml and incubated for 1 h and 4 h at 37°C. After the incubation period, cells were washed with PBS and then trypsinized. Cell pellet obtained after centrifugation was re-suspended in PBS prior to analysis by flow cytometer (Amnis, EMD Millipore, USA). Control cells did not receive any treatment. For each sample, a minimum of 10,000 events were collected. The geo mean fluorescence of the cells was calculated from the IDEAS software V6.0.

3.3.7 Cytotoxicity Study

The cytotoxic activity of free PTX, G4-PTX-PEG, and G4-PTX-PEG-Biotin was determined by MTT assay. The 96-well plates were seeded with A549 cells at a density

of 10,000 cells/well on the day before treatment. To the wells, formulations equivalent to a PTX concentration ranging from 0-50 µg/ml were added and incubated at 37°C and 5% CO_2 for 24 h and 48 h. Following incubation, formulations were removed and 50 µl of MTT reagent (5 mg/ml solution) was added to each well. The plates were further incubated for another 4 h, and MTT reagent was discarded. DMSO (150 µl) was added to each well to dissolve the purple colored formazan crystals. The absorbance at 570 nm was measured using a microplate reader (Spectramax™, Molecular Devices, USA) with a reference wavelength of 630 nm. Cells without PTX treatment were used as control. Percentage cell viability was calculated from the absorbance of sample against absorbance of control.

3.3.8 Evaluation of multifunctional dendrimer conjugates in 3D spheroid model

3.3.8.1 Formation of A549spheroids

Spheroids are 3D structures which mimic the *in vivo* tumors. In the current study, A549 cancer cell spheroids were prepared by liquid overlay method (Sarisozen, Abouzeid, and Torchilin 2014; Perche and Torchilin 2012). Briefly, 1.5% (w/v) agar solution was prepared in serum free DMEM medium and autoclaved. To each well of a 96-well plate, 50 µL of the agar solution was added to the bottom to prevent cell adhesion. Care should be taken so as to not let the agar solution solidify before adding to wells. In case of 8-well glass chamber slides, 150 µl of agar solution was added. The agar coated plates were allowed to cool down for 45 min.

From the culture flasks, A549 cells were harvested using trypsin and centrifuged to obtain cell pellet. Cells were counted and then seeded at a density of 8,000 cells per each well. Plates were centrifuged for 15 min at room temperature. After centrifugation, plates are left in the incubator. The formation of spheroids was continuously monitored using an

inverted microscope (Leica DMi8, Leica Microsystems, Germany). Spheroids of 3 – 5 days old were used in the further studies.

3.3.8.2 Penetration efficiency in 3D cancer cell spheroids

The penetration of targeted and non-targeted dendrimer conjugates into the spheroids was studied using confocal microscopy. F-G4-PEG-Biotin and F-G4-PEG were added to the spheroids grown in 8-well glass chamber slides and incubated for 1 h and 4 h. Following that, the cancer cell spheroids were washed with PBS and then observed by laser scanning confocal microscope (Leica DMi8, Leica Microsystems, Germany) at 10X magnification. Z-stack images were obtained from the surface where fluorescence is observed towards the tumor spheroid equatorial plane at every 10 μm thickness. Images were analyzed using Image *J* software.

3.3.8.3 Uptake of dendrimer conjugates in 3D spheroids by flow cytometry

Flow cytometry technique was utilized to quantitatively determine the uptake of targeted and non-targeted dendrimer conjugates in 3D cell spheroids. Five-day-old spheroids were employed in the study and incubated with F-G4-PEG and F-G4-PEG-Biotin for 1 h and 4 h. After the treatment period, 10 spheroids each of every treatment were pooled up to achieve required cell population for flow cytometry analysis. The spheroids were washed with PBS and broken down using Accutase cell detachment solution. Accutase solution is used to create single cell suspensions from a clump of cells. It contains proteolytic and collagenolytic enzymes. The obtained cell suspension after Accutase treatment was centrifuged and re-suspended in PBS to analyze using flow cytometer. A minimum of 10,000 events were collected for each sample. Same instrument conditions were maintained to study the uptake in monolayers and spheroids. The fluorescence intensity

histograms were captured in the FITC channel for each sample. A bar diagram of geo mean fluorescence exhibited by F-G4-PTX-PEG and F-G4-PEX-PEG-Biotin was plotted.

3.3.8.4 Inhibitory effect on the 3D spheroids

The inhibitory effect of PTX formulations on the growth of A549 cancer cell spheroids was studied to evaluate the potential of synthesized conjugates in delivering the drug to tumors. The cancer cell spheroids were incubated with free PTX, G4-PTX-PEG, and G4-PTX-PEG-Biotin at a PTX concentration of 25 μg/mL. After 24 h, the medium with formulations was carefully removed and fresh growth medium was added. The media was further changed on alternate days. The magnitude of inhibition of growth in spheroids was observed under inverted microscope (Leica DMi8, Leica Microsystems, Germany) at 10X magnification and images were captured. The data is represented as mean diameter of three spheroids with standard deviation.

3.3.8.5 In vitro cytotoxicity in spheroids

Cytotoxicity imposed by various PTX formulations in 3D spheroids was studied using Presto blue assay following the manufacturer's instructors. Presto Blue reagent is a cell permeable resazurin-based solution which turns to a red fluorescent complex upon reduction by viable cells. The fluorescence/absorbance of the sample is measured and the cell viability is calculated. Visually compact spheroids (typically 3-5 days after seeding) were treated with free PTX, G4-PTX-PEG, and G4-PTX-PEG-Biotin (PTX concentration: 25 μg/mL) for 24 h. Each formulation was added to 10 spheroids individually. Following the treatment period, the spheroids were washed with PBS and added with 50 μL of Accutase solution. Then, the spheroids were gently shaken and the resulting suspension was centrifuged at 1200 rpm for 5 min. Samples for analysis were prepared by re-suspending the cell pellet in 90 μL of growth medium and adding 10 μL of

Presto Blue reagent. The samples were incubated at 37 °C for 2 h. The absorbance was measured at 570 nm using 600 nm as reference.

3.3.8.6 Live/Dead cell assay in 3D spheroids

The amount of live and dead population developed as a result of various PTX treatments to A549 cell spheroids was assessed by live/dead cell assay using Calcein Blue AM reagent. Briefly, the spheroids were treated with free PTX, G4-PTX-PEG, and G4-PTX-PEG-Biotin at a PTX concentration of 50 μg/mL. After 24 h of incubation, the spheroids were washed with PBS and stained with calcein blue AM reagent and propidium iodide (PI). Calcein blue AM ester passively diffuses into the cells and gets cleaved by the intracellular esterases in viable cells to yield calcein blue. The resultant calcein blue retains in the cell and emits blue fluorescence. Additionally, dead cells were stained by PI and can be observed using red filter of fluorescence microscope (Leica DMi8, Leica Microsystems, Germany) at 10X magnification. Bright field and fluorescence images were captured and processed using Image J software.

3.3.9 Statistical analysis

All experiments were performed in triplicate and data are expressed as mean ± SD. The statistical significance among the groups was established using Student's *t*-test using Graph Pad prism 5 (GraphPad Software, Inc.; San Diego, CA). Any value with p less than 0.05 were considered statistically significant. The representation of *, ** or ##, *** or ### in figures corresponds to p values < 0.05, 0.01 and 0.001, respectively.

3.4 Results and Discussion

3.4.1 Synthesis and characterization of multifunctional dendrimer conjugate

The formation of hemisuccinate form of PTX at 2' position was confirmed by mass spectrometry. A peak at 954.5 (MH+) and 976.5 (MNa+) was observed which matches the mass of hemisuccinate form of PTX (Figure 2.5). The proton NMR of the intermediate conjugates G4-PTX and F-G4 was represented in figure 2.3 and 2.4. In the NMR spectrum, the aromatic groups of PTX resulted in peaks at δ (ppm) 7-8.5. Further, the protons of PEG chains can be seen at δ (ppm) 3.2-4.1 whereas the protons corresponding to the PAMAM dendrimer molecule were observed at δ (ppm) 1.5-3.5. In figure 3.2, the peak at δ (ppm) 4.4 and 4.6 relates to the ring juncture protons of Biotin. These signals confirm the successful conjugation of biotin to the dendrimer surface to form G4-PTX-PEG-Biotin.

In addition, from the GPC analysis relative mass of each conjugate was identified. From the mass value, the approximate number of molecules attached to each dendrimer molecule was calculated. It was observed that approximately 2.5 molecules of PTX, 10.5 molecules of PEG.

Further, the HABA/Avidin assay revealed the biotinylation degree of the dendrimer molecule. The number of biotin molecules attached to each dendrimer was calculated to be 20.98 (See Table 3.1). Moreover, a change in the zeta potential value as shown in Table 3.2 after every synthetic step supports the successful construction of the conjugates.

Table 3.1 Relative mass and approximate number of molecules of each type attached to dendrimer.

Multifunctional Dendrimer Conjugate	**Relative Mass (Da)**	**No. of molecules attached approximately per each dendrimer**
G4	14843	-
G4-PTX	17263	2.53 of PTX
G4-PTX-PEG	38391	10.56 of PEG
G4-PTX-PEG-Biotin	-	20.98 of Biotin (from HABA/Avidin assay)

Table 3.2 Zeta potential values of multifunctional dendrimer conjugates (Mean±SD, n=3).

Dendrimer conjugate	**Zeta potential (mV)**
G4	18.1±2.2
G4-PTX	13.3±1.8
G4-PTX-PEG	6.3±1.26
G4-PTX-PEG-Biotin	4.8±1.35

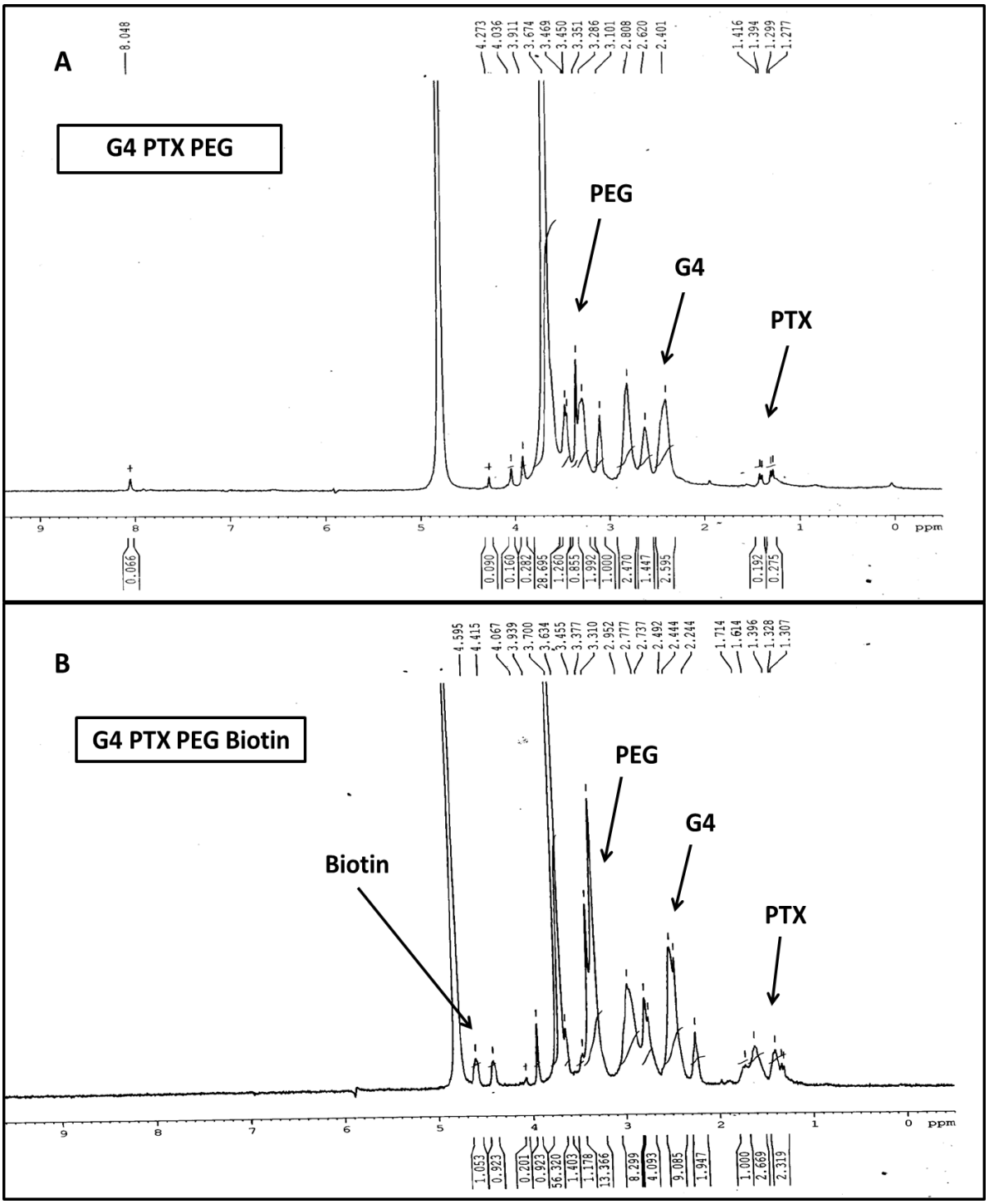

Figure 3.2 ^{1}H NMR spectrum of (A) G4-PTX-PEG and (B) G4-PTX-PEG-Biotin in D2O at 300 MHz.

3.4.3 Cellular Uptake by Confocal microscopy

The uptake of F-G4-PEG and F-G4-PEG-Biotin by the A549 cells after 1 h and 4 h incubation was observed by confocal microscopy. A strong green fluorescence was noticed in the cells treated with biotin targeted dendrimer conjugate compared to the cells treated with the non-targeted ones. The green fluorescence caused by F-G4-PEG-Biotin in cells saturated with free biotin was seen to be less in intensity than the cells without excess biotin. This suggests that the biotin targeted dendrimers internalize actively by the biotin receptors present markedly high on the surface of the A549 cells. The less significant uptake occurring in the presence of free biotin also suggests that the dendrimer conjugates also undergo charge based adsorptive endocytosis. The adsorptive endocytosis of positively charged moieties and the biotin receptor mediated uptake significantly improves the cellular association of the synthesized dendrimer conjugates. Further, the confocal microscopy results are in agreement with flow cytometry data that the cells treated with F-G4-PEG-Biotin demonstrated higher internalization compared to F-G4-PEG at both the time points. Photomicrographs of the cells after 1 h and 4 h incubation were represented in Figure 3.3.

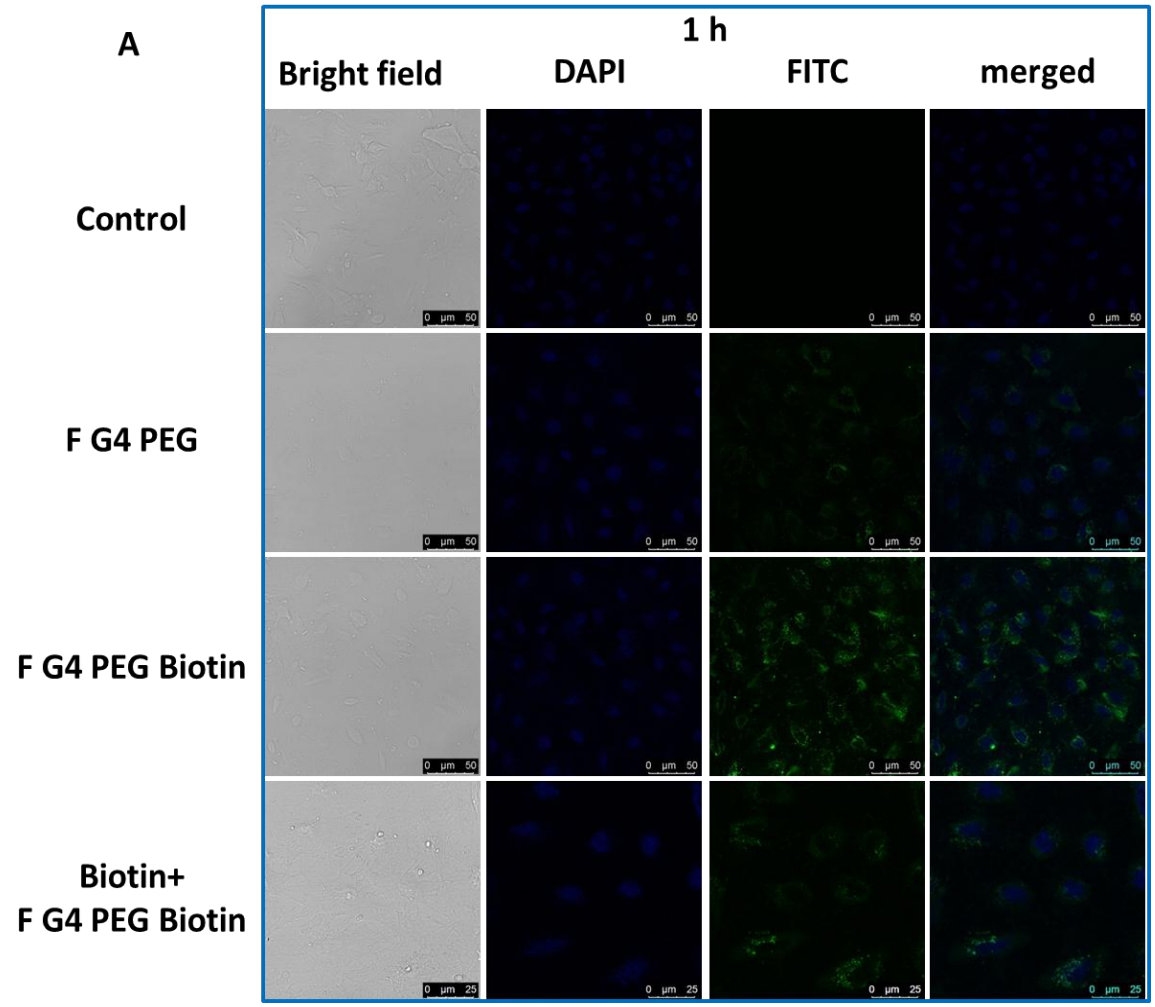
A
1 h
Bright field
DAPI
FITC
merged
Control
F G4 PEG
F G4 PEG Biotin
Biotin+
F G4 PEG Biotin

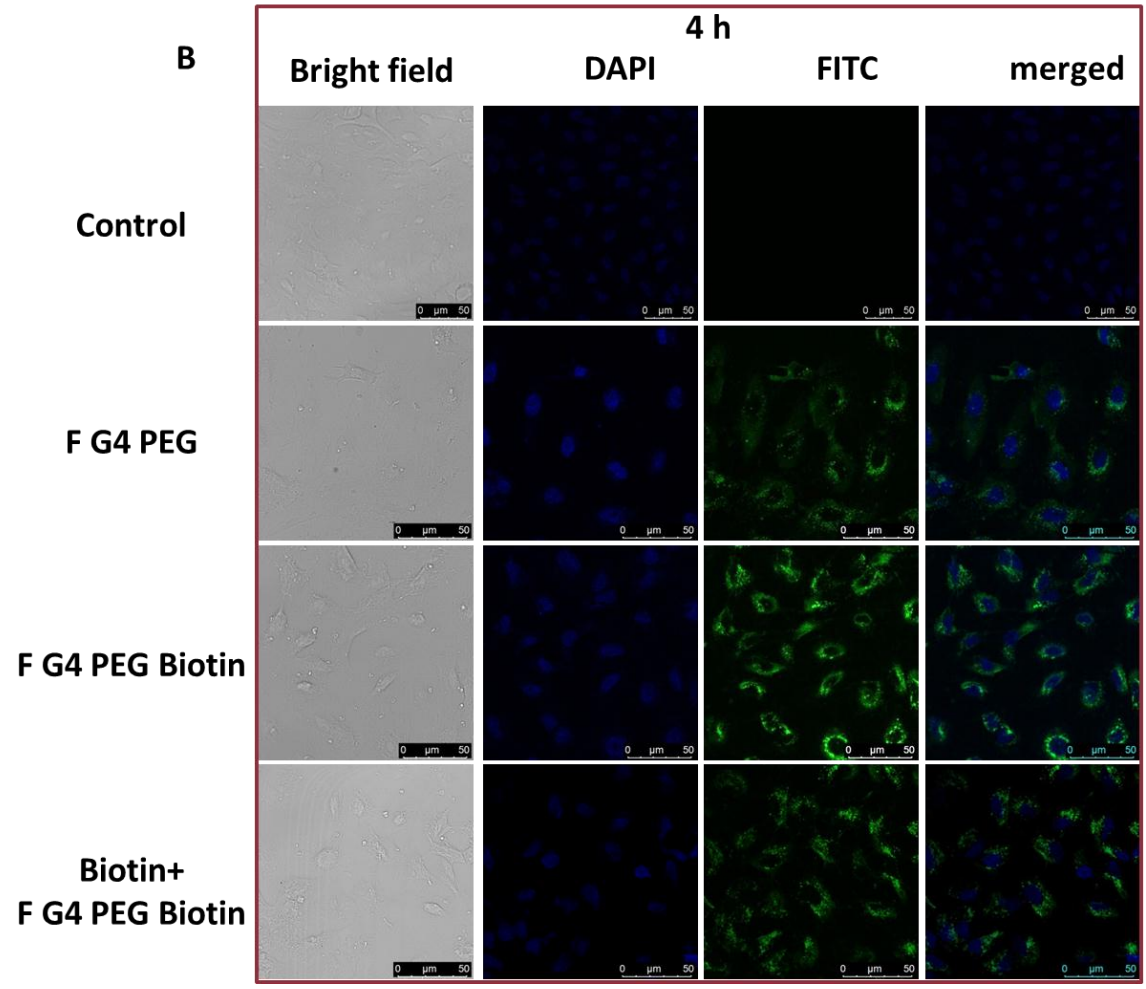

Figure 3.3 Confocal microscopy images of A549 cells after (A) 1 h and (B) 4 h of incubation with F-G4-PEG and F-G4-PEG-Biotin and, Biotin+F-G4-PEG-Biotin.

3.4.4 Cellular uptake by flow cytometry

Quantitative assessment of cellular uptake was made using flow cytometry. Similar to the microscopy studies, influence of free biotin on the uptake of targeted dendrimers was also studied. The saturation of the biotin vitamin transporters resulted in decreased intensity of the fluorescence in the cells treated with F-G4-PEG-Biotin. From the results, a time dependent increase in the uptake was witnessed at 1 h and 4 h treatment. A 1.53 fold and 1.94 fold increase in the uptake was observed at 1 h and 4 h respectively for F-G4-PEG-Biotin compared to F-G4-PEG.

The flow cytometry data indicated that the Biotin tagged dendrimer conjugates were promptly internalized via the biotin receptors. The role of biotin receptors in uptake of actively targeted dendrimer conjugates was understood and the data was in accordance with the confocal microscopy data. Geo Mean Fluorescence of different treatments at 1 h and 4 h was represented as bar graph along with the histograms of events captured by flow cytometer in Figure 3.4.

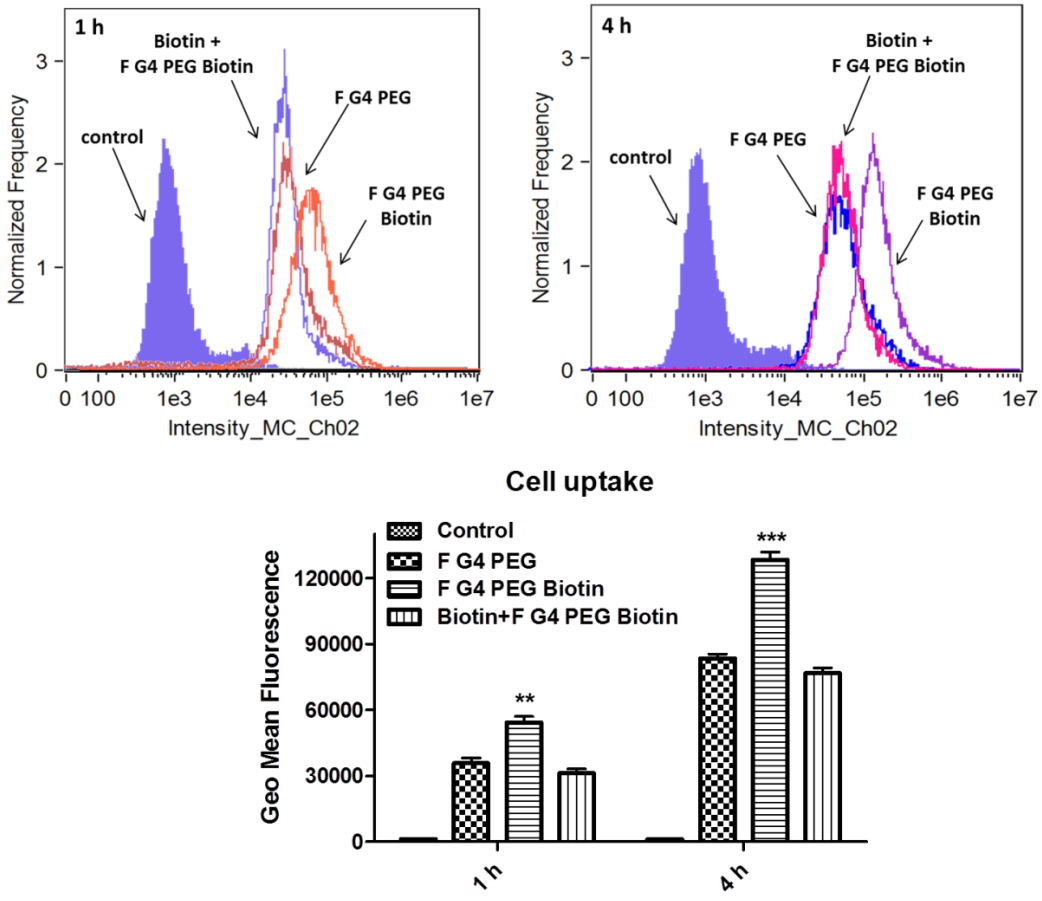

Figure 3.4 Cellular uptake of fluorescently tagged G4 conjugates in A549 cells after 1 h and 4 h incubation as assessed by flow cytometer and represented as histograms and bar graph of geo mean fluorescence (Mean±SD, n=3).

3.4.5 Cytotoxicity Study

The cytotoxic activity displayed by the dendrimer-drug conjugates compared to free drug was calculated by MTT assay. Cells were treated with free PTX, G4-PTX-PEG, and G4-PTX-PEG-Biotin at 0-50 µg/ml concentration and incubated for 24 h and 48 h. The results of the study revealed that there was a decrease in the cell viability with increase in treatment time and concentration of the drug treatment given to the cells (Figure 3.5). Of all the treatments, G4-PTX-PEG-Biotin was found to be more active in killing the cells compared to other treatments. At the end of 24 h, G4-PTX-PEG-Biotin exhibited 32.7±5.14% cell viability against 51.62±3.9% of G4-PTX-PEG and 62.3±3% of free PTX. Further, the cell viability declined to 14.5±3.44%, 29.8±3.2%, and 43.2±2.8% for G4-PTX-PEG-Biotin, G4-PTX-PEG, and free PTX respectively after 48 h treatment. Dendrimer-drug conjugates were more active at all the time points compared to free PTX. Also, G4-PTX-PEG-Biotin had shown highest cytotoxicity which can be attributed to its ability to internalize actively into the cells via the biotin receptors resulting in delivering PTX in higher amount in the tumor cells compared to unmodified G4-PTX-PEG or free PTX. In addition, the uptake of the dendrimer conjugates by receptor mediated/adsorptive endocytosis help avoid the drug efflux by P-glycoprotein. A reason for lesser cytotoxicity noticed in free PTX treated cells could be due to the drug being pushed out of the cell by P-glycoprotein transporter system.

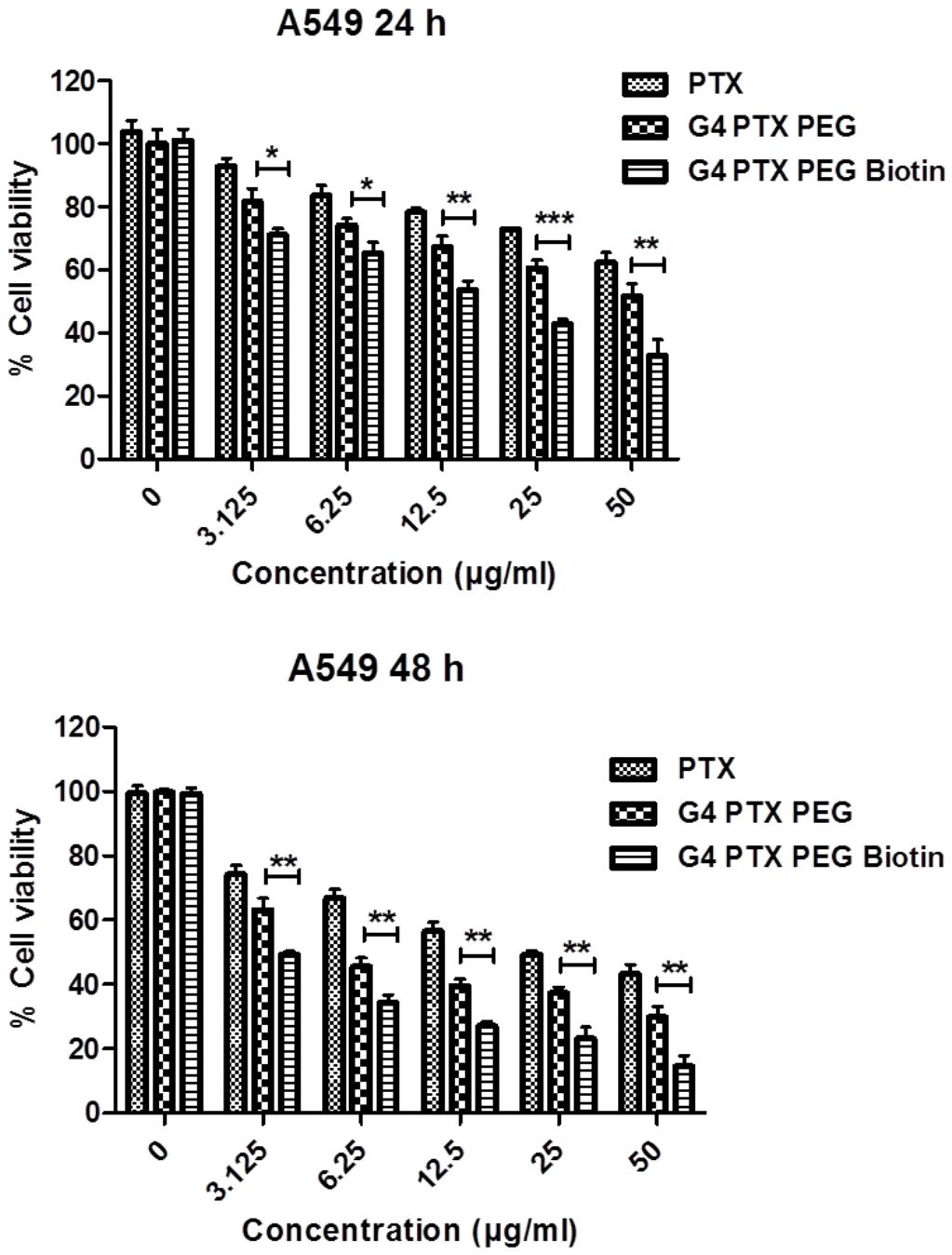

Figure 3.5 Percentage cell viability of A549 cells treated with different concentrations of PTX, G4-PTX-PEG, and G4-PTX-PEG-Biotin at 24 h and 48 h (Mean ± SD; n = 3).

3.4.6 Penetration efficiency in 3D cancer cell spheroids

3D cell culture spheroidal models mimic the *in vivo* tumors terms in terms of tumor structure and tumor microenvironment. 3D spheroids retain cancer cells in a better natural morphology in presence of extracellular matrix, and pH and oxygen gradients. Moreover, 3D spheroid models mimic the drug resistance in solid tumors better than 2D monolayer cell system. (van den Brand et al. 2017; Yang et al. 2017). These features makes the 3D spheroid cancer cell model an attractive alternative to understand the movement of molecules into the cancer tissue.

From the Z-stack images captured using confocal microscopy, it was witnessed that the fluorescence was deeper in spheroids treated with biotin tagged dendrimers in comparison to the untargeted conjugate. Also, with increase in the time of incubation from 1 h to 4 h, the conjugates moved into the core of the spheroids as evidenced by the bright green fluorescence at depths (Figure 3.6). Biotin receptor mediated uptake of F-G4-PEG-Biotin resulted in superior diffusion of dendrimer conjugate into the 3D tumor spheroids. This observation ascertains the advantage of active targeting to tumors by biotinylation of the delivery systems.

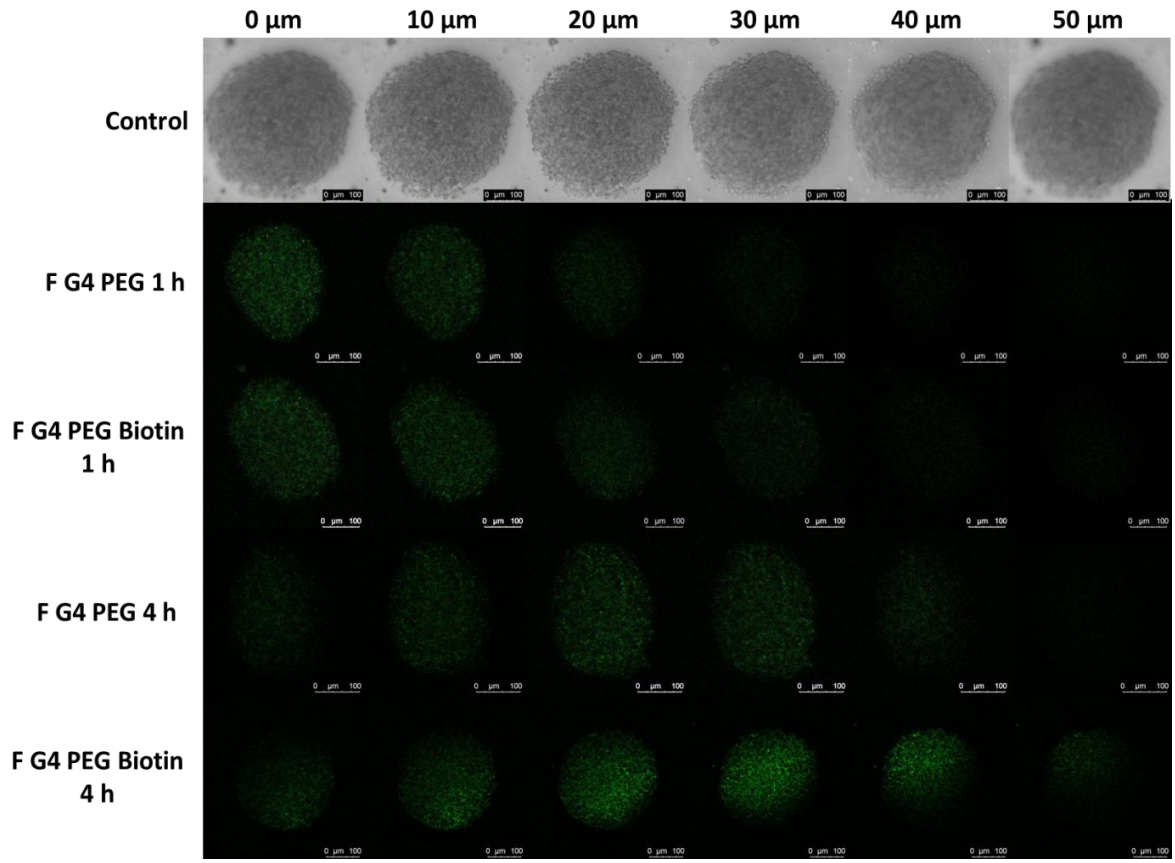

Figure 3.6 (A) Penetration of G4 conjugates in 3D cultured spheroids at various depths after 1 h and 4 h incubation captured as Z-stacks by confocal microscopy.

3.4.8 Uptake of dendrimer conjugates in 3D spheroids by flow cytometry

The internalization of biotin targeted and non-targeted dendrimers in the 3D multicellular cancer spheroids was quantified by flow cytometry. The single cell suspension attained after breaking down of spheroids by Accutase solution was suspended in PBS and analyzed. The fluorescence intensity was observed to be higher with F-G4-PEG-Biotin conjugate treatment compared to F-G4-PEG. The biotin tagged dendrimer conjugate exhibited a 1.63 fold and 1.7 fold higher geo mean fluorescence value in comparison to the F-G4-PEG after 1 h and 4 h of incubation.

The flow cytometry data supports the confocal microscopy results, where time-dependent increase in the accumulation in spheroids was observed. It can be affirmed that the biotin conjugation on the surface remarkably improved the uptake of the dendrimer conjugates. Data obtained after analysis by flow cytometer was represented as Figure 3.7.

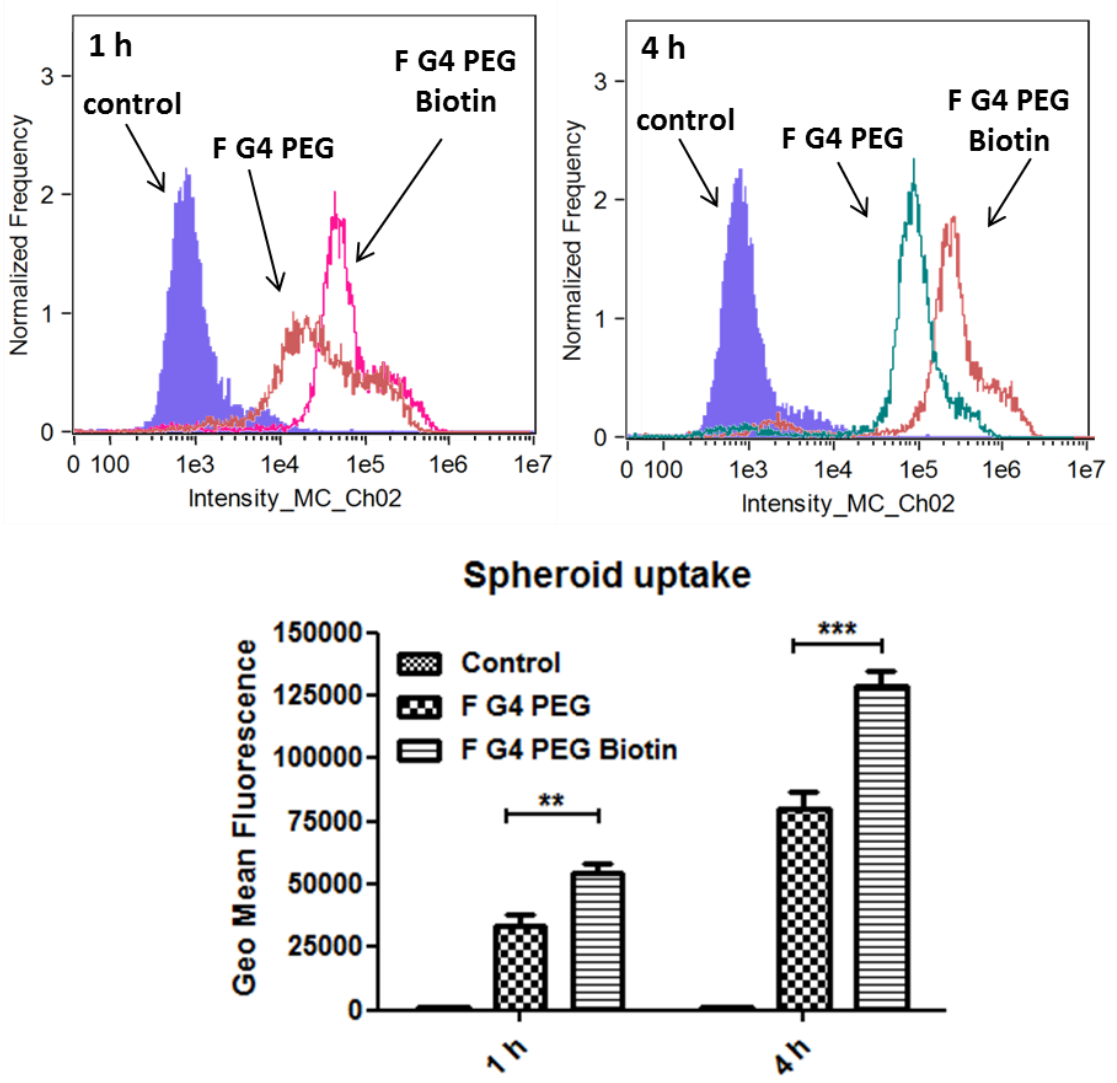

Figure 3.7 Quantitative assessment of cellular uptake in 3D tumor spheroids treated with F-G4-PEG and F-G4-PEG-Biotin by flow cytometry (Mean ± SD; n = 3).

3.4.9 Inhibitory effect of dendrimer conjugates on 3D cancer cell spheroids

Growth inhibition caused due to exposure of multicellular cancer spheroids to free PTX, G4-PTX-PEG, and G4-PTX-PEG-Biotin was evaluated by measuring the diameter of the tumor spheroids over time. The spheroids were examined for 6 days and brightfield images were captured on Day 0, Day 3, and Day 6. The diameter of the spheroids was noted down to analyze the growth of spheroids. As shown in Figure 3.8A, it was observed that the diameter of spheroids was significantly less on treatment with dendrimer conjugates in comparison to free PTX. Moreover, a sweeping increase in the diameter of control spheroids was observed over the period of time in comparison to drug treated spheroids with size reaching up to 1000 µm diameter. The average diameter of spheroids at the end of 6 days was found to be 531.3 ± 13.5 µm, 647 ± 32.6 µm, 791.6 ± 38.2 µm, and 927.3 ± 10 µm after treatment with G4-PTX-PEG-Biotin, G4-PTX-PEG, Free PTX, and control respectively. The plot of diameters of spheroids is represented as a line graph in Figure 3.8B.

This can be explained based on the cellular association data that the active targeting via biotin receptors helped the delivery system to internalize efficiently in-turn leading to localization of PTX in the spheroids subsequently inhibiting their growth progression. This was supported by the uptake studies performed in the 3D spheroid model, where it was observed that the dendrimer conjugate significantly internalized into the spheroids, making more drug available for action at the target location. Since 3D spheroid model mimics in vivo solid tumors, it would not be wrong to extrapolate that the Biotin conjugated dendrimer could significantly reduce the tumor progression *in vivo*.

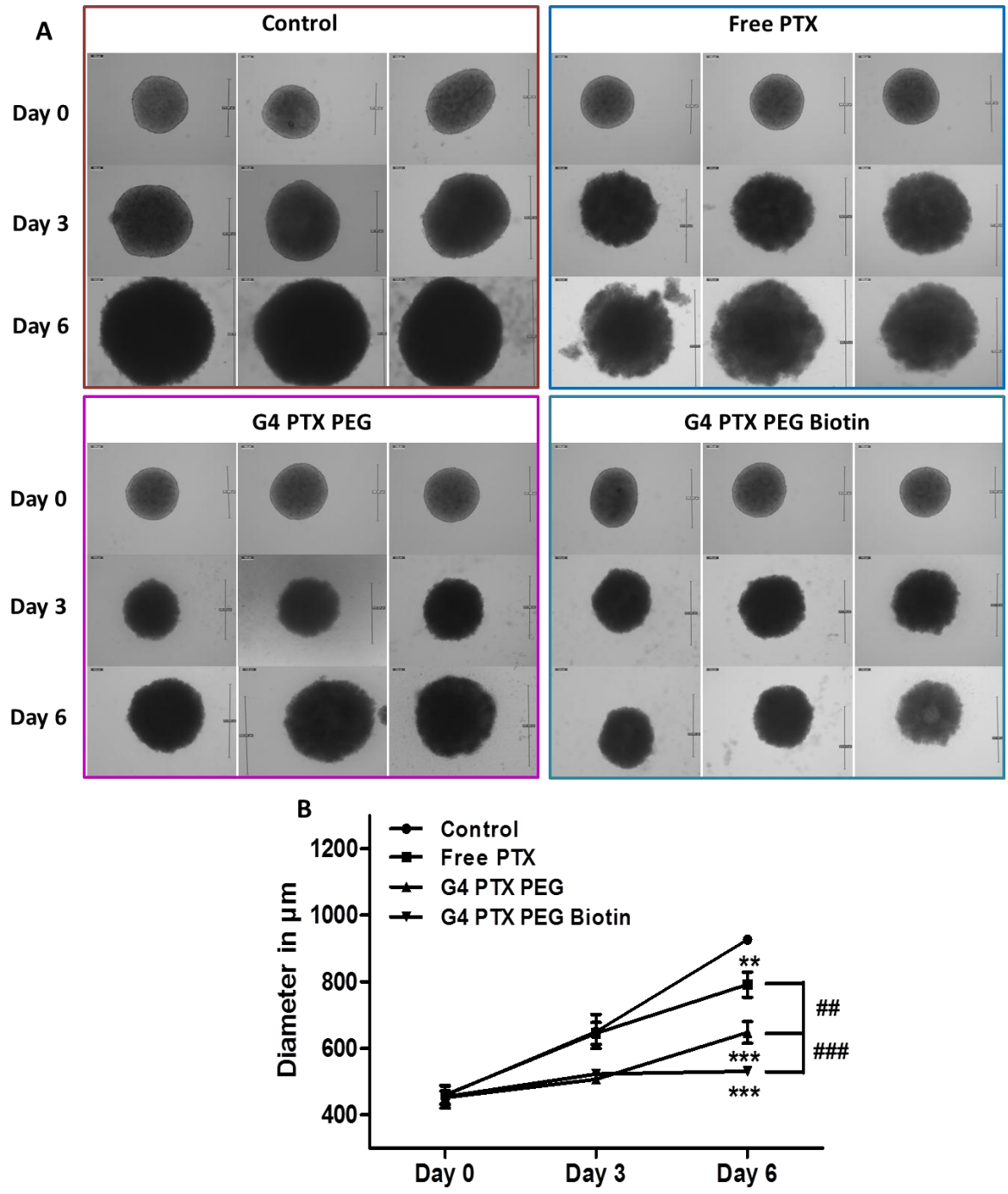

Figure 3.8 (A) Photomicrograph of spheroids after different PTX treatments captured at Day 0, Day 3, and Day 6 using bright field microscope at 10X magnification. (B) Graphical representation of spheroid growth inhibition (Mean of diameter in µm ± SD; n = 3).

3.4.10 In vitro cytotoxicity in spheroids

The reducibility of Presto Blue reagent upon treatment with PTX formulations was used as a measure to quantify the cytotoxic activity exhibited by the formulations in the A549 multicellular spheroids. Treatment of spheroids with G4-PTX-PEG-Biotin and G4-PTX-PEG resulted in higher cytotoxicity in comparison to free PTX after treatment for 24 h. The cytotoxicity was highest in case of G4-PTX-PEG-Biotin with a cell viability of 39.35 ± 2.6% in comparison to G4-PTX-PEG and free PTX with a viability of 50.5 ± 3.7% and 68.9 ± 1.48% respectively. The data is represented as a bar graph in Figure 3.9. The dendrimer conjugates were found to be effective in tumor spheroids as was observed in the monolayers although a slight reduction in cytotoxicity was noted. This can be explained based on the fact that the permeation of carrier system becomes limited in tumor spheroids compared to free access to cells in monolayers. The efficiency of biotin tagged dendrimers to enter the cells actively helps in superior buildup of PTX in cells to show its action.

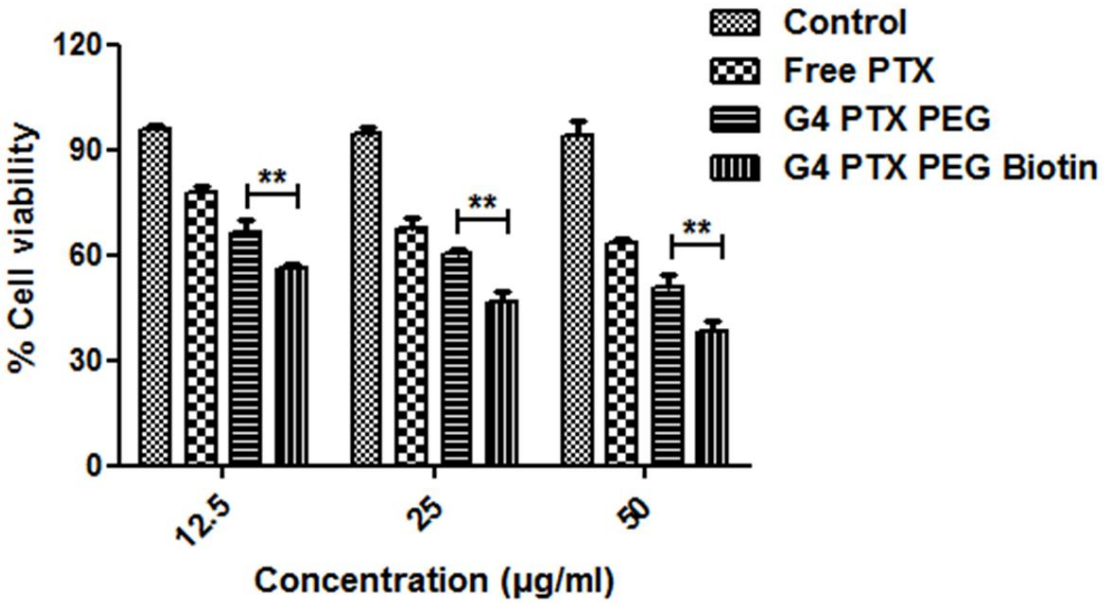

Figure 3.9 In vitro cytotoxicity induced by PTX, G4-PTX-PEG, and G4-PTX-PEG-Biotin at 24 h in tumor spheroids as assessed by Presto Blue assay (Mean of percentage cell viability ± SD; n = 3).

3.4.11 Live/Dead cell assay in 3D spheroids

To study the live and dead cell population induced in the multicellular spheroids as a response to treatment with PTX conjugates, the spheroids were incubated with Calcein Blue AM reagent. When internalized by the live cells, the calcein blue AM produces bright blue fluorescence due to intracellular esterase activity. The dead cells cannot convert the calcein blue AM reagent yielding no fluorescence. The dead cells can be identified by PI staining.

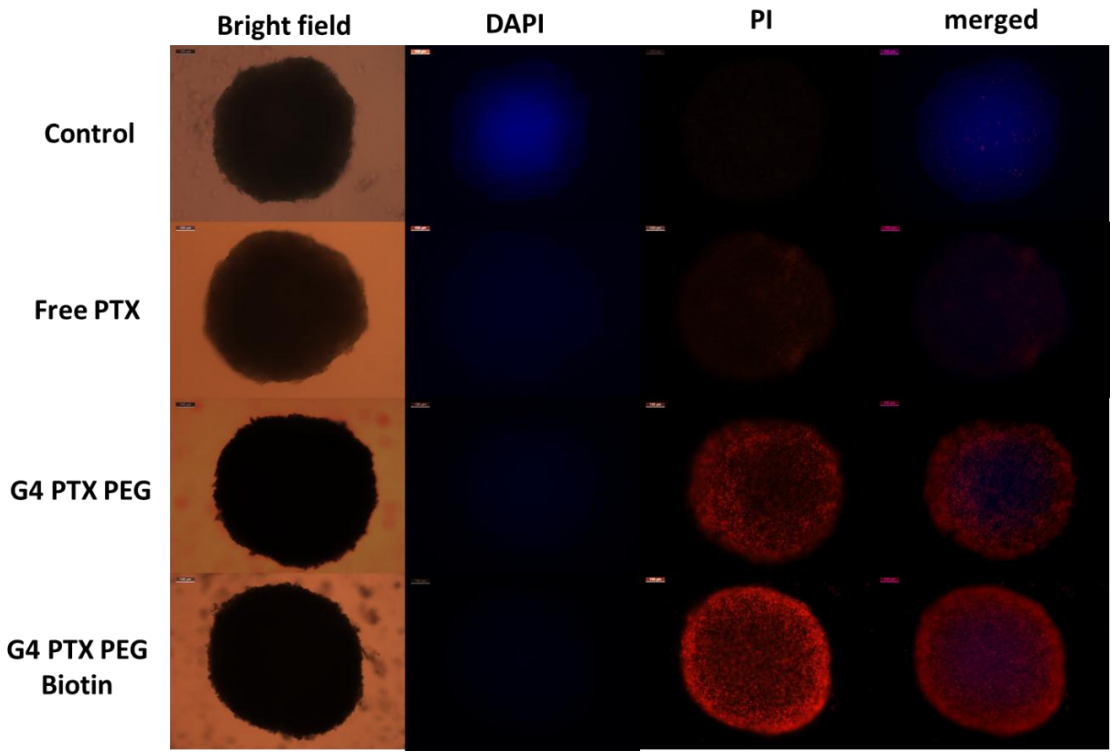

Figure 3.10 Live/dead cell micrographs of tumor spheroids captured using fluorescence microscope at 10X magnification. Red fluorescence (PI) depicts dead population and blue fluorescence (calcein blue) depicts live population.

The fluorescence micrographs of spheroids as represented in Figure 3.10, suggest that the G4-PTX-PEG-Biotin had maximum red fluorescence in comparison to G4-PTX-PEG and free PTX. Control spheroids did not show any significant dead population. Free PTX treated spheroids, dead cells were majorly observed towards the circumference suggesting limited penetration of PTX deeper into the spheroid. In spheroids treated with free PTX, dead population was present mostly on the periphery indicating the inability of free drug to reach deeper parts of spheroid.

On the other hand, with G4-PTX-PEG and G4-PTX-PEG-Biotin treated spheroids, dead cell population was observed clearly on the periphery as well as within the central regions

of spheroid. This indicates significantly better targeting and penetration of G4-PTX-PEG-Biotin in cancer cells.

3.5 Conclusion

In this study, we have developed a G4 PAMAM dendrimer system to deliver paclitaxel (PTX) specifically to the cancer cells by following active-targeting approach. Biotin was anchored on to surface of the dendrimers to target the vitamin uptake receptors overexpressed in the cancer cells. PTX was covalently linked to the surface of the G4 PAMAM dendrimer using a succinate linker. Further, to avoid the toxicity of dendrimers due to their cationic nature, PEG has been attached which also imparts stability and prolonged circulation to the delivery system. Biotin was attached by acid/amine coupling reaction and has been quantified using HABA/Avidin assay. The dendrimer conjugates were characterized by proton NMR and zeta potential analysis which confirmed their formation. GPC analysis of G4-PTX, and G4-PTX-PEG revealed the attachment of around 2.5 molecules of PTX and 10.5 molecules of PEG per molecule of G4 PAMAM dendrimer. From the HABA assay, it was observed that approximately 20.98 molecules of Biotin were present on the surface of dendrimers. Cytotoxicity study by MTT assay and, cellular uptake studies performed on A549 cells revealed that dendrimer–drug conjugates were efficient in cellular internalization and cell killing activity. Biotin saturation studies demonstrated the role of biotin receptor in mediating cellular uptake. Further, in 3D cancer cell spheroids, biotin tagged conjugate displayed superior cytotoxicity, inhibition of growth, and penetration in comparison to non-targeted conjugate and free drug. Considering all the above results, it can be affirmed that the newly developed active targeted dendrimer system could be a promising option for cancer treatment.

Chapter 4

Conclusion

4. CONCLUSION

The drawbacks associated with the conventional chemotherapy have led the researchers on a quest to find alternate approaches for delivery of anti-cancer agents. Nanotechnology is a fast growing area which has profound applications in the field of drug delivery owing to innumerable advantages it offers in medicine. Various Nano drug delivery systems have been investigated in the anti-cancer drug delivery in an attempt to overcome the problems faced by most of the drugs such as low solubility, non-specific drug distribution, unwanted adverse effects, systemic toxicity, drug resistance to name a few. Poly(amidoamine) dendrimers (PAMAM) are a class of branched polymers which are characterized by well-defined architecture, size and monodispersity. PAMAM dendrimers have been explored to deliver anti-cancer agents either by physical entrapment in the internal cavities or by covalently conjugating them to the wide variety and number of functional groups they offer. The current study was designed to utilise the advantages of PAMAM dendrimers in delivery of a chemotherapeutic molecule, paclitaxel (PTX) whose therapeutic potential is limited by its poor physicochemical properties. Further, to improve the delivery of PTX intracellularly, PAMAM dendrimers are modified on surface with a cell penetrating peptide (CPP), octa-arginine (R8) or with biotin, which actively targets the biotin vitamin uptake receptors overexpressed on the surface of cancer cells. PEGylation was performed to reduce the toxicity of cationic PAMAM dendrimers and prolonged blood circulation. The dendrimers were fluorescently labelled for experiments which need fluorescence measurement. The proton NMR spectra of dendrimer conjugates revealed successful attachment of different functional moieties. Further, GPC analysis gave an approximation of number of molecules attached per dendrimer molecule. The change in zeta potential values with each step of synthesis also supports the formation of conjugates.

In the first part of the work, octa-arginine (R8) was used to deliver PTX intracellularly to human cervical cancer (HeLa) cells. The synthesized dendrimer system was found to be non-toxic to blood cells in haemolytic assay. The cellular uptake of G4-PTX-PEG-R8 in vitro was significantly higher than the unmodified conjugate and the cellular association improved with time as assessed by confocal microscopy and flow cytometry experiments. MTT assay results revealed that dendrimer conjugates conferred maximum cytotoxicity to cancer cells in comparison to free drug after 24 h and 48 h treatment. Also, the G4-PTX-PEG-R8 induced higher apoptosis in HeLa cells which can be attributed to the greater cellular uptake and hence more availability of drug in the cells. Further, the dendrimer conjugates were evaluated in 3D multicellular HeLa spheroids. The ability of R8 to internalize deeper into the tissues has resulted in increased permeation, uptake, growth inhibition, and cytotoxicity of R8-modified dendrimer conjugates over G4-PTX-PEG and free PTX in the spheroid model. As the spheroids mimic the microenvironment of in vivo cancers, it can be fairly said that the developed G4-PTX-PEG-R8 can efficiently deliver PTX intracellularly to tumor tissues. Attachment of octa-arginine (R8) greatly influenced the cellular association of the dendrimer construct. However, the localization of this system in tumor tissues would solely rely on the EPR effect, a passive diffusion phenomenon.

In the later part of this work, Biotin, a small molecule ligand has been tagged on surface of PAMAM dendrimers to actively target the cancer cells overexpressing biotin receptors (A549). HABA/Avidin assay revealed an attachment of around 20.98 molecules of biotin per dendrimer. The active targeting of cancer cells by biotin has significantly improved the cellular uptake and cytotoxicity caused by G4-PTX-PEG-Biotin over G4-PTX-PEG and free PTX. Saturation of biotin receptors by excess free biotin revealed that the uptake mechanism was receptor mediated. Also, due to the cationic nature of the

dendrimer conjugates, adsorptive endocytosis also adds to the uptake mechanisms. Further, the evaluation in multicellular A549 cell spheroids resulted in biotin tagged conjugates being more effective in therapeutic outcome by inhibition of spheroid growth and cell killing. The designed biotin conjugate is selective to cancer cells overexpressing biotin receptors and can minimize non-specific toxicities.

The surface modification of PAMAM dendrimers with PEG imparted the required biocompatibility to be able to employ them as delivery carrier for PTX without any carrier mediated toxicity. The covalent attachment of PTX to G4 PAMAM dendrimer by a succinate linker gives an advantage of preventing drug loss during circulation which helps tune the release specifically in the tumor environment besides solubility enhancement. Also, the conjugation has significantly increased the cytotoxic potential of the PTX than the pure drug alone. Further, the attachment of both targeting moieties R8 and biotin on the surface showed a positive influence on the cellular internalization and biological activity of the conjugate in comparison to the unmodified ones suggesting the benefits of tumor targeting.

Overall, the developed multifunctional dendrimer-drug conjugates could be an effective treatment strategy in delivery of poorly soluble chemotherapeutic agents to cancer tissues.

Future Perspectives

Over the past few decades, dendrimers have evolved from a concept to becoming a new class of polymers with a distinctive structural design and flexible chemical configurations. Advancement in the polymerization and synthetic procedures have paved a way to the progress of well-structured dendrimers with a high number of surface functionalities that can be employed to hold a variety of biological moieties including peptides, proteins, sugars, and targeting agents while carrying a large therapeutic payload either in the interior pockets of the dendrimers or on their surface.

The greater entrapment capability of dendrimers makes them extremely attractive carriers for delivering anti-cancer drugs to tumor tissue for cancer treatment. The surface of dendrimers can be fabricated to attach ligands or peptides such as cell penetrating peptides along with receptor specific targeting ligands together which serve different functions making them dual-targeted delivery systems. In addition, dendrimers are suited for administration via most of the routes including intravenous, ocular, transdermal, oral, and intranasal along with possibility of active or passive targeting of drugs. This strategy of targeting is a part of 'precision medicine' approach which can deliver the bioactives/contrast agents to exact location where action is needed.

The developed dendrimer system can be explored to deliver other anti-cancer agents whose clinical potential is compromised due to their poor physico-chemical properties. We anticipate that future exploration will emphasize on the rational design and creation of specific linkers that will be recognized and cleaved selectively by enzymatic and chemical environment present exclusively in the tumor cells offering

superior level of governance over the location and rate of anti-cancer drug release from dendrimer-drug conjugates.

More precision in synthesis of dendrimer conjugates having a control over each step and in a cost-effective way, reducing batch-to-batch variation in terms of number of molecules of each type attached to the dendrimer molecule, and further understanding of dendrimer characteristics may lead to successful clinical translation of the developed dendrimer system. Also, the variations in the biodistribution and pharmacokinetic profile, drug release, and stability of the dendrimer based delivery system with the type and magnitude of the modification needs thorough investigation to be able to predict their in vivo behavior in a clinical setup.

Further research is warranted for better understanding of the absorption and uptake mechanisms of dendrimer based nanomedicine in the body to translate into clinically viable targeting approach for delivery of chemotherapeutics in cancer.

Overall, the future appears extremely promising for the dendrimer based nanomedicine in targeted anti-cancer therapies.

Bibliography

Abraham, Sheela A, Dawn N Waterhouse, Lawrence D Mayer, Pieter R Cullis, Thomas D Madden, and Marcel B Bally. 2005. 'The liposomal formulation of doxorubicin.' in, *Methods in Enzymology* (Elsevier).

Agrahari, Vivek. 2017. 'The exciting potential of nanotherapy in brain-tumor targeted drug delivery approaches', *Neural Regeneration Research*, 12: 197-200.

Akhter, Md Habban, Md Rizwanullah, Javed Ahmad, Mohamed Jawed Ahsan, Md Ali Mujtaba, and Saima Amin. 2017. 'Nanocarriers in advanced drug targeting: setting novel paradigm in cancer therapeutics', *Artificial Cells, Nanomedicine, and Biotechnology*: 1-12.

Asthana, Abhay, Abhay Singh Chauhan, Prakash Vamanrao Diwan, and Narendra Kumar Jain. 2005. 'Poly (amidoamine)(PAMAM) dendritic nanostructures for controlled sitespecific delivery of acidic anti-inflammatory active ingredient', *AAPS PharmSciTech*, 6: E536-E42.

Babu, Anish, Amanda K Templeton, Anupama Munshi, and Rajagopal Ramesh. 2014. 'Nanodrug delivery systems: a promising technology for detection, diagnosis, and treatment of cancer', *AAPS PharmSciTech*, 15: 709-21.

Bae, You Han. 2009. 'Drug targeting and tumor heterogeneity', *Journal of controlled release: official journal of the Controlled Release Society*, 133: 2.

Bannon-Peppas, L, and JO Blanchette. 2004. 'Nanoparticle and targeted system for cancer therapy', *Adv. Drug Deliv. Rev*, 56: 1649-59.

Barth, Rolf F, Gong Wu, Weilian Yang, Peter J Binns, Kent J Riley, Hemant Patel, Jeffrey A Coderre, Werner Tjarks, AK Bandyopadhyaya, and BTS

Thirumamagal. 2004. 'Neutron capture therapy of epidermal growth factor (+) gliomas using boronated cetuximab (IMC-C225) as a delivery agent', *Applied radiation and isotopes*, 61: 899-903.

Bar-Zeev, Maya, Yoav D Livney, and Yehuda G Assaraf. 2017. 'Targeted nanomedicine for cancer therapeutics: Towards precision medicine overcoming drug resistance', *Drug Resistance Updates*, 31: 15-30.

Bellocq, Nathalie C, Suzie H Pun, Gregory S Jensen, and Mark E Davis. 2003. 'Transferrin-containing, cyclodextrin polymer-based particles for tumor-targeted gene delivery', *Bioconjugate chemistry*, 14: 1122-32.

Bhadra, D, S Bhadra, S Jain, and NK Jain. 2003. 'A PEGylated dendritic nanoparticulate carrier of fluorouracil', *International journal of pharmaceutics*, 257: 111-24.

Bhadra, Dipankar, Sulekha Bhadra, and NK Jain. 2005. 'Pegylated lysine based copolymeric dendritic micelles for solubilization and delivery of artemether', *J Pharm Pharm Sci*, 8: 467-82.

Biswas, Swati, Namita S Dodwadkar, Pranali P Deshpande, Shruti Parab, and Vladimir P Torchilin. 2013. 'Surface functionalization of doxorubicin-loaded liposomes with octa-arginine for enhanced anticancer activity', *European Journal of Pharmaceutics and Biopharmaceutics*, 84: 517-25.

Biswas, Swati, Namita S. Dodwadkar, Aleksandr Piroyan, and Vladimir P. Torchilin. 2012. 'Surface conjugation of triphenylphosphonium to target poly(amidoamine) dendrimers to mitochondria', *Biomaterials*, 33: 4773-82.

Biswas, Swati, Pranali P Deshpande, Federico Perche, Namita S Dodwadkar, Shailendra D Sane, and Vladimir P Torchilin. 2013. 'Octa-arginine-modified

pegylated liposomal doxorubicin: an effective treatment strategy for non-small cell lung cancer', *Cancer Letters*, 335: 191-200.

Biswas, Swati, Pranali P Deshpande, Gemma Navarro, Namita S Dodwadkar, and Vladimir P Torchilin. 2013. 'Lipid modified triblock PAMAM-based nanocarriers for siRNA drug co-delivery', *Biomaterials*, 34: 1289-301.

Bobo, Daniel, Kye J Robinson, Jiaul Islam, Kristofer J Thurecht, and Simon R Corrie. 2016. 'Nanoparticle-based medicines: a review of FDA-approved materials and clinical trials to date', *Pharmaceutical Research*, 33: 2373-87.

Bolhassani, Azam, Behnaz Sadat Jafarzade, and Golnaz Mardani. 2017. 'In vitro and in vivo delivery of therapeutic proteins using cell penetrating peptides', *Peptides*, 87: 50-63.

Bray, F., J. S. Ren, E. Masuyer, and J. Ferlay. 2013. 'Global estimates of cancer prevalence for 27 sites in the adult population in 2008', *Int J Cancer*, 132: 1133-45.

Brigger, I., C. Dubernet, and P. Couvreur. 2002. 'Nanoparticles in cancer therapy and diagnosis', *Advanced drug delivery reviews*, 54: 631-51.

Bu, Le, Liang-Chun Gan, Xiao-Qiang Guo, Feng-Zheng Chen, Qin Song, Xiao-Jun Gou, Shi-Xiang Hou, and Qian Yao. 2013. 'Trans-resveratrol loaded chitosan nanoparticles modified with biotin and avidin to target hepatic carcinoma', *International Journal of Pharmaceutics*, 452: 355-62.

Byrne, James D, Tania Betancourt, and Lisa Brannon-Peppas. 2008. 'Active targeting schemes for nanoparticle systems in cancer therapeutics', *Advanced drug delivery reviews*, 60: 1615-26.

'Cancer Registration and Surveillance Modules'. U. S. National Institutes of Health, National Cancer Institute, Accessed 8, May 2018. https://training.seer.cancer.gov/disease/cancer/.

'Cancer Statistics'. Accessed 09 April 2018. http://cancerindia.org.in/statistics/.

Celik, F, C Gocmez, M Bozkurt, I Kaplan, K Kamasak, E Akil, E Dogan, A Guzel, and E Uzar. 2013. 'Neuroprotective effects of carvacrol and pomegranate against methotrexate-induced toxicity in rats', *European Review for Medical and Pharmacological Sciences*, 17: 2988-93.

Cerrato, Carmine Pasquale, Kadri Künnapuu, and Ülo Langel. 2017. 'Cell-penetrating peptides with intracellular organelle targeting', *Expert opinion on drug delivery*, 14: 245-55.

Chai, Stella, Kenneth KW To, and Ge Lin. 2010. 'Circumvention of multi-drug resistance of cancer cells by Chinese herbal medicines', *Chinese Medicine*, 5: 26.

Chen, Shuyi, Xianrui Zhao, Jingyi Chen, Jin Chen, Larisa Kuznetsova, Stanislaus S. Wong, and Iwao Ojima. 2010. 'Mechanism-Based Tumor-Targeting Drug Delivery System. Validation of Efficient Vitamin Receptor-Mediated Endocytosis and Drug Release', *Bioconjugate chemistry*, 21: 979-87.

Cheng, Yiyun, Zhenhua Xu, Minglu Ma, and Tongwen Xu. 2008. 'Dendrimers as drug carriers: applications in different routes of drug administration', *Journal of pharmaceutical sciences*, 97: 123-43.

Chidambaram, Moorthi, R Manavalan, and K Kathiresan. 2011. 'Nanotherapeutics to overcome conventional cancer chemotherapy limitations', *Journal of Pharmacy & Pharmaceutical Sciences*, 14: 67-77.

Conniot, João, Joana M Silva, Joana G Fernandes, Liana C Silva, Rogério Gaspar, Steve Brocchini, Helena F Florindo, and Teresa S Barata. 2014. 'Cancer immunotherapy: nanodelivery approaches for immune cell targeting and tracking', *Frontiers in chemistry*, 2: 105.

Cui, Yani, Junhui Sui, Mengmeng He, Zhiyi Xu, Yong Sun, Jie Liang, Yujiang Fan, and Xingdong Zhang. 2016. 'Reduction-degradable polymeric micelles decorated with parg for improving anticancer drug delivery efficacy', *ACS Applied Materials & Interfaces*, 8: 2193-203.

Debnath, Shawon, Darin Saloum, Sukanta Dolai, Chong Sun, Saadyah Averick, Krishnaswami Raja, and Jimmie E Fata. 2013. 'Dendrimer-curcumin conjugate: a water soluble and effective cytotoxic agent against breast cancer cell lines', *Anti-Cancer Agents in Medicinal Chemistry (Formerly Current Medicinal Chemistry-Anti-Cancer Agents)*, 13: 1531-39.

D'emanuele, Antony, Rachaneekorn Jevprasesphant, Jeffrey Penny, and David Attwood. 2004. 'The use of a dendrimer-propranolol prodrug to bypass efflux transporters and enhance oral bioavailability', *Journal of controlled release*, 95: 447-53.

Deshpande, Pranali, Aditi Jhaveri, Bhushan Pattni, Swati Biswas, and Vladimir Torchilin. 2018. 'Transferrin and octaarginine modified dual-functional liposomes with improved cancer cell targeting and enhanced intracellular delivery for the treatment of ovarian cancer', *Drug Delivery*, 25: 517-32.

Dissanayake, Shama, William A. Denny, Swarna Gamage, and Vijayalekshmi Sarojini. 2017. 'Recent developments in anticancer drug delivery using cell

penetrating and tumor targeting peptides', *Journal of Controlled Release*, 250: 62-76.

Dubikovskaya, Elena A, Steve H Thorne, Thomas H Pillow, Christopher H Contag, and Paul A Wender. 2008. 'Overcoming multidrug resistance of small-molecule therapeutics through conjugation with releasable octaarginine transporters', *Proceedings of the National Academy of Sciences*, 105: 12128-33.

Duncan, Ruth, and Lorella Izzo. 2005. 'Dendrimer biocompatibility and toxicity', *Advanced drug delivery reviews*, 57: 2215-37.

Duncan, Ruth. 2003. 'The dawning era of polymer therapeutics', *Nature reviews Drug discovery*, 2: 347.

Esfand, Roseita, and Donald A Tomalia. 2001. 'Poly (amidoamine)(PAMAM) dendrimers: from biomimicry to drug delivery and biomedical applications', *Drug discovery today*, 6: 427-36.

Estanqueiro, Marilene, Maria Helena Amaral, Jaime Conceição, and José Manuel Sousa Lobo. 2015. 'Nanotechnological carriers for cancer chemotherapy: The state of the art', *Colloids and Surfaces B: Biointerfaces*, 126: 631-48.

Ferlay, J., H. R. Shin, F. Bray, D. Forman, C. Mathers, and D. M. Parkin. 2010. 'Estimates of worldwide burden of cancer in 2008: GLOBOCAN 2008', *Int J Cancer*, 127: 2893-917.

Ferlay, J., I. Soerjomataram, R. Dikshit, S. Eser, C. Mathers, M. Rebelo, D. M. Parkin, D. Forman, and F. Bray. 2015. 'Cancer incidence and mortality worldwide: sources, methods and major patterns in GLOBOCAN 2012', *Int J Cancer*, 136: E359-86.

Floor, S. L., J. E. Dumont, C. Maenhaut, and E. Raspe. 2012. 'Hallmarks of cancer: of all cancer cells, all the time?', *Trends Mol Med*, 18: 509-15.

Freres, P., G. Jerusalem, and M. Moonen. 2017. 'Chapter 2 - Categories of Anticancer Treatments.' in Patrizio Lancellotti, Jose L. Zamorano Gómez and Maurizio Galderisi (eds.), *Anti-Cancer Treatments and Cardiotoxicity* (Academic Press: Boston).

Fu, Fanfan, Yilun Wu, Jingyi Zhu, Shihui Wen, Mingwu Shen, and Xiangyang Shi. 2014. 'Multifunctional lactobionic acid-modified dendrimers for targeted drug delivery to liver cancer cells: investigating the role played by PEG spacer', *ACS applied materials & interfaces*, 6: 16416-25.

Gerber, David E. 2008. 'Targeted therapies: a new generation of cancer treatments', *American Family Physician*, 77.

Gillies, Elizabeth R, and Jean MJ Frechet. 2005. 'Dendrimers and dendritic polymers in drug delivery', *Drug discovery today*, 10: 35-43.

Greish, Khaled. 2007. 'Enhanced permeability and retention of macromolecular drugs in solid tumors: a royal gate for targeted anticancer nanomedicines', *Journal of drug targeting*, 15: 457-64.

Griffiths AJF, Miller JH, Suzuki DT, et al. 2000. *An Introduction to Genetic Analysis* (W. H. Freeman: New York).

Gullotti, Emily, and Yoon Yeo. 2009. 'Extracellularly activated nanocarriers: a new paradigm of tumor targeted drug delivery', *Molecular pharmaceutics*, 6: 1041-51.

Guo, Hejian, Dianrui Zhang, Tingting Li, Caiyun Li, Yuanyuan Guo, Guangpu Liu, Leilei Hao, Jingyi Shen, Lisi Qi, and Xinquan Liu. 2014. 'In vitro and in vivo

study of Gal-OS self-assembled nanoparticles for liver-targeting delivery of doxorubicin', *Journal of Pharmaceutical Sciences*, 103: 987-93.

Hackett, Gavin S. 2012. 'Intracellular delivery of therapeutic antibodies', University of Nottingham.

Hanahan, Douglas, and Robert A Weinberg. 2011. 'Hallmarks of Cancer: The Next Generation', *Cell*, 144: 646-74.

Hao, Mengze, Fengju Song, Xiaoling Du, Guowen Wang, Yun Yang, Kexin Chen, and Jilong Yang. 2015. 'Advances in targeted therapy for unresectable melanoma: new drugs and combinations', *Cancer Letters*, 359: 1-8.

Hartwell, LH, and TA Weinert. 1989. 'Checkpoints: controls that ensure the order of cell cycle events', *Science*, 246: 629-34.

He, Hai, Yan Li, Xin-Ru Jia, Ju Du, Xue Ying, Wan-Liang Lu, Jin-Ning Lou, and Yan Wei. 2011. 'PEGylated Poly (amidoamine) dendrimer-based dual-targeting carrier for treating brain tumors', *Biomaterials*, 32: 478-87.

He, Xuedan, Carla S Alves, Nilsa Oliveira, João Rodrigues, Jingyi Zhu, István Bányai, Helena Tomás, and Xiangyang Shi. 2015. 'RGD peptide-modified multifunctional dendrimer platform for drug encapsulation and targeted inhibition of cancer cells', *Colloids and Surfaces B: Biointerfaces*, 125: 82-89.

Heldin, Carl-Henrik, Kristofer Rubin, Kristian Pietras, and Arne Östman. 2004. 'High interstitial fluid pressure—an obstacle in cancer therapy', *Nature Reviews Cancer*, 4: 806.

Horwitz, SB. 1994. 'Taxol (paclitaxel): mechanisms of action', *Annals of oncology: official journal of the European Society for Medical Oncology*, 5: S3-6.

Ingole, Sangita P, Aruna U Kakde, and Priti B Bonde. 2016. 'A Review on Statistics of Cancer in India'.

Jain, Keerti, Prashant Kesharwani, Umesh Gupta, and NK Jain. 2010. 'Dendrimer toxicity: Let's meet the challenge', *International Journal of Pharmaceutics*, 394: 122-42.

Jansen, Johan FGA, and EW Meijer. 1994. 'Encapsulation of guest molecules into a dendritic box', *Science*, 266: 1226-29.

Jia, Xiao, and Lee Jia. 2012. 'Nanoparticles improve biological functions of phthalocyanine photosensitizers used for photodynamic therapy', *Current Drug Metabolism*, 13: 1119-22.

Jiang, Yan-Yan, Guo-Tao Tang, Li-Hong Zhang, Shu-Yi Kong, Sai-Jie Zhu, and Yuan-Ying Pei. 2010. 'PEGylated PAMAM dendrimers as a potential drug delivery carrier: in vitro and in vivo comparative evaluation of covalently conjugated drug and noncovalent drug inclusion complex', *Journal of Drug Targeting*, 18: 389-403.

Kakde, Deepak, Deepti Jain, Vivek Shrivastava, Rajendra Kakde, and AT Patil. 2011. 'Cancer therapeutics-opportunities, challenges and advances in drug delivery'.

Kang, Min Hyung, Min Jung Park, Hyun Joon Yoo, Kwon Yie hyuk, Sang Gon Lee, Sung Rae Kim, Dong Woo Yeom, Myung Joo Kang, and Young Wook Choi. 2014. 'RIPL peptide (IPLVVPLRRRRRRRRC)-conjugated liposomes for enhanced intracellular drug delivery to hepsin-expressing cancer cells', *European Journal of Pharmaceutics and Biopharmaceutics*, 87: 489-99.

Kesharwani, Prashant, and Arun K Iyer. 2015. 'Recent advances in dendrimer-based nanovectors for tumor-targeted drug and gene delivery', *Drug discovery today*, 20: 536-47.

Kesharwani, Prashant, Keerti Jain, and Narendra Kumar Jain. 2014. 'Dendrimer as nanocarrier for drug delivery', *Progress in Polymer Science*, 39: 268-307.

Khalil, Ikramy A, and Hideyoshi Harashima. 2018. 'An Efficient PEGylated Gene Delivery System with Improved Targeting: Synergism between Octaarginine and a Fusogenic Peptide', *International Journal of Pharmaceutics*.

Khalil, Ikramy A, Kentaro Kogure, Shiroh Futaki, and Hideyoshi Harashima. 2006. 'High density of octaarginine stimulates macropinocytosis leading to efficient intracellular trafficking for gene expression', *Journal of Biological Chemistry*, 281: 3544-51.

Khandare, Jayant J, Sreeja Jayant, Ajay Singh, Pooja Chandna, Yang Wang, Nicholi Vorsa, and Tamara Minko. 2006. 'Dendrimer versus linear conjugate: influence of polymeric architecture on the delivery and anticancer effect of paclitaxel', *Bioconjugate chemistry*, 17: 1464-72.

Kitagishi, Hiroaki, Fumihiko Chai, Shigeru Negi, Yukio Sugiura, and Koji Kano. 2015. 'Supramolecular intracellular delivery of an anionic porphyrin by octaarginine-conjugated per-O-methyl-β-cyclodextrin', *Chemical Communications*, 51: 2421-24.

Kloß, Alexander, Peter Henklein, Dagmar Siele, Marion Schmolke, Sébastien Apcher, Lothar Kuehn, Paul W Sheppard, and Burkhardt Dahlmann. 2009. 'The cell-penetrating peptide octa-arginine is a potent inhibitor of proteasome

activities', *European Journal of Pharmaceutics and Biopharmaceutics*, 72: 219-25.

Köhler, Georges, and Cesar Milstein. 1975. 'Continuous cultures of fused cells secreting antibody of predefined specificity', *Nature*, 256: 495.

Koren, Erez, and Vladimir P Torchilin. 2012. 'Cell-penetrating peptides: breaking through to the other side', *Trends in Molecular Medicine*, 18: 385-93.

Koshkaryev, Alexander, Aleksandr Piroyan, and Vladimir P Torchilin. 2013. 'Bleomycin in octaarginine-modified fusogenic liposomes results in improved tumor growth inhibition', *Cancer Letters*, 334: 293-301.

Kulhari, Hitesh, Deep Pooja, Shweta Shrivastava, Madhusudana Kuncha, VGM Naidu, Vipul Bansal, Ramakrishna Sistla, and David J Adams. 2016. 'Trastuzumab-grafted PAMAM dendrimers for the selective delivery of anticancer drugs to HER2-positive breast cancer', *Scientific reports*, 6: 23179.

Kumari, Preeti, Omkara Swami Muddineti, Sri Vishnu Kiran Rompicharla, Pratyusha Ghanta, Adithya Karthik BBN, Balaram Ghosh, and Swati Biswas. 2017. 'Cholesterol-conjugated poly (D, L-lactide)-based micelles as a nanocarrier system for effective delivery of curcumin in cancer therapy', *Drug Delivery*, 24: 209-23.

Kuwada, Eri, Toshimasa Tadaki, Kaori Kambara, Kohji Egawa, and Katsuo Noguchi. 2011. 'Conjugation to octa-arginine via disulfide bonds confers solubility to denatured proteins in physiological solution and enables efficient cell internalization', *Biotechnology and applied biochemistry*, 58: 439-48.

Kwak, Tae Won, Do Hyung Kim, Young-Il Jeong, and Dae Hwan Kang. 2015. 'Antitumor activity of vorinostat-incorporated nanoparticles against human cholangiocarcinoma cells', *Journal of Nanobiotechnology*, 13: 1-13.

Layek, Buddhadev, Lindsey Lipp, and Jagdish Singh. 2015. 'Cell penetrating peptide conjugated chitosan for enhanced delivery of nucleic acid', *International Journal of Molecular Sciences*, 16: 28912-30.

Leamon, Christopher P, and Joseph A Reddy. 2004. 'Folate-targeted chemotherapy', *Advanced drug delivery reviews*, 56: 1127-41.

Lee, Jun H, and Anjan Nan. 2012. 'Combination drug delivery approaches in metastatic breast cancer', *Journal of drug delivery*, 2012.

Li, Yuhuan, Robert J. Lee, Kongtong Yu, Ye Bi, Yuhang Qi, Yating Sun, Yujing Li, Jing Xie, and Lesheng Teng. 2016. 'Delivery of siRNA Using Lipid Nanoparticles Modified with Cell Penetrating Peptide', *ACS Applied Materials & Interfaces*, 8: 26613-21.

Li, Zhen, Shirui Tan, Shuan Li, Qiang Shen, and Kunhua Wang. 2017. 'Cancer drug delivery in the nano era: An overview and perspectives', *Oncology reports*, 38: 611-24.

Liao, Huihui, Hui Liu, Yulin Li, Mengen Zhang, Helena Tomás, Mingwu Shen, and Xiangyang Shi. 2014. 'Antitumor efficacy of doxorubicin encapsulated within PEGylated poly (amidoamine) dendrimers', *Journal of Applied Polymer Science*, 131.

Liu, Yayuan, Ling Mei, Qianwen Yu, Chaoqun Xu, Yue Qiu, Yuting Yang, Kairong Shi, Qianyu Zhang, Huile Gao, Zhirong Zhang, and Qin He. 2015. 'Multifunctional Tandem Peptide Modified Paclitaxel-Loaded Liposomes for the

Treatment of Vasculogenic Mimicry and Cancer Stem Cells in Malignant Glioma', *ACS Applied Materials & Interfaces*, 7: 16792-801.

Livaniou, Evangelia, Danae Costopoulou, Irene Vassiliadou, Leondios Leondiadis, John O Nyalala, Dionyssis S Ithakissios, and Gregory P Evangelatos. 2000. 'Analytical techniques for determining biotin', *Journal of Chromatography A*, 881: 331-43.

Lodish H, Berk A, Zipursky SL, et al. . 2000. "Molecular Cell Biology." In *Section 8.1, Mutations: Types and Causes*. New York: W. H. Freeman.

Luo, Zhong, Yan Hu, Kaiyong Cai, Xingwei Ding, Quan Zhang, Menghuan Li, Xing Ma, Beilu Zhang, Yongfei Zeng, and Peizhou Li. 2014. 'Intracellular redox-activated anticancer drug delivery by functionalized hollow mesoporous silica nanoreservoirs with tumor specificity', *Biomaterials*, 35: 7951-62.

Luong, Duy, Prashant Kesharwani, Rahul Deshmukh, Mohd Cairul Iqbal Mohd Amin, Umesh Gupta, Khaled Greish, and Arun K Iyer. 2016. 'PEGylated PAMAM dendrimers: Enhancing efficacy and mitigating toxicity for effective anticancer drug and gene delivery', *Acta Biomaterialia*, 43: 14-29.

Ma, Pengkai, Xuemei Zhang, Ling Ni, Jinming Li, Fengpu Zhang, Zheng Wang, Shengnan Lian, and Kaoxiang Sun. 2015. 'Targeted delivery of polyamidoamine-paclitaxel conjugate functionalized with anti-human epidermal growth factor receptor 2 trastuzumab', *International Journal of Nanomedicine*, 10: 2173.

Madani, F., S. Lindberg, U. Langel, S. Futaki, and A. Graslund. 2011. 'Mechanisms of cellular uptake of cell-penetrating peptides', *J Biophys*, 2011: 414729.

Maeda, Hiroshi. 2001. 'The enhanced permeability and retention (EPR) effect in tumor vasculature: the key role of tumor-selective macromolecular drug targeting', *Advances in enzyme regulation*, 41: 189-207.

Majoros, István J, Andrzej Myc, Thommey Thomas, Chandan B Mehta, and James R Baker. 2006. 'PAMAM dendrimer-based multifunctional conjugate for cancer therapy: synthesis, characterization, and functionality', *Biomacromolecules*, 7: 572-79.

Malam, Yogeshkumar, Marilena Loizidou, and Alexander M Seifalian. 2009. 'Liposomes and nanoparticles: nanosized vehicles for drug delivery in cancer', *Trends in pharmacological sciences*, 30: 592-99.

Matsumura, Yasuhiro, and Hiroshi Maeda. 1986. 'A new concept for macromolecular therapeutics in cancer chemotherapy: mechanism of tumoritropic accumulation of proteins and the antitumor agent smancs', *Cancer research*, 46: 6387-92.

Mehdizadeh, Mozhdeh, Hasti Rouhani, Nima Sepehri, Reyhaneh Varshochian, Mohammad Hossein Ghahremani, Mohsen Amini, Mehdi Gharghabi, Seyed Nasser Ostad, Fatemeh Atyabi, and Azin Baharian. 2017. 'Biotin decorated PLGA nanoparticles containing SN-38 designed for cancer therapy', *Artificial cells, nanomedicine, and biotechnology*, 45: 495-504.

Mendelsohn, John. 1997. 'Epidermal growth factor receptor inhibition by a monoclonal antibody as anticancer therapy', *Clinical Cancer Research*, 3: 2703-07.

Menjoge, Anupa R, Rangaramanujam M Kannan, and Donald A Tomalia. 2010. 'Dendrimer-based drug and imaging conjugates: design considerations for nanomedical applications', *Drug discovery today*, 15: 171-85.

Mignani, Serge, Saïd El Kazzouli, Mosto Bousmina, and Jean-Pierre Majoral. 2013. 'Expand classical drug administration ways by emerging routes using dendrimer drug delivery systems: a concise overview', *Advanced drug delivery reviews*, 65: 1316-30.

Milhem, OM, C Myles, NB McKeown, D Attwood, and A D'Emanuele. 2000. 'Polyamidoamine Starburst® dendrimers as solubility enhancers', *International journal of pharmaceutics*, 197: 239-41.

Milletti, Francesca. 2012. 'Cell-penetrating peptides: classes, origin, and current landscape', *Drug discovery today*, 17: 850-60.

Minko, Tamara, Pankaj V Paranjpe, Bo Qiu, Anita Lalloo, Roney Won, Stanley Stein, and Patrick J Sinko. 2002. 'Enhancing the anticancer efficacy of camptothecin using biotinylated poly (ethyleneglycol) conjugates in sensitive and multidrug-resistant human ovarian carcinoma cells', *Cancer Chemotherapy and Pharmacology*, 50: 143-50.

Mishra, Prajna, Bismita Nayak, and RK Dey. 2016. 'PEGylation in anti-cancer therapy: An overview', *asian journal of pharmaceutical sciences*, 11: 337-48.

Nair, M Krishnan, Cherian Varghese, and R Swaminathan. 2005. 'Cancer: Current scenario, intervention strategies and projections for 2015', *NCHM Background papers-Burden of Disease in India*: 219-25.

Najlah, Mohammad, Sally Freeman, David Attwood, and Antony D'Emanuele. 2006. 'Synthesis, characterization and stability of dendrimer prodrugs', *International journal of pharmaceutics*, 308: 175-82.

Nasongkla, Norased, Xintao Shuai, Hua Ai, Brent D Weinberg, John Pink, David A Boothman, and Jinming Gao. 2004. 'cRGD-functionalized polymer micelles for targeted doxorubicin delivery', *Angewandte Chemie*, 116: 6483-87.

Nateghian, Navid, Navid Goodarzi, Mohsen Amini, Fatemeh Atyabi, Mohammad Reza Khorramizadeh, and Rassoul Dinarvand. 2016. 'Biotin/folate-decorated human serum albumin nanoparticles of docetaxel: comparison of chemically conjugated nanostructures and physically loaded nanoparticles for targeting of breast cancer', *Chemical Biology & Drug Design*, 87: 69-82.

Noor Kamil, Saba Kamil. 2015. 'Global Cancer Incidences, Causes and Future Predictions for Subcontinent Region', *Systematic Reviews in Pharmacy*, 6: 13-17.

O'Connor, Clare M, Jill U Adams, and Jennifer Fairman. 2010. 'Essentials of cell biology', *Cambridge: NPG Education*.

Ojima, Iwao, Brendan Lichtenthal, Siyeon Lee, Changwei Wang, and Xin Wang. 2016. 'Taxane anticancer agents: a patent perspective', *Expert Opinion on Therapeutic Patents*, 26: 1-20.

Papadopoulou, Lefkothea C, and Asterios S Tsiftsoglou. 2013. 'The potential role of cell penetrating peptides in the intracellular delivery of proteins for therapy of erythroid related disorders', *Pharmaceuticals*, 6: 32-53.

Patri, Anil K, Andrzej Myc, James Beals, Thommey P Thomas, Neil H Bander, and James R Baker. 2004. 'Synthesis and in vitro testing of J591 antibody− dendrimer conjugates for targeted prostate cancer therapy', *Bioconjugate chemistry*, 15: 1174-81.

Peer, Dan, Jeffrey M. Karp, Seungpyo Hong, Omid C. Farokhzad, Rimona Margalit, and Robert Langer. 2007. 'Nanocarriers as an emerging platform for cancer therapy', *Nature Nanotechnology*, 2: 751.

Perche, F., and V. P. Torchilin. 2012. 'Cancer cell spheroids as a model to evaluate chemotherapy protocols', *Cancer Biology & Therapy*, 13: 1205-13.

Pirollo, Kathleen F, and Esther H Chang. 2008. 'Does a targeting ligand influence nanoparticle tumor localization or uptake?', *Trends in biotechnology*, 26: 552-58.

Pourianazar, Negar Taghavi, Pelin Mutlu, and Ufuk Gunduz. 2014. 'Bioapplications of poly (amidoamine)(PAMAM) dendrimers in nanomedicine', *Journal of Nanoparticle Research*, 16: 2342.

Prabhakar, U., H. Maeda, R. K. Jain, E. M. Sevick-Muraca, W. Zamboni, O. C. Farokhzad, S. T. Barry, A. Gabizon, P. Grodzinski, and D. C. Blakey. 2013. 'Challenges and key considerations of the enhanced permeability and retention effect for nanomedicine drug delivery in oncology', *Cancer Res*, 73: 2412-7.

Pratt, William B, William D Ensminger, and Raymond W Ruddon. 1994. *The anticancer drugs* (Oxford University Press, USA).

Quan, Yu Hua, Byungji Kim, Ji-Ho Park, Yeonho Choi, Young Ho Choi, and Hyun Koo Kim. 2014. 'Highly sensitive and selective anticancer effect by conjugated HA-cisplatin in non-small cell lung cancer overexpressed with CD44', *Experimental Lung Research*, 40: 475-84.

Ren, Wen Xiu, Jiyou Han, Soojin Uhm, Yu Jin Jang, Chulhun Kang, Jong-Hoon Kim, and Jong Seung Kim. 2015. 'Recent development of biotin conjugation in biological imaging, sensing, and target delivery', *Chemical Communications*, 51: 10403-18.

Rompicharla, Sri Vishnu Kiran, Prakruti Trivedi, Preeti Kumari, Pratyusha Ghanta, Balaram Ghosh, and Swati Biswas. 2017. 'Polymeric micelles of suberoylanilide hydroxamic acid to enhance the anticancer potential in vitro and in vivo', *Nanomedicine*, 12: 43-58.

Ruoslahti, Erkki. 2017. 'Tumor penetrating peptides for improved drug delivery', *Advanced drug delivery reviews*, 110: 3-12.

Russell-Jones, Gregory, Kirsten McTavish, John McEwan, John Rice, and David Nowotnik. 2004. 'Vitamin-mediated targeting as a potential mechanism to increase drug uptake by tumours', *Journal of Inorganic Biochemistry*, 98: 1625-33.

Saranath, Dhananjaya, and Aparna Khanna. 2014. 'Current status of cancer burden: global and Indian scenario', *Biomed Res J*, 1: 1-5.

Sarisozen, Can, Abraham H. Abouzeid, and Vladimir P. Torchilin. 2014. 'The effect of co-delivery of paclitaxel and curcumin by transferrin-targeted PEG-PE-based mixed micelles on resistant ovarian cancer in 3-D spheroids and in vivo tumors', *European Journal of Pharmaceutics and Biopharmaceutics*, 88: 539-50.

Scholar, Eric. 2007. 'Antimetabolites.' in S. J. Enna and David B. Bylund (eds.), *xPharm: The Comprehensive Pharmacology Reference* (Elsevier: New York).

Senapati, Sudipta, Arun Kumar Mahanta, Sunil Kumar, and Pralay Maiti. 2018. 'Controlled drug delivery vehicles for cancer treatment and their performance', *Signal transduction and targeted therapy*, 3: 7.

Sharma, Anupama, Surya Prakash Gautam, and Arun Kumar Gupta. 2011. 'Surface modified dendrimers: synthesis and characterization for cancer targeted drug delivery', *Bioorganic & Medicinal Chemistry*, 19: 3341-46.

Sherwood, Lauralee. 2015. *Human physiology: from cells to systems* (Cengage learning).

Shi, Jing-Fang, Ping Wu, Zi-Hua Jiang, and Xiao-Yi Wei. 2014. 'Synthesis and tumor cell growth inhibitory activity of biotinylated annonaceous acetogenins', *European Journal of Medicinal Chemistry*, 71: 219-28.

Shin, Meong Cheol, Jian Zhang, Kyoung Ah Min, Kyuri Lee, Youngro Byun, Allan E David, Huining He, and Victor C Yang. 2014. 'Cell-penetrating peptides: Achievements and challenges in application for cancer treatment', *Journal of Biomedical Materials Research Part A*, 102: 575-87.

Shukla, Rameshwer, Thommey P Thomas, Jennifer Peters, Alina Kotlyar, Andrzej Myc, and James R Baker Jr. 2005. 'Tumor angiogenic vasculature targeting with PAMAM dendrimer–RGD conjugates', *Chemical communications*: 5739-41.

Šimůnek, Tomáš, Martin Štěrba, Olga Popelová, Michaela Adamcová, Radomír Hrdina, and Vladimír Geršl. 2009. 'Anthracycline-induced cardiotoxicity: overview of studies examining the roles of oxidative stress and free cellular iron', *Pharmacological Reports*, 61: 154-71.

Singh, Jaspreet, Keerti Jain, Neelesh Kumar Mehra, and N. K. Jain. 2016. 'Dendrimers in anticancer drug delivery: mechanism of interaction of drug and dendrimers', *Artificial Cells, Nanomedicine, and Biotechnology*, 44: 1626-34.

Sowinska, Marta, and Zofia Urbanczyk-Lipkowska. 2014. 'Advances in the chemistry of dendrimers', *New Journal of Chemistry*, 38: 2168-203.

Stortecky, Stefan, and Thomas M Suter. 2010. 'Insights into cardiovascular side-effects of modern anticancer therapeutics', *Current opinion in oncology*, 22: 312-17.

Sudimack, Jennifer, and Robert J Lee. 2000. 'Targeted drug delivery via the folate receptor', *Advanced drug delivery reviews*, 41: 147-62.

Svenson, Sönke, and Donald A Tomalia. 2012. 'Dendrimers in biomedical applications—reflections on the field', *Advanced drug delivery reviews*, 64: 102-15.

Taheri, Azade, Rassoul Dinarvand, Faranak Salman Nouri, Mohammad Reza Khorramizadeh, Atefeh Taheri Borougeni, Pooria Mansoori, and Fatemeh Atyabi. 2011. 'Use of biotin targeted methotrexate–human serum albumin conjugated nanoparticles to enhance methotrexate antitumor efficacy', *International Journal of Nanomedicine*, 6: 1863.

Thomas, Thommey P, Istvan J Majoros, Alina Kotlyar, Jolanta F Kukowska-Latallo, Anna Bielinska, Andrzej Myc, and James R Baker. 2005. 'Targeting and inhibition of cell growth by an engineered dendritic nanodevice', *Journal of medicinal chemistry*, 48: 3729-35.

Tomalia, Donald A. 2005. 'Birth of a new macromolecular architecture: dendrimers as quantized building blocks for nanoscale synthetic polymer chemistry', *Progress in Polymer Science*, 30: 294-324.

Tripodo, Giuseppe, Delia Mandracchia, Simona Collina, Marta Rui, and Daniela Rossi. 2014. 'New perspectives in cancer therapy: the biotin-antitumor molecule conjugates', *Medicinal Chemistry (Shariqah, United Arab Emirates)*, 8: 1-4.

Tseng, Ching-Li, Wen-Yun Su, Ko-Chung Yen, Kai-Chiang Yang, and Feng-Huei Lin. 2009. 'The use of biotinylated-EGF-modified gelatin nanoparticle carrier to enhance cisplatin accumulation in cancerous lungs via inhalation', *Biomaterials*, 30: 3476-85.

Uchida, Masaki, Hisanori Kosuge, Masahiro Terashima, Deborah A Willits, Lars O Liepold, Mark J Young, Michael V McConnell, and Trevor Douglas. 2011. 'Protein cage nanoparticles bearing the LyP-1 peptide for enhanced imaging of macrophage-rich vascular lesions', *ACS nano*, 5: 2493-502.

Vadlapudi, Aswani Dutt, Ramya Krishna Vadlapatla, Dhananjay Pal, and Ashim K Mitra. 2013. 'Biotin uptake by T47D breast cancer cells: functional and molecular evidence of sodium-dependent multivitamin transporter (SMVT)', *International Journal of Pharmaceutics*, 441: 535-43.

van den Brand, D., L. F. Massuger, R. Brock, and W. P. Verdurmen. 2017. 'Mimicking Tumors: Toward More Predictive In Vitro Models for Peptide- and Protein-Conjugated Drugs', *Bioconjugate chemistry*, 28: 846-56.

Vega, Javier, Shi Ke, Zhen Fan, Sidney Wallace, Chusilp Charsangavej, and Chun Li. 2003. 'Targeting doxorubicin to epidermal growth factor receptors by site-specific conjugation of C225 to poly (L-glutamic acid) through a polyethylene glycol spacer', *Pharmaceutical Research*, 20: 826-32.

Ventola, C. Lee. 2017. 'Progress in Nanomedicine: Approved and Investigational Nanodrugs', *Pharmacy and Therapeutics*, 42: 742-55.

Vogelstein, Bert, and Kenneth W Kinzler. 2004. 'Cancer genes and the pathways they control', *Nature Medicine*, 10: 789.

Wang, Shengpeng, Jiange Qiu, Zhi Shi, Yitao Wang, and Meiwan Chen. 2015. 'Nanoscale drug delivery for taxanes based on the mechanism of multidrug resistance of cancer', *Biotechnology Advances*, 33: 224-41.

Wang, Yin, Rui Guo, Xueyan Cao, Mingwu Shen, and Xiangyang Shi. 2011. 'Encapsulation of 2-methoxyestradiol within multifunctional poly (amidoamine) dendrimers for targeted cancer therapy', *Biomaterials*, 32: 3322-29.

Wang, Yin, Xueyan Cao, Rui Guo, Mingwu Shen, Mengen Zhang, Meifang Zhu, and Xiangyang Shi. 2011. 'Targeted delivery of doxorubicin into cancer cells using a folic acid–dendrimer conjugate', *Polymer Chemistry*, 2: 1754-60.

Wen, Xiaoxia, Qing-Ping Wu, Shi Ke, Lee Ellis, Chusilp Charnsangavej, Abraham S Delpassand, Sidney Wallace, and Chun Li. 2001. 'Conjugation with 111In-DTPA-poly (ethylene glycol) improves imaging of anti-EGF receptor antibody C225', *Journal of Nuclear Medicine*, 42: 1530-37.

White, Mary C., Dawn M. Holman, Jennifer E. Boehm, Lucy A. Peipins, Melissa Grossman, and S. Jane Henley. 2014. 'Age and Cancer Risk: A Potentially Modifiable Relationship', *American Journal of Preventive Medicine*, 46: S7-15.

Xu, Heng, Celeste AS Regino, Yoshinori Koyama, Yukihiro Hama, Andrew J Gunn, Marcelino Bernardo, Hisataka Kobayashi, Peter L Choyke, and Martin W Brechbiel. 2007. 'Preparation and preliminary evaluation of a biotin-targeted, lectin-targeted dendrimer-based probe for dual-modality magnetic resonance and fluorescence imaging', *Bioconjugate chemistry*, 18: 1474-82.

Yamada, Yuma, Masahiro Hashida, and Hideyoshi Harashima. 2015. 'Hyaluronic acid controls the uptake pathway and intracellular trafficking of an octaarginine-modified gene vector in CD44 positive-and CD44 negative-cells', *Biomaterials*, 52: 189-98.

Yang, Wenjun, Yiyun Cheng, Tongwen Xu, Xueyuan Wang, and Long-ping Wen. 2009. 'Targeting cancer cells with biotin–dendrimer conjugates', *European Journal of Medicinal Chemistry*, 44: 862-68.

Yang, Wenzhi, Miaomiao Wang, Lilan Ma, Haiying Li, and Le Huang. 2014. 'Synthesis and characterization of biotin modified cholesteryl pullulan as a novel anticancer drug carrier', *Carbohydrate Polymers*, 99: 720-27.

Yang, Yang, Aniruddha Roy, Yucheng Zhao, Elijus Undzys, and Shyh-Dar Li. 2017. 'Comparison of Tumor Penetration of Podophyllotoxin–Carboxymethylcellulose Conjugates with Various Chemical Compositions in Tumor Spheroid Culture and In Vivo Solid Tumor', *Bioconjugate chemistry*, 28: 1505-18.

Yao, Xin, Kessarin Panichpisal, Neil Kurtzman, and Kenneth Nugent. 2007. 'Cisplatin nephrotoxicity: a review', *The American journal of the medical sciences*, 334: 115-24.

Yellepeddi, Venkata K, Ajay Kumar, and Srinath Palakurthi. 2009. 'Biotinylated poly (amido) amine (PAMAM) dendrimers as carriers for drug delivery to ovarian cancer cells in vitro', *Anticancer Research*, 29: 2933-43.

Yuan, X., W. Ji, S. Chen, Y. Bao, S. Tan, S. Lu, K. Wu, and Q. Chu. 2016. 'A novel paclitaxel-loaded poly(d,l-lactide-co-glycolide)-Tween 80 copolymer nanoparticle overcoming multidrug resistance for lung cancer treatment', *Int J Nanomedicine*, 11: 2119-31.

Zhang, Yong, and Dev K Chatterjee. 2007. 'Liposomes, Dendrimers and other Polymeric Nanoparticles for Targeted Delivery of Anticancer Agents–A Comparative Study', *Nanotechnologies for the Life Sciences*.

Zhou, Benqing, Lingzhou Zhao, Mingwu Shen, Jinhua Zhao, and Xiangyang Shi. 2017. 'A multifunctional polyethylenimine-based nanoplatform for targeted anticancer drug delivery to tumors in vivo', *Journal of Materials Chemistry B*, 5: 1542-50.

Zhu, Jingyi, Linfeng Zheng, Shihui Wen, Yueqin Tang, Mingwu Shen, Guixiang Zhang, and Xiangyang Shi. 2014. 'Targeted cancer theranostics using alpha-tocopheryl succinate-conjugated multifunctional dendrimer-entrapped gold nanoparticles', *Biomaterials*, 35: 7635-46.

"National Center for Biotechnology Information, PubChem Compound Database; CID=36314."

2007. 'In vitro evaluation of dendrimer prodrugs for oral drug delivery', *International journal of pharmaceutics*, 336: 183-90.

2008. 'Octaarginine-modified liposomes: enhanced cellular uptake and controlled intracellular trafficking', *International Journal of Pharmaceutics*, 354: 39-48.

Appendix

List of publications

From thesis work:

1. **Rompicharla SVK**, Kumari P, Ghosh B, Biswas S**.** "Octa-Arginine Modified Poly(amidoamine) Dendrimers for Improved Delivery and Cytotoxic Effect of Paclitaxel in Cancer". *Artificial Cells, Nanomedicine, and Biotechnology*, 2018, 1-13.

Other publications:

1. Bhatt H, **Rompicharla SVK**, Komanduri N, Shah A, Paradkar S, Ghosh B, Biswas S. "Development of curcumin-loaded solid lipid nanoparticles utilizing glyceryl monostearate as single lipid using QbD approach: Characterization and evaluation of anticancer activity against human breast cancer cell line". *Current Drug Delivery*, 2018. (Manuscript accepted)

2. **Rompicharla, SVK.**, Bhatt H, Shah A, Komanduri N, Vijayasarathy D, Ghosh, B, Biswas S. "Formulation optimization, characterization, and evaluation of in vitro cytotoxic potential of curcumin loaded solid lipid nanoparticles for improved anticancer activity". *Chemistry and Physics of Lipids*, 2017, 208, 10-18.

3. **Rompicharla SVK**, Trivedi P, Kumari P, Ghanta P, Ghosh B, Biswas S. "Polymeric micelles of suberoylanilide hydroxamic acid to enhance the anticancer potential in vitro and in vivo". *Nanomedicine*, 2017, 12(1):43-58.

4. Kumari P, **Rompicharla SVK**, Muddineti OS, Ghosh B, & Biswas S. "Transferrin-anchored poly (lactide) based micelles to improve anticancer activity of curcumin in hepatic and cervical cancer cell monolayers and 3D spheroids". *International journal of biological macromolecules*, 2018, 116: 1196-1213.

5. Muddineti OS, Vanaparthi A, **Rompicharla SVK**, Kumari P, Ghosh, B, Biswas S "Cholesterol and vitamin E-conjugated PEGylated polymeric micelles for efficient delivery and enhanced anticancer activity of curcumin: evaluation in 2D monolayes and 3D spheroids". *Artificial Cells Nanomedicine Biotechnology,* 2018, 9: 1-14.

6. Muddineti OS, Shah A, **Rompicharla SVK**, Ghosh B, Biswas S. "Cholesterol-grafted chitosan micelles as a nanocarrier system for drug-siRNA co-delivery to the lung cancer cells". *International journal of biological macromolecules*. 2018.

7. Kumari P, Muddineti OS, **Rompicharla SVK**, Ghanta P, Adithya Karthik BBN, Ghosh B, Biswas S. "Choltesterol-conjugated poly(D,L-Lactide)-based micelles as a nanocarrier system for effective delivery of curcumin in cancer therapy". *Drug Delivery*. 2017, 24(1), 209-223.

8. Lakhani PM, **Rompicharla SVK**, Ghosh B, Biswas S. "An overview of synthetic strategies and current applications of gold nanorods in cancer treatment". *Nanotechnology*, 2015, 26(43), 432001

List of poster presentations at conferences

1. "Biotin Conjugated Multifunctional PAMAM Dendrimers for the Delivery of Paclitaxel". 16th International Symposium on Advances in Technology and Business Potential of New Drug Delivery Systems organized by Controlled Release Society Indian Chapter, February 23rd-24th, 2018 at Mumbai, India.

2. "Cell Penetrating Peptide Octa-Arginine Anchored Multifunctional PAMAM Dendrimer for the Delivery of Paclitaxel". American Association of Pharmaceutical Scientists (AAPS) 2016, November 13-17 at Colorado, USA.

3. "Curcumin Loaded Solid Lipid nano particles for Improved Delivery to cancer cells". International conference on "Pharmaceutical Education-Academia Relation to Industry-Current Scenario" 17th & 18th March 2017, Organized by Centre for Pharmaceutical Sciences Institute of Science and Technology, JNTUH, Kukatpally, Hyderabad, India.

Rompicharla Sri Vishnu Kiran

Biography

Mr R. S. V. Kiran completed his Bachelor of Pharmacy from Acharya Nagarjuna University, Andhra Pradesh, India in 2011. He completed his M. S. (Pharm.) (Pharmaceutics) from NIPER, Hyderabad in 2013. Post his one year stint at Biocon, Bangalore, Mr Kiran joined Dr Swati Biswas's lab at BITS Pilani Hyderabad Campus for carrying out his doctoral research work. Mr Kiran worked on a DBT funded project based on dendrimer technology to target cancer for his doctoral research. Mr Kiran has received international travel support from Department of Science and Technology (DST) to present his research work at various international conferences. He has co-authored 12 scientific peer review publications in well-renowned international journals, one Indian Patent application and presented papers in various international and national conferences.

Dr. Swati Biswas

Biography

Dr. Swati Biswas is presently working as Assistant Professor, in Department of Pharmacy, Birla Institute of Technology and Science, Pilani, Hyderabad Campus. She received her B. Pharm degree (1998) and M.Pharm (2000) from Jadavpur University, India. She was awarded her Ph.D. in Pharmaceutical Sciences in the year 2008 from Wayne State University, USA. After completion of doctoral studies, she pursued her postdoctoral studies in Northeastern State University, USA (2013). She has been involved in research for the last 15 years. She has to her credit more than 40 research publications, two US patents and two Indian Patents. She has authored 3 book chapters in "Dendrimers: Synthesis, Applications and Role in Nanotechnology", "Drug Delivery Strategies for Poorly Water-Soluble Drugs" and "Handbook of Polymers for Pharmaceutical technologies, Volume 2: Processing and Applications". She has successfully completed many sponsored projects and currently handling projects sponsored by DST, DBT and DST-LVPEI. She has guided one Ph.D student and currently four students are pursuing their Ph.D. work under her supervision.